The Petrography of the Longnose Peridotite and Its Relationship to the Duluth Complex

A THESIS

SUBMITTED TO THE FACULTY OF THE GRADUATE SCHOOL

BY

Eric Kendall Linscheid

IN PARTIAL FULFILLMENT OF THE REQUIREMENTS

FOR THE DEGREE OF

MASTER OF SCIENCE

January, 1991

ABSTRACT

The Longnose Peridotite is a funnel-shaped, ultramafic body intruded into middle Proterozic (1.1 b. y.) troctolitic series rocks of the Duluth Complex. The body is located approximately 83 kilometers north of Duluth, Minnesota. The geometry of the Longnose Peridotite is based on drill core logs and gravity data. In plan view, the body is tear drop in shape, measuring about 760 meters long and narrowing from 490 meters at the widest point to 76 meters at the narrowest point. In longitudinal section, it forms an asymmetrical funnel with a maximum thickness of 167 meters. A crude zonal arrangement of cumulate rocks exists. Going stratigraphically up section, they are oxide clinopyroxenite, oxide peridotite (wehrlite), oxide dunite, and feldspathic dunite. The marginal zone of the body is characterized by xenoliths of troctolitic rocks from the Duluth Complex and locally exhibits inversed stratigraphy. Discordant massive oxide zones composed of ilmenite and titanomagnetite are primarily hosted by oxide dunite and to a lesser extent by oxide clinopyroxenite. The zones vary from less than 0.1 meter in thickness and perhaps to several meters in lateral extent to up to 30 m in thickness and 130 m in length. These zones are thought to have formed by filter pressing or by primary precipitation of ilmenite/titanomagnetite from a Fe-Ti rich ultramafic magma, and subsequent annealing at subsolidus oxide terperatures.

Mineral chemical analyses of olivine, plagioclase, and augite show a similar mineralogy between the Longnose Peridotite and other troctolitic, gabbroic, and dunitic rocks in the Duluth Complex.

The Longnose Peridotite was introduced soon after the intrusion of the troctolitic country rocks of the Duluth Complex based on the lack of alteration of the country rock and lack of chilled margins in the Longnose Peridotite. The stratigraphy of the Longnose Peridotite can be explained by multiple injections of magma. The inverted stratigraphy in the marginal zones and the sparcity of igneous foliation suggest that the injections may have been vigorous in nature.

TABLE OF CONTENTS

LIST OF PLATES

LIST OF FIGURES

LIST OF TABLES

LIST OF APPENDICES

Acknowledgements

This thesis was made possible by the cooperation of several people and organizations. Nicor Mineral Ventures (now Westmont Mining) gave access to drill core. Mr. William Ulland of American Shield Corporation who consults for Nicor Mineral Ventures, supplied geophysical data, TiO2 analyses, drill core logs, and space in which to log the drill core. He also answered questions about the geometry of the deposit. Mr. Leon Gladen, previously of the Minnesota D.N.R. proposed the thesis and the D.N.R. graciously funded the project. Dr. Penny Morton's patience and dedication made the completion of this thesis possible. Ms. Sarah Mills helped with the initial identification of minerals in drill core. Dr. Dexter Perkins and Dr. Bob Stevenson at the University of North Dakota, Grand Forks, graciously offered their time and expertise in microprobe analyses.

Chapter 1

Introduction

A. Statement of Problem

The Longnose Peridotite is a funnel-shaped, ultramafic body intruded into the lower troctolite series rocks of the Duluth Complex, near Hoyt Lakes, Minnesota. The pluton displays a crude concentric zonation, going up section, of oxide clinopyroxenite and oxide-olivine clinopyroxenite, oxide peridotite (wehrlite), oxide dunite, and feldspathic oxide dunite at the top. Discordant, massive titaniferous oxide zones occur within some of the dunitic and peridotitic rocks. Inclusions of footwall rock occur largely in the marginal zones of the deposit. Sulfides are a minor component of the body.

The peridotite body was discovered by airborn electromagnetics in the late 1950's by Bear Creek Mining Company while searching for massive sulfides. The intrusion is currently being explored for ilmenite-titanomagnetite by Westmont Mining.

The objective of this thesis is twofold: 1) to describe the petrography and establish the petrogenesis of the Longnose Peridotite by the study of drill core samples and microprobe analysis, and 2) to investigate the relationship between the Longnose Peridotite and the Duluth Complex.

B. Location

The Longnose Peridotite is located in the western part of the Duluth Complex (Figs. 1 and 2) approximately 83 air kilometers (52 miles) north of Duluth, Minnesota. Access is via Minnesota Highway 137

north out of Hoyt Lakes, and east on U.S. Forest Service road 117 for 6.6 km (4.1 miles). The intrusion occupies the center of section 30, T.59N., R.14W., in the Allen 7.5 minute U.S.G.S. quadrangle.

C. Methods of Study

The map area covers 6.7 square kilometers (2.64 by 2.54 km) and was mapped at a scale of 1:4800 (see Plate 1 in back jacket). The area was selected to include the country rocks surrounding the Longnose Peridotite and to insure adequate outcrop exposure. Twenty-four thin sections were made of samples thought to be representative of rock units mapped in the field. Four diamond drill cores, supplied by Westmont Mining were selected to give what was thought at the time the best stratigraphic cross-section of the deposit. Three cores were of 2.5 inch diameter and approximately 550′ (168 m) in length, the fourth core was 1.44 inches in diameter and 3085′ (940 m) in length. Only the top 66′ (20 m) of the fourth core intersected the Longnose Peridotite; the remaining core consists of troctolitic rocks of the Duluth Complex. The first three drill cores and the top 66′ of the fourth drill core were originally logged at a scale of 1:60, and later reduced to 1:300 (see Plate 2; all measurements are reported in feet as the drill cores were recorded in feet). The purpose of the log was to determine the stratigraphy within the Longnose Peridotite, including the relationship between the oxide zones and the ultramafic (silicate) rocks of the body.

Sampling of the drill core for thin sections and polished sections was done upon completion of each log. Samples were selected based on textural, mineralogical, and lithologic changes. Eighty-nine thin

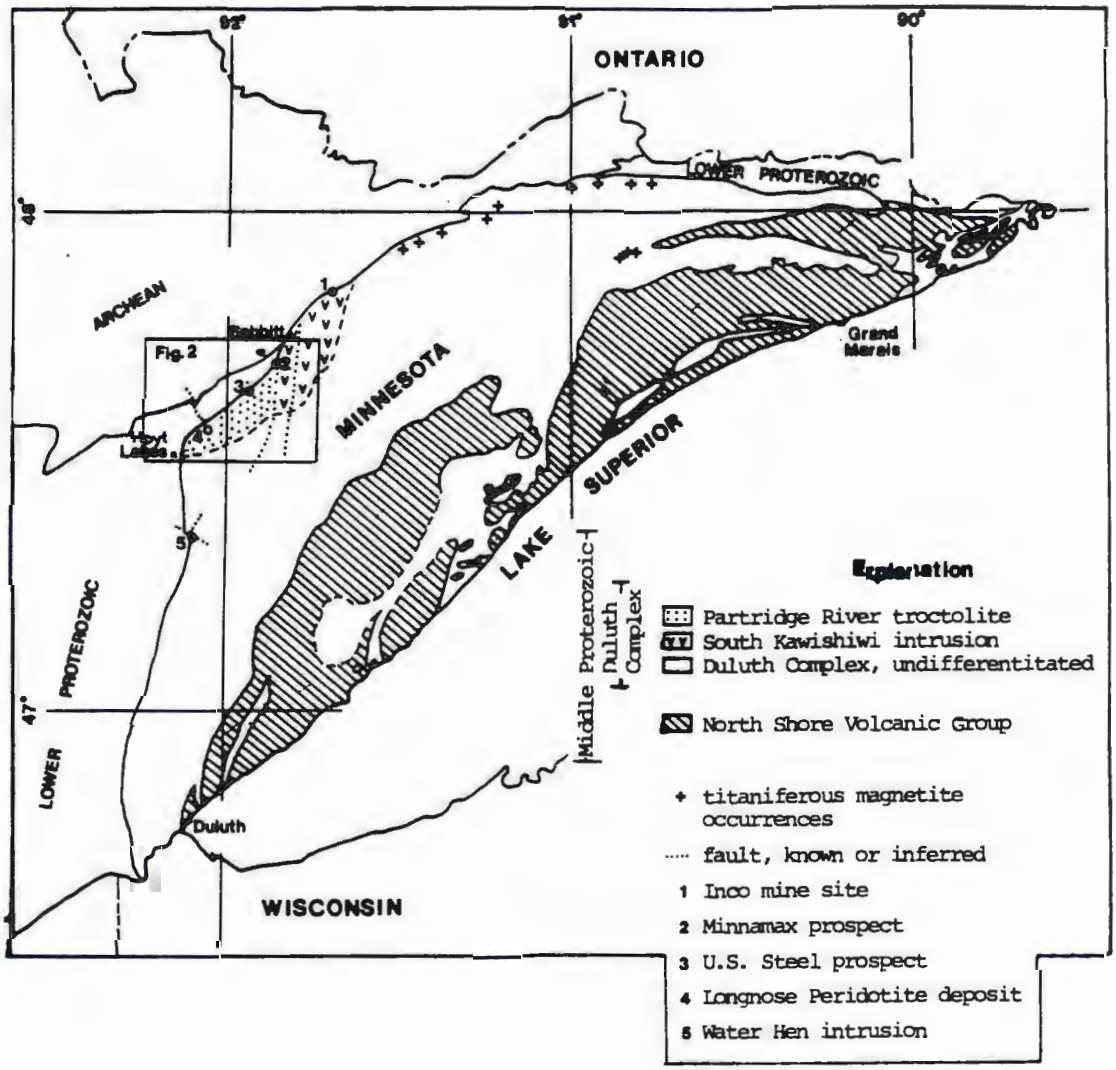

Fig. 1. Bedrock geology of Northeastern Minnesota. (After Cooper, 1978)

sections and 59 polished sections were examined. Polished sections were made from thin section "heels" wherever possible. This aided in establishing the textural and mineralogical relationships among different silicate phases and oxide phases.

Electron microprobe analyses were made on 10 polished thin sections which were selected after completion of the petrographic study. Two to four phases in each section were analyzed for the following elements: Si,Al, Ti, Fe, Mn, Mg, Ca, Na, and in the case of oxides, V and Cr were added. This work was completed at the University of North Dakota under the direction of Dr. Dexter Perkins and Dr. Bob Stevenson. Samples were selected to represent the major rock types, to compare the composition of minerals within the same rock type in different drill cores, and to monitor the compositon of silicates and oxides up section in one drill core (LN-2).

D. Previous work

Grout (1950) gives the most extensive summary of titaniferous magnetite in Minnesota. The majority of deposits are concentrated in the Duluth Complex in Lake and Cook counties in northeastern Minnesota (Fig. 1). According to Grout (1950), titaniferous magnetite was reported as early as 1876 by N.H. Winchell of the Minnesota Geological and Natural History Survey. He was followed by Peckman (1877), Irving (1883), Winchell (1891) and Van Hise and Leith (1911). Diamond drilling was done in 1898 and 1908 by Johnson Nickel Mining Company (Grout, 1950). The first extensive study was completed by T.M. Broderick in 1917 who classified the titaniferous magnetite deposits into four types: 1) inclusions of Gunflint Iron Formation; 2) banded

segregations of gabbro with oxide layers; 3) irregular bodies of recrystallizd Gunflint Iron Formation inclusions; and 4) dike-like bodies. In 1947, the Minnesota Geological Survey (M.G.S.) initiated an extensive drilling program to evaluate the titaniferous magnetite deposits in Cook County. Their results showed that 94 million tons of indicated and inferred "marginal" ore were extractable by shallow surface mining (Grout, 1950). However, much of this, if not most, now lies within the Boundary Waters Canoe Area Wilderness and is inaccessable to mining.

Nathan (1969) mapped part of the Duluth Complex along the Gunflint Trail in Cook County and suggested several areas most favorable for future exploration. The most current exploration of titaniferous oxides in the Duluth Complex is being carried out by Westmont Mining on the Longnose Peridotite and adjacent Long Ear body in St. Louis County. Severson (1988) and Severson & Hauck (1990) represent the most recent studies of the structure of the Partridge River intrusion and the geology, geochemistry and stratigraphy of the Partridge River intrusion and related oxide ultramafic intrusions. This thesis represents the first description of the Longnose Peridotite.

Chapter 2

General and Field Geology

A. Regional Geology

The Duluth Complex is one of the largest stratiform basic intrusions in the world (Taylor, 1964), covering nearly 4050 square km (2500 square miles) in the form of an arcuate belt that extends from Duluth northeastward nearly 243 km (150 miles) to near Hovland, Minnesota on the North Shore of Lake Superior (Phinney, 1972). The Duluth Complex was intruded generally along a unconformity between the overlying 1.1 b.y. Keweenawan North Shore Volcanic Group (NSVG) and underlying igneous and metasedimentary rocks which range in age from Archean to lower Proterozoic (Figs. 1 and 2).

The stratigraphy of the Duluth Complex consists of two main units of Middle Proterozoic (1120 m.y. plus or minus 15 m.y.) age (Phinney, 1972):

1) an older, anorthositic-gabbroic portion which forms the upper part of the Complex, and 2) younger troctolitic and gabbroic rocks which compose the lower 2/3 of the Complex and underlie and intrude the upper anorthositic-gabbroic rocks (Phinney, 1972). Bonnichsen (1972) called the two units the anorthositic series and troctolitic series, respectively. Taylor (1964) had called the two units the anorthositic gabbro and the layered series. Both are composed of multiple intrusions (Taylor, 1964. Bonnichsen, 1972. Weiblen and Morey, 1980). Minor ferrogranodiorite and granophyre occur as late-stage intrusions, principally along the contact between the two units. Small ultramafic

EXPLANATION

Middle Proterozoic — Duluth Complex — Troctolitic Series

tpg Powerline gabbro of Bonnichsen, 1974

tpt Partridge River troctolite of Bonnichsen, 1974

tr Railroad troctolite of Bonnichsen, 1974

tg tap South Kawishiwi intrusion of Green et al., 1966
tt

- tap troctolite with less than 5% augite
- tt troctolite
- tg ferrogabbro of Bonnichsen, 1974

tu troctolitic and/or gabbroic rocks, undivided

Anorthositic Series

agu anorthositic gabbro, undivided

h hornfels inclusions, undivided

Lower Proterozoic

v Virginia Formation

if Biwabik Iron Formation

pq Poqegama Quartzite

Archean

grg Giants Range batholith

lv Lake Vermilion Formation eg Ely Greenstone

SYMBOLS

- —— fault, mapped
- — — — fault, inferred from topographic and aeromagnetic lineaments
- — — — contact, inferred
- ▭ map area

after Cooper, 1978

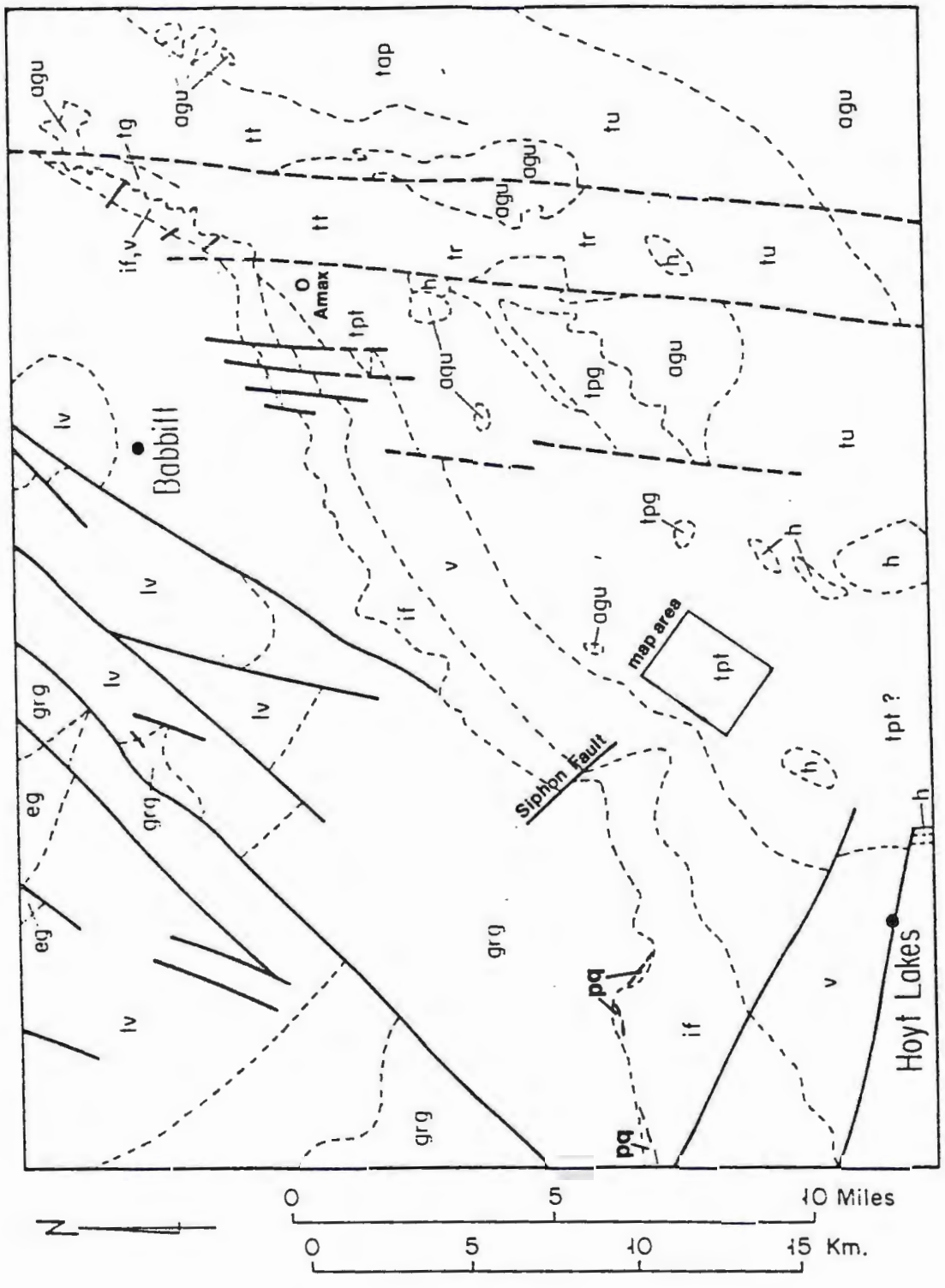

Fig. 2. General geology of the Hoyt Lakes - South Kawishiwi area. (After Cooper, 1978)

bodies consisting mainly of dunite, clinopyroxenite, and peridotite with associated titanomagnetite and Cu-Ni sulfides occur along the basal contact of the complex, within the troctolitic series (Bonnichsen, 1972; Wieblen, 1982). Ultramafic bodies include a 20 m wide dike of clinopyroxenite in the Dunka pit area located in the Babbitt 7.5 minute quadrangle, the Longnose Peridotite body and the adjacent Long Ear body, and the Water Hen intrusion (Fig. 1), which is discussed in chapter 6. The Long Ear body is composed largely of clinopyroxenite with titaniferous oxides and is located approximately 620 meters to the north of the Longnose Peridotite (see Plate 1).

Weiblen and Morey (1980) propose that the geometry of individual intrusions in the Hoyt-Lakes-Kawishiwi area is representative of the Duluth Complex as a whole. According to their interpretation, the geometry consists of a set of normal faults trending NNE and dipping steeply to the SE, and another set which offsets these and trend NW and are nearly vertical. They envision this pattern to represent an extensive half-graben system which formed in a rift-transform environment. Based on major element compositions, structure, and igneous textures, they propose a two-stage magmatic model. The first stage is characterized by extensive and efficient gravity segregation of olivine and clinopyroxene from a low-Al magma to produce the anorthositic series rocks and minor late-stage ultramafic (ilmenite wehrlite) and granophyric rocks. The second magmatic event was dominated by magmatic current flow of a high-Al magma to form the troctolitic series.

Green (1983), however, gives several lines of geological and geochemical evidence which contradict the above models, and suggests an alternative model of sequences of eruption and subsidence of plateau lavas (NSVG). The lavas were extruded via fissures and compositionally are high-Al olivine tholeiite. Great volumes of mafic intrusive rocks (Duluth Complex) were emplaced penecontemporaneously as large sills, intracrustal half-grabens, or other forms.

B. General Geology of the Hoyt Lakes-South Kawishiwi Area

The Longnose Peridotite deposit is located in what Bonnichsen (1972) informally calls the Partridge River troctolite (PRT)-- a basal intrusion of the troctolitic series in the Hoyt Lakes-Babbitt area (unit tpt, Fig. 2). The Duluth Complex in this region is underlain by the Archean Giants Range Granite and Lower Proterozoic Animikie Group, and subordinate Keweenawan basaltic lavas (Phinney, 1972). The general geology is shown in Fig. 2. The Giants Range Granite is nonconformably overlain by the Animikie group. The Animikie group consists of the Pokegama Quartzite, the Biwabik Iron Formation (BIF), and the Virginia Formation, in ascending stratigraphic order. The Biwabik Iron Formation conformably overlies the Pokegama Quartzite (Morey, 1972) and ranges in lithology from a bedded ferruginous chert to cherty siderite. The ferruginous chert contains 25-30% iron and is 61 to 229 m thick. The Virginia Formation, an interlayered argillite, argillaceous siltstone and greywacke, with lesser carbonate, chert and cherty siderite, conformably overlies the BIF (Morey, 1972) and forms the footwall rock to the Duluth Complex in the Hoyt Lakes area. Adjacent

to the Duluth Complex the Virginia Formation has been metamorphosed to a fine-grained feldspar-bearing cordierite-biotite hornfels (Phinney, 1972). Inclusions of hornfels, most measuring less than 30 m in diameter, occur in the base of the Complex. In the Hoyt Lakes area the contact between the Duluth Complex and Virginia Formation is not exposed, but is interpreted to lie within an area 1.6 to 2.5 km wide parallel to the two formations from geophysical surveys (Bonnichsen, 1972).

In the Babbitt-Hoyt Lakes area, the lower part of the Duluth Complex consists of the basal troctolitic series and the lowest part of the anorthositic series. Contacts are predominantly inferred as outcrop is sparse (Plate 1). The troctolitic series is divided into two main intrusions: the South Kawishiwi intrusion (Green et al., 1966; Phinney, 1969) and the Partridge River troctolite (PRT) (Bonnichsen 1972). Tyson (1979) divided the South Kawishiwi intrusion into a basal zone and an upper zone. The basal zone is composed of troctolite, gabbro, norite, picrite, dunite, and augite troctolite. The augite troctolite locally contains xenoliths of anorthosite and hornfelsed basalt. The upper zone consists of troctolite. The PRT is composed of troctolite to anorthositic troctolite and augite troctolite with subordinate picrite (Cooper, 1978; Tyson, 1979). The PRT forms an elongate body trending N45^{o} E based on map boundaries and foliation trends. It is in apparent fault contact to the east with the Railroad troctolite (see Fig. 2) and part of the South Kawishiwi intrusion and to the SE with anorthositic series rocks which are inferred from

aeromagnetic data (Cooper, 1978).

The PRT can be distinguished from the South Kawishiwi intrusion by its different stratigraphic sequence, weaker foliation of plagioclase (Tyson, 1979), greater olivine and intercumulus mineral content, and possibly better cyclic layering (Cooper, 1978). Although the intrusions have different strata and textures according to available reports, their differences may in part be due to different people mapping the area (Phinney, pers. comm., 1984). The PRT has been less extensively studied due to poorer outcrop exposure than the South Kawishiwi intrusion (Tyson, 1979). Cooper (1978) gives a succinct summary of the petrography of the rock types in the area.

Tyson (1979) studied 14 drill cores, 4 in detail, in the Partridge River troctolite in the Babbitt-Hoyt Lakes area. Five major units were distinguished in the basal 1800' some of which could be correlated among drill cores. These are unit A, unit B, unit C, the main unit, and unit P, in ascending order. Unit A occurs at the base and lies directly above the Virginia Formation. It consists of a picrite which grades into augite troctolite of unit B. Unit B in turn grades into olivine gabbro and augite troctolite of unit C. The top is termed the main unit and consists of troctolites, gabbro, troctolitic anorthosite, and inclusions of anorthosite series rocks which are unit P.

C. Structure in the Hoyt Lakes-South Kawishiwi Area

Mancuso and Dolence (1970) suggest that the structure of the Duluth Complex in the Babbitt area was controlled by pre-existing conditions. These conditions include the nature of the contact between the BIF and Virginia Formation, a pre-intrusion anticline in the

Animikie rocks at the base of the Complex, and adjustments of the floor of the Complex by pre- and post-Duluth Complex faulting. In their view the troctolite was intruded as irregular sheets from the SE along the BIF and Virginia Formation contact, rafting pre-Complex rocks with it. The strike of the basal contact is to the northeast, and the dip is variable to the southeast. The dip is approximately 10^{o} SE in the Dunka River area to as much as 60^{o} SE near Hoyt Lakes (Bonnichsen, 1972), with an average dip of about 30^{o} (Holst et al., 1986).

Cooper (1978) has done the most extensive structural analysis in the Hoyt Lakes-South Kawishiwi area and has extrapolated his results to the Duluth Complex as a whole. Few faults had been previously mapped or inferred (Weiblen & Morey, 1980). Using as evidence aeromagnetic and topographic lineament data, field mapping of joints and fault zones, and joint analyses, Cooper (1978) drew faults if three requirements were met: 1) the presence of a topographic lineament; 2) the presence of an aeromagnetic gradient; and 3) the presence of disrupted structural elements. He found two distinct fault sets, one trending N45-55^{o} W and the other N10-30^{o} E. Each fault set is accompanied by a parallel joint set. In the PRT and South Kawishiwi intrusions aeromagnetic lineaments and topographic lineaments coincide at N39^{o} E and probably reflect the original trend of individual or separate intrusions or layering in the Duluth Complex. A strong N51^{o} E trend in aeromagnetic lineaments in the South Kawishiwi intrusion and in topographic lineaments in the PRT corresponds with the overall trend of glacial lateral moraines in much of the area, suggesting that the

moraines may be controlled in part by bedrock geology (Cooper, 1978). Based on Cooper's study, Weiblen and Morey (1980) suggest that the area may consist of two distinct structural blocks with a northeast trend of faults east of the International Nickel Company property and a northwest-trending fault in the vicinity of the Minnamax prospect east of Babbitt (Figs. 1 and 2). The Siphon Fault (Figs. 1 and 2) roughly coincides with the lithologic boundary between the Giants Range Granite and Animikie group. The fault is downthrown to the east with an estimated vertical offset in excess of 400' (122m). Evidence is not sufficient to continue the fault into the Duluth Complex (Holst et al., 1986).

The Keweenawan history of the Hoyt Lakes-South Kawishiwi area starts with mid-continental rifting and the beginning of fissure eruption of the NSVG. This was soon followed by multiple intrusion of the anorthositic series and ended with intrusion of the troctolitic series. The first intrusion of the troctolitic series in this area is the South Kawishiwi intrusion (Figs. 1 and 2). The PRT was intruded soon after the South Kawishiwi intrusion based on the lack of chilled margins in the PRT. The PRT contains inclusions thought to be Virginia Formation and NSVG. The Powerline Gabbro (tpg, Fig. 2) was the last major intrusion in the area. A new stress system, producing the faults and joints mentioned above, developed after intrusion of the troctolitic series and cessation of rifting (Cooper, 1978).

D. Pleistocene Geology

The morphology of the Hoyt Lakes-South Kawishiwi area is largely the result of the advance of the Rainy Lobe ice (Fig. 3) during the

late-Wisconsin glaciation at 20,000-10,000 B.P. (Stark, 1977). The first advance of the Rainy Lobe is termed the St. Croix phase, which moved SW from Canada depositing the Toimi drumlin field just north of Duluth. This lobe later merged with the Superior Lobe as it climbed out of the Lake Superior Basin and flowed southwestward to produce the St. Croix moraine (not shown on Fig. 3). Wright (1972) determined the glacial trend was N45^{o} E from the long axis of the Toimi drumlins. After retreat of both lobes, the Rainy Lobe readvanced into the Hoyt Lakes area. This advance is termed the Automba phase by Wright (1972). The Superior Lobe stopped to the east of the area, and the Rainy Lobe, upon retreat, deposited a series of three moraines trending east-west.

Stark (1977) divided the area between moraines based on morphology (Fig. 3); a northern ice-scoured plain with thin and patchy till, a central area bordered on the south by the first moraine and to the north by the third moraine, and a southern area dominated by the Toimi Drumlin field. The map area for the present study lies between the first and second moraines.

Evidence of glaciation in the field area include: 1) northeast-trending ridges with or without outcrop; 2) concentration of outcrop on the west and southwest of topographic highs indicating ice movement from the NE; 3) 1-5 m high roche moutonnees; and 4) glacial erratics, in decreasing proportions, of BIF and Giants Range Granite, greenstone, and biotite schist. The map area has a total relief of 14 m, and is dominated by spruce bog. Longnose Creek cuts through the area and joins the Partridge River to the east. The Longnose Peridotite lies beneath a semicircular spruce bog.

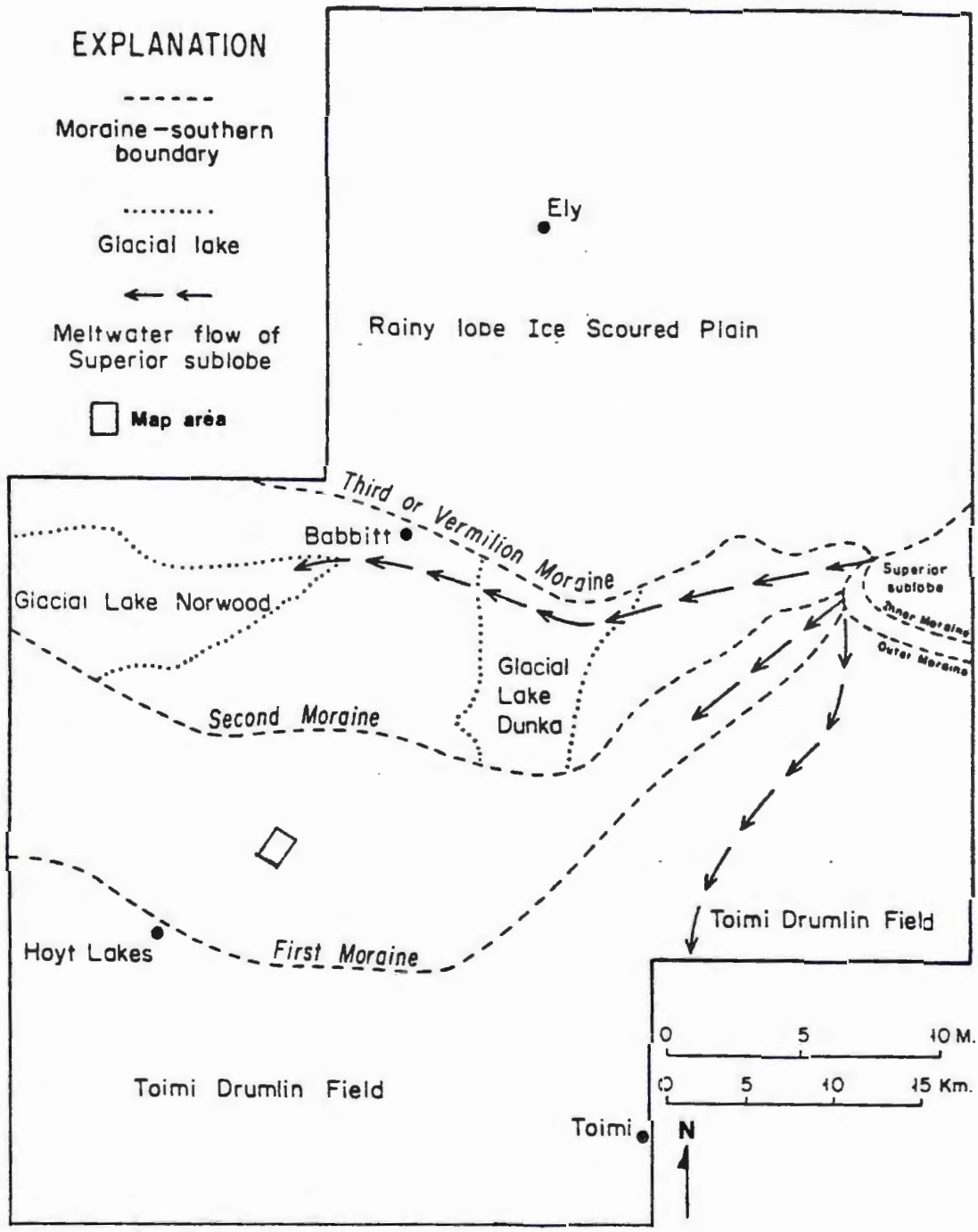

Fig. 3. Pleistocene morphology of the Hoyt Lakes-South Kawishiwi area.
(After Stark, 1977)

E. Detailed Geology

Nine major lithologic units were distinguished in the area using Phinney's (1972) classification (Fig. 4). Age relationships between units are obscure due to discontinuous outcrop exposure and lack of, or scarcity of contacts. Relative ages are based on the attitude of foliation, on the premise that foliation is the result of cumulus and/or magmatic flow processes in the troctolitic series rocks and that the Law of Superposition is applicable. The general foliation trend of the rocks in the field area is NE with a dip to the SE. The rock units are therefore inferred to young eastward, and will be described accordingly. Point counts, estimated mineral modes in thin section and outcrop, and anorthite content of plagioclase (as determined with the Michel - Levy method) are listed in Appendix 1. The geologic map is in the back jacket as Plate 1.

Unit 1. Troctolitic anorthosite to anorthositic troctolite

Unit 1 is exposed in the west-central part of the map area along Forest Road 117 (Plate 1). In outcrop it is a light to medium grey, coarse - to medium-grained, equigranular, fresh troctolite. It weathers to a medium grey with positive relief of brownish-orange olivine and dull black augite. The unit is distinguished by its coarse grain size and lack of foliation. Plagioclase occurs as subhedral laths 0.3-1.5 cm in length and composes 75-87% of the rock. Fresh amber brown olivine forms amoeboid grains 0.2 - 1 cm across. On a local scale (1 - 2 meters) the olivine mode varies between 10 - 25%. Augite occurs sporadically as individually ophitic grains up to 1 cm across as several grains up to 4 cm across which may host oxide "clots"

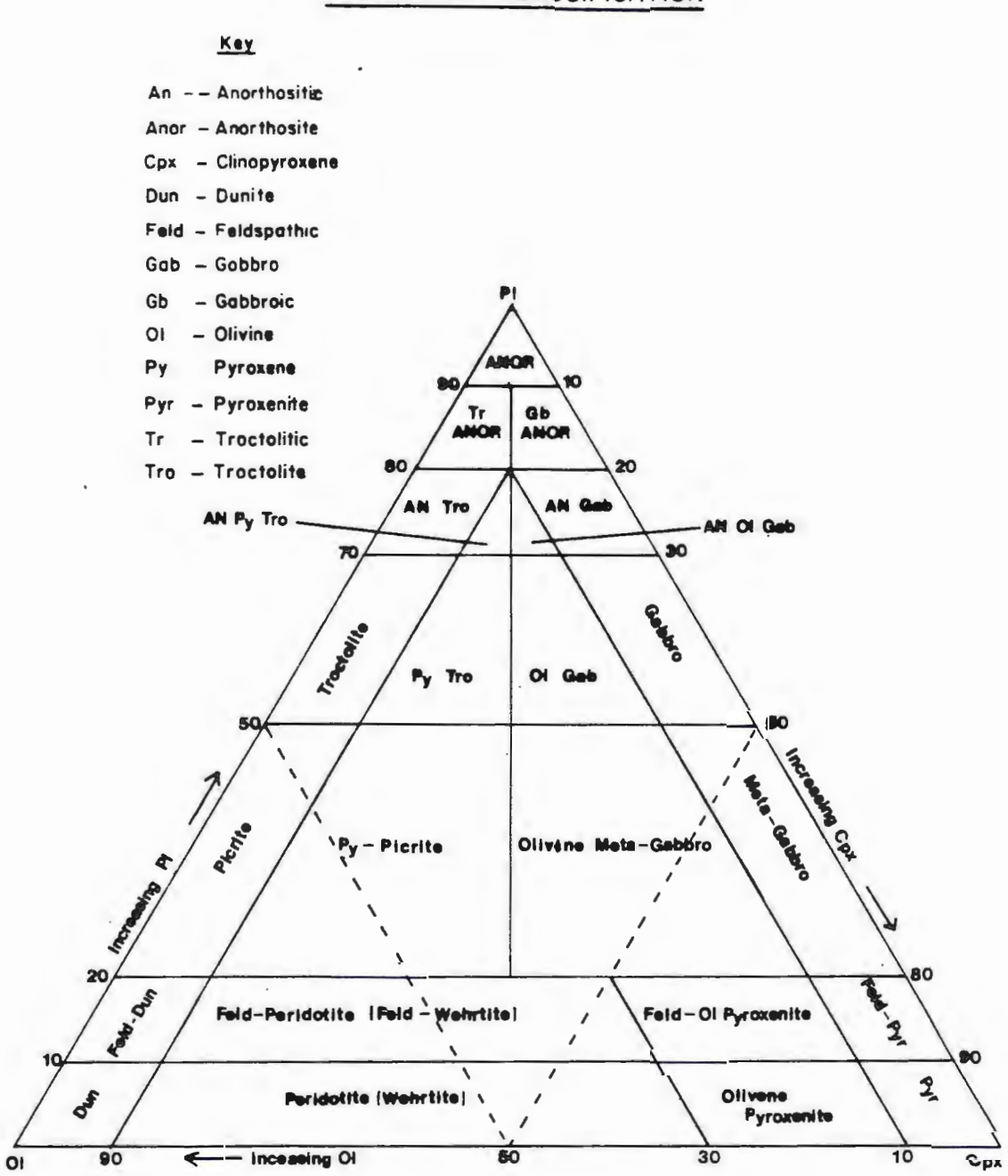

Fig. 4. Rock classification.
(From Phinney, 1972)

up to 1 cm across. Augite averages less than 4% of the rock. Oxides (less than 2% of the rock) generally occur as medium-sized, anhedral, disseminated grains. Reddish-brown botite is a minor constituent and is associated with oxides.

In thin section, plagioclase (An_{69}) forms fresh tabular laths with patchy zonation and minor (less than 1%) opaque rods. Olivine occurs as suboval to anhedral grains 0.5-6 mm across and in places subpoikilitically encloses plagioclase. Augite is interstitial and shows exsolution of orthopyroxene and irregular zones with 5-30% opaque rods. Orthoyroxene forms partial rims on olivine and as symplectite with oxides. The oxides ilmenite and magnetite occur as 0.1-1 mm interstitial grains and uncommonly magnetite occurs as euhedra in plagioclase.

Unit 2a. Augite-biotite bearing troctolitic anorthosite to olivine-bearing anorthositic gabbro

Unit 2a is exposed in the western half of the map area and appears to be the host rock for the Longnose Peridotite, although no contacts were observed. The unit forms ridges trending predominantly NE. Foliation strikes predominantly northeasterly and dips gently to the southeast (see Fig. 16). In outcrop it is medium- to dark-grey, medium-grained, ophitic, foliated, and modally heterogeneous. The unit weathers to medium grey with positive relief of brownish-orange altered olivine, dull black augite, and metallic black oxides. The unit is distinguished by its grain size, ubiquitous biotite, and variance in mineral modes over meters to tens of meters within and/or between outcrops (see Appendix 1). Jointing is commonly parallel to foliation

planes (Fig. 5). No modal layering of minerals was observed in outcrops.

Plagioclase occurs as subparallel 2-5 mm long, subhedral tabular grains and composes between 68% and 83% of the rock. It rarely occurs as isolated, tabular phenocrysts up to 4 cm in length. Olivine forms amber-brown 1-3 mm subequant to rounded grains and makes up 12% to 20% of the rock. Augite (5-12%) occurs as 0.5-1 cm wide ophitic grains and in 4-16 cm "pods" of small grains (Fig. 6). Oxides (trace to 2%) form anhedral to platy grains 1-6 mm with conchoidal fracture. Red biotite forms 1-3 mm flakes in close association with oxides.

In thin section, plagioclase forms fresh, 1-6 mm subhedral tabular grains which are subparallel. Grains typically exhibit overgrowth, patchy zonation and opaque rods. Four samples were collected in one outcrop from the base (14490-36A) to the top (14491) of the outcrop at 0.3-1 m intervals. Anorthite content of the plagioclase decreases going up from An_{73} to An_{66} (Appendix 1). Subhedral olivine and euhedra of magnetite may be included. Olivine forms 0.2-3 mm oval to subhedral prisms and lesser anhedral grains. Augite content varies between samples, but everywhere occurs as ophitic to subpoikilitic grains up to 7 mm and invariably contains 5-20% opaque rods parallel to two cleavages. Examination of one polished section identified these rods as ilmenite. Orthopyroxene forms rims on olivine (Fig. 7) or as symplectite with oxides. No orthopyroxene was observed in augite. Deep red-brown pleochroic biotite forms minor flakes with cleavage perpendicular to olivine, augite, and oxides.

Fig. 5. Plagioclase foliation planes parallel to joint sets in unit 2a.

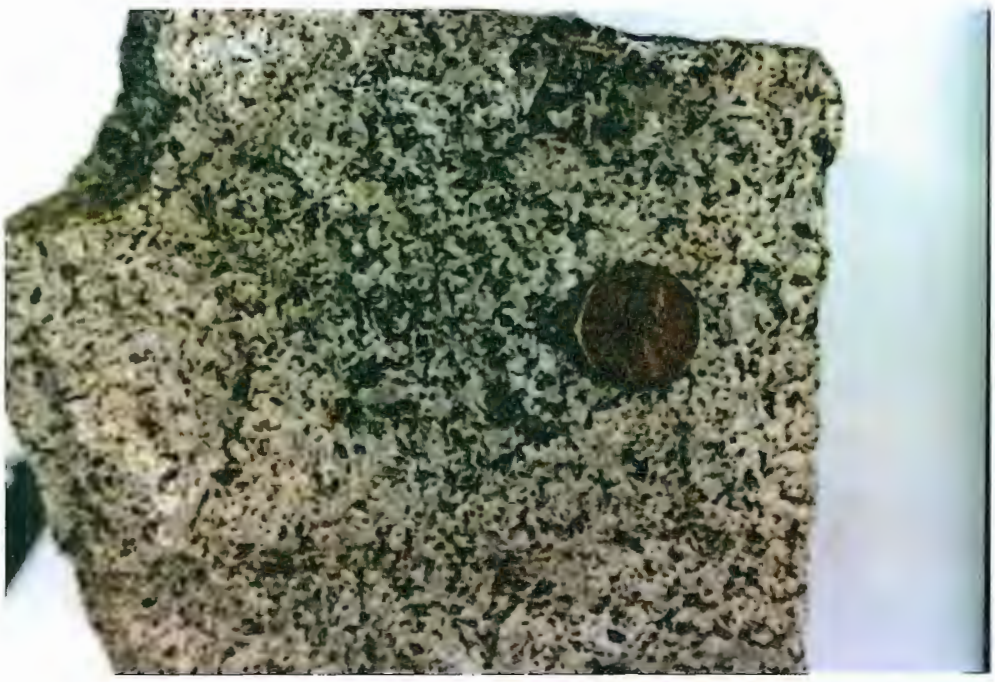

Fig. 6. Ophitic augite (black) in unit 2a.

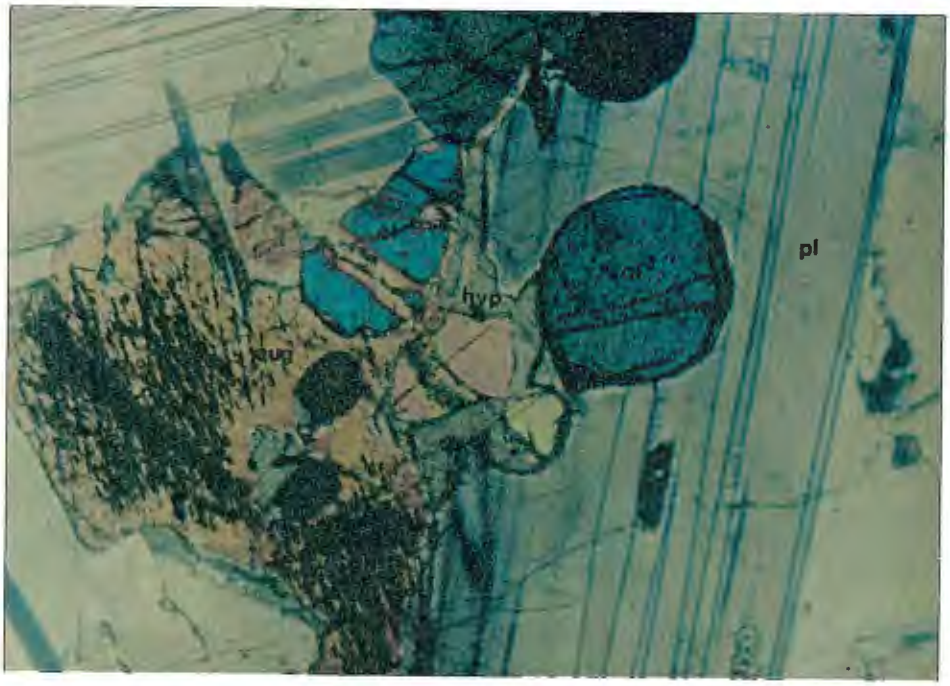

Fig. 7. Olivine-plagioclase cumulate with interstitial augite (orange) with exsolved opaques in unit 2a. Orthopyroxene (light grey) partially rims olivine (round grains). (Field of view approx. 5 mm across)

Unit 2b. Pyroxene troctolite hornfels

Unit 2b occurs in three outcrops in the eastern part of the map area; two are xenoliths in sharp, exposed contact with Unit 7, and the third is an isolated out crop in apparent contact with Unit 7. Unit 2b is distinguished by its fine-grained granoblastic texture and burgundy weathered color.

In thin section, the hornfels displays a fine-grained granoblastic texture of plagioclase, olivine, and augite with trace amount of oxides. In one instance olivine occurs as an oikocryst in the hornfels.

Unit 3. Olivine oikocryst- bearing anorthosite

Unit 3 crops out in two locations, in the northwest where it forms a 5 m high by 18 m long ridge and is in apparent contact with Unit 2a, and as a small isolated outcrop in the southern part of the map area. This unit is readily distinguished by 0.5-1.5 cm diameter round olivine oikocrysts which weather brown with positive relief (Fig. 8) and a high plagioclase content (approx. 92%). The rock is medium grey, medium-grained, and well-foliated. Plagioclase forms well aligned, 1-5 mm long tabular grains which in some cases reach 1 cm in length. Olivine oikocrysts include 50% plagioclase. Augite and oxide constitute less than 3% of the rock and are interstitial to plagioclase.

Examination of one thin section shows fresh, well-aligned subhedral tabular to equant grains of plagioclase (An_{75}) 0.5-4 mm long with minor intercumulus overgrowth. No opaque rods were seen. Olivine forms an oikocryst 1.5 cm across and also occurs as minor interstital blebs. Orthopyroxene forms partial rims on olivine. Oxides occur interstitially as 0.2 mm grains in trace amounts.

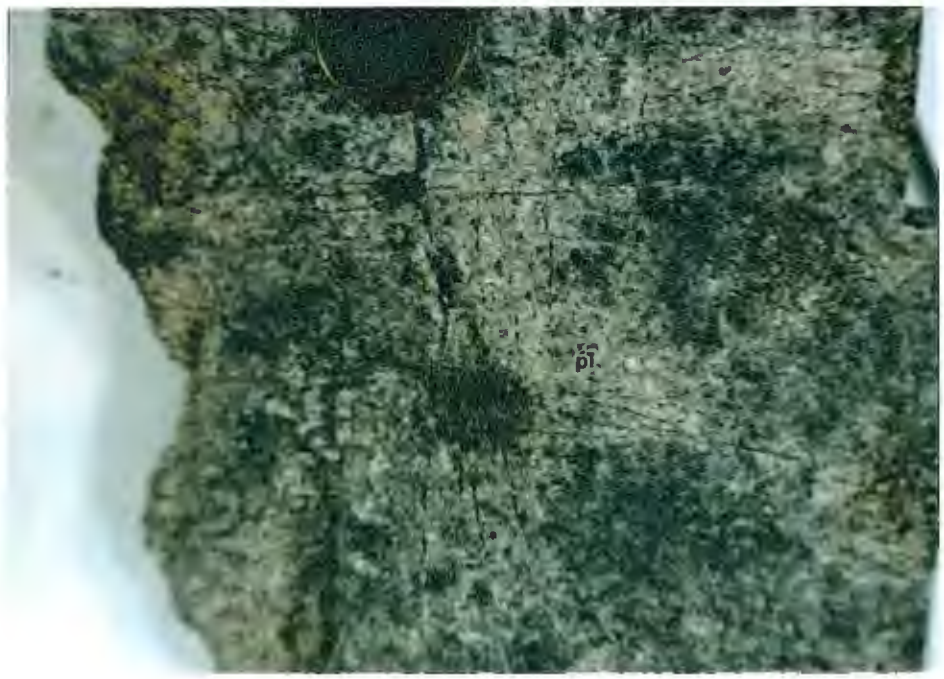

Fig. 8. Olivine oikocrysts in unit 3.

Unit 4. Anorthositic pyroxene troctolite

Unit 4 occurs in the northwest portion of the map area in apparent contact with Unit 2a. It forms three fairly continuous and sub-parallel ridges trending roughly N30^{o} E. In outcrop it is medium grey to greenish-grey, coarse- to medium-grained, and poorly foliated to massive. It is distinguished from other units by its green hue, higher augite content and very poor foliation. It weathers to a dark grey with positive relief of brownish-orange olivine and black augite (Fig 9). The unit is inhomogeneous, with olivine and augite contents varying within and/or between outcrops by as much as 12% each. It thus grades into Unit 2a.

Plagioclase forms predominantly 3-6 mm anhedral grains and more rarely subhedral tabular grains and composes 65-80% of the rock. Olivine forms irregular 2-6 mm olive-green to amber-brown grains, and makes up 10-20% of the rock. Augite (5-15%) is vitreous black when fresh, and forms ophitic and poikilitic grains up to 2 cm across enclosing olivine. Oxides are a minor constituent and are interstitial to plagioclase and/or rim augite as 1-3 mm grains. Unit 4 is the only unit in which chalcopyrite was observed. It occurs as irregular 1-2 mm grains bordering augite and/or plagioclase. It makes up less than 0.1% of the rock.

In thin section it is very similiar to samples from Unit 2a, both in texture and mineral modes except that plagioclase is poorly aligned. The anorthite content of plagioclase is 70%.

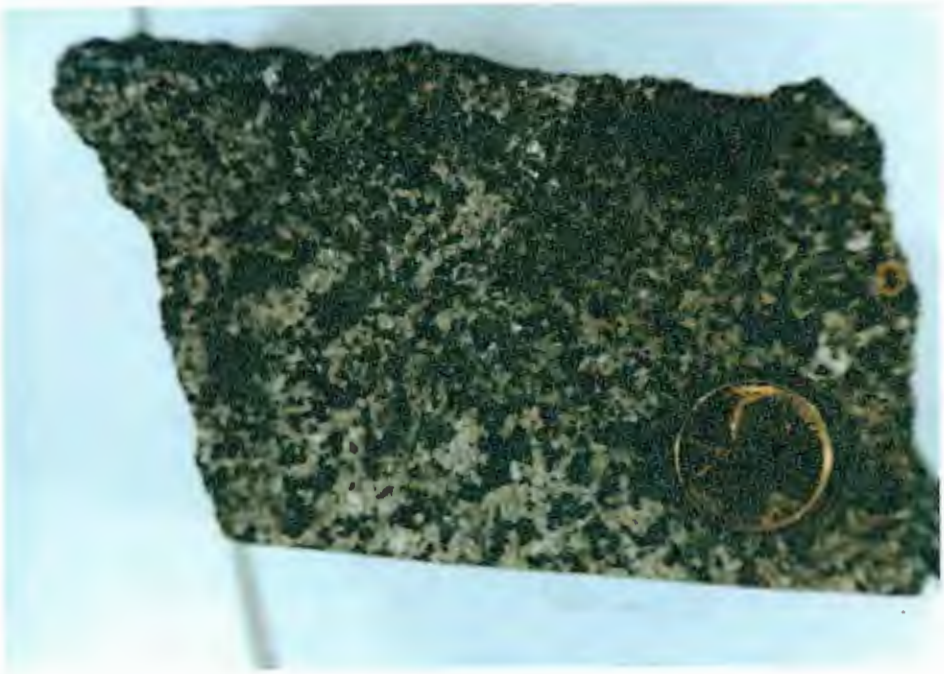

Fig. 9. Anorthositic pyroxene troctolite with ophitic augite (black) in unit 4.

Unit 5. Augite-bearing troctolitic anorthosite

Unit 5 forms 1-2 m high ledges in the southern portion of the map area. It is in apparent contact with units 2a and 3. It is light to medium grey, medium-grained, and ophitic, weathering to a light grey. It is distinguished from unit 2a by its generally higher plagioclase content (80-90%), although locally these units are indistinguishable. Plagioclase is light to medium grey and typically forms 2-5 mm anhedral grains with grains locally 1.5 cm in length. Tabular, subparallel grains were observed in only one outcrop. Olivine composes about 8% of the rock. It is light amber brown to dark olive green, and forms 1-3 mm irregular to round grains. Augite (5%) forms 0.2-1 cm ophitic grains, but locally may be as large as 5 cm in diameter. Oxides are metallic black and interstitial to the silicates. Red biotite makes up less than 2% of the rock.

Unit 6. Fine - grained troctolite

Unit 6 forms a 60 m long by 3 m high ridge in the northeast part of the map area between units 2a and 7. No contacts were observed. It is light grey in fresh hand sample, weathering to a dark grey with positive relief of brownish-orange olivine. It is easily distinguished by its fine grain size, excellent plagioclase and olivine foliation, and paucity of augite and oxides. Plagioclase and olivine compose approximately 69% and 30% of the rock, respectively, with augite and oxides composing less than 1%.

In thin section, plagioclase (An 71) occurs as 0.5-1 mm long tabular grains with minor intercumulus overgrowth. It is highly fractured. Olivine forms euhedral to subhedral prismatic grains 0.2-1

mm in length which lie in the plane of plagioclase foliation. Olivine is rimmed by iddingsite with or without magnetite or it is rimmed by a thick vestige of augite with opaque rods. Ilmenite forms plates 0.1-0.2 mm in length.

Unit 7. Troctolite to anorthositic troctolite

Unit 7 covers the eastern half of the map area. Outcrops occur predominantly on the western side of hills and form 2-5 m high ridges. It is a medium grey, coarse- to medium-grained, foliated troctolite. The unit varies locally in olivine within and/or between outcrops. The unit weathers dark grey with positive relief of brownish-orange olivine, dull black augite, and metallic black oxides. It is distinguished from other units by: 1) generally coarser olivine and greater modal olivine (approx. 25%); 2) local olivine oikocrysts and anorthosite xenoliths (o and x in Plate 1 and 3) a paucity of augite (Fig. 10). The unit varies locally in olivine content within and/or between outcrops (see Appx. 1). Plagioclase foliation planes are atypical.

Plagioclase forms poor to well-aligned tabular grains 1-10 mm, averaging 3-5 mm in length. Olivine is light to dark amber-brown to dark olive-green when fresh. Grains are typically isolated, 2-3 mm across and round, although it also forms in 4-15 mm sinuous aggregates of grains or as clusters up to 3 cm across. In the oikocryst - bearing variety, olivine includes plagioclase and/or augite in 1-4 cm subrounded to amoeboid grains (Fig. 11). Only one of the olivine textures is prevalent in any one outcrop. Augite is vitreous black when fresh. It is a minor constituent of the unit, forming individual

Fig. 10. Typical troctolite of unit 7. Olivine-orange, plagioclase-grey, augite-black

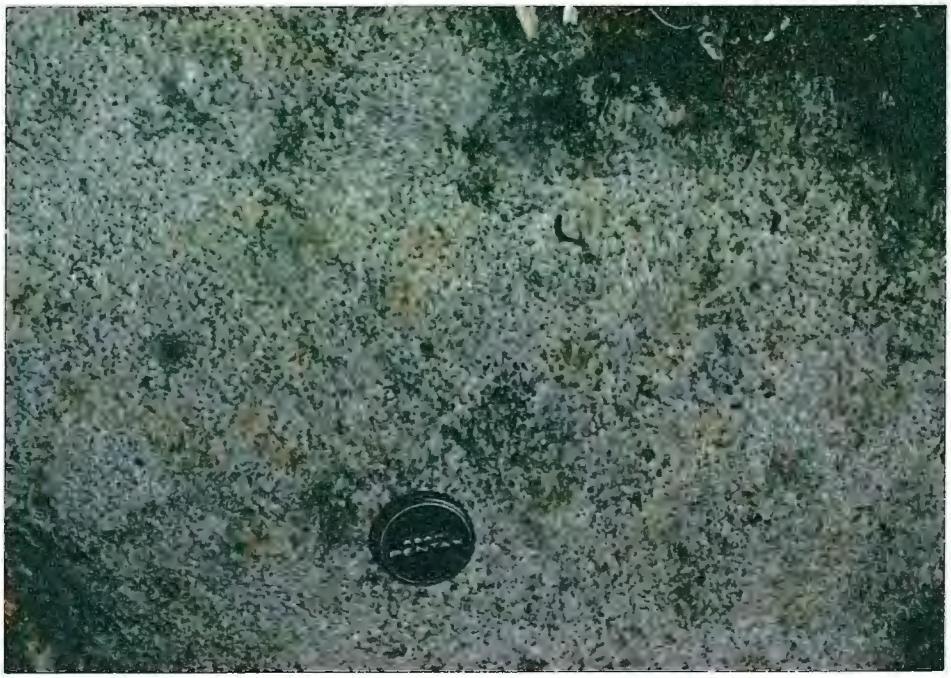

Fig. 11. Olivine-oikocryst variety of unit 7. Olivine-orange, plagioclase-grey, augite-black.

ophitic to sub-poikilitic grains 0.5-2 cm across, and is enriched in local areas 0.3-1 m square where the rock type is olivine gabbro. Oxides occur interstitially to the other silicates as disseminated grains or less commonly as an amalgamation of several grains to form a "clump" of irregular shape 0.5-2 cm across.

The anorthositic xenoliths are in sharp contact with the troctolite. No alteration or foliation differences of plagioclase are evident at the contact between the two rock types. The xenoliths are 10-60 cm in diameter and consist of 90% medium-grained plagioclase and 10% olivine oikocrysts 5-10 cm across of irregular shape (Fig. 12).

Eight thin sections of this unit were examined. Six were selectd from different stratigraphic horizons within a typical outcrop of troctolite to check for mineral mode and textural variations, starting with sample 14496-52A at the base and going sequentially up to 14496-52F at 0.2-1 m intervals. The other two were selected to represent the unit (14494) and to check the anorthosite xenolith-troctolite contact (14503).

The stratigraphic sequence of samples showed no major mineral mode or textural variation from 52A-52E. Sample 52F, however, shows a decrease in modal plagioclase and An content from approximately An 71% to An 68% with concomitant increase in olivine and augite (see Appendix 1). The textures of the bottom five samples are very similiar to units 2 and 4. Plagioclase invariably occurs as fresh, well-aligned, subhedral tabular laths 1-7 mm in length with opaque rods and displays both patchy and minor oscillatory zonation. Olivine forms oval to subhedral prismatic grains 0.2-3 mm long with the prismatic grains

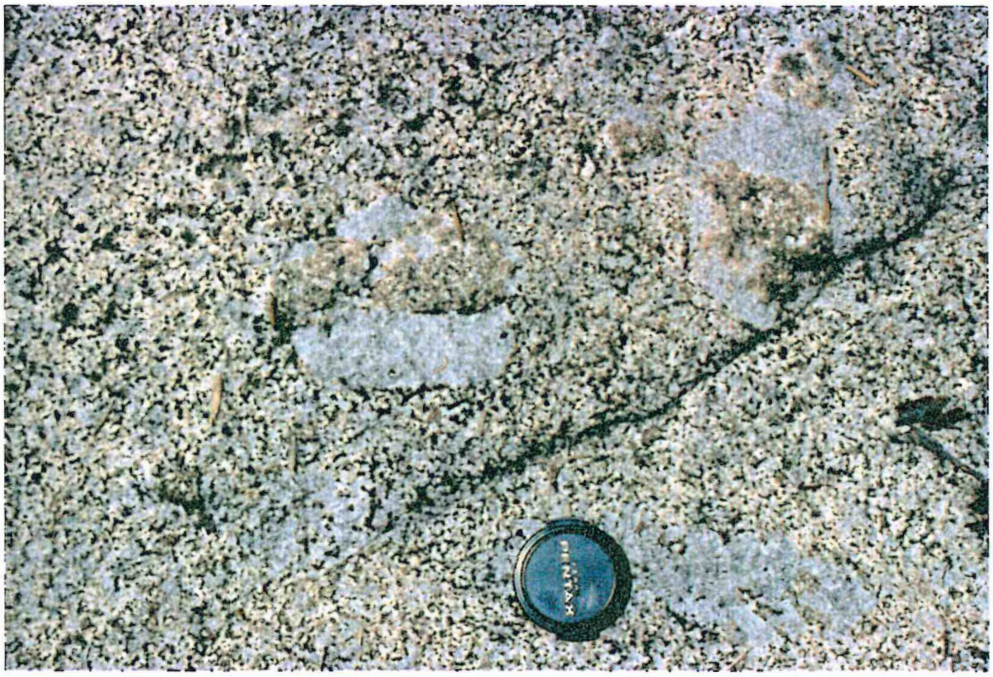

Fig. 12. Anorthosite xenolith in troctolite of unit 7. Olivine-orange, augite/oxides-black, plagioclase-grey.

parallel to plagioclase foliation and minor interstitial blebs in samples 52A-52E. In sample 52F olivine also occurs as oikocrysts 1.5 cm across (Fig. 13). Augite occurs interstitially to plagioclase, olivine, and magnetite in samples 52A-C, but is ophitic and subpoikilitic in samples 52D-F. Orthopyroxene occurs in minor amounts as mantles on olivine and augite and as symplectite with plagioclase. Red-brown pleochroic biotite forms flakes perpendicular to magnetite.

Unit 8. Dunite to picrite

Unit 8 occurs in the northwest part of the map area as a 1.2 m high by 6 m long by 1 m wide outcrop. The outcrop trends N72^{o} W. It is dark greenish-black where fresh, and weathers to a dark rusty black. Olivine composes 40-95% of the rock, and forms suboval grains 1-5 mm in length. Plagioclase is medium grey, forms 1-4 mm anhedral grains, and varies from 5-60% over a distance of centimeters. A medium-grained troctolite to picrite outcrops approximately 1 m above the dunite and is traceable for 30 m along strike. No contact was visible. This rock type also occurs along the same strike of the dunite 35 m to the west where it is stratigraphically 3 m below the dunite.

In thin section the rock is an olivine cumulate with interstitial plagioclase. Olivine forms oval to prismatic grains 0.5-4 mm long. It is highly fractured and altered to iddingsite, serpentine, and magnetite. It typically hosts round inclusions of plagioclase 0.1-0.3 mm across and subhedral to oval grains of oxides. Plagioclase (An_{69}) forms anhedral grains 0.3-1 mm across with patchy zonation and moderate alteration to clay, sericite, and epidote. Several grains commonly occur together in the intercumulus space of olivine grains.

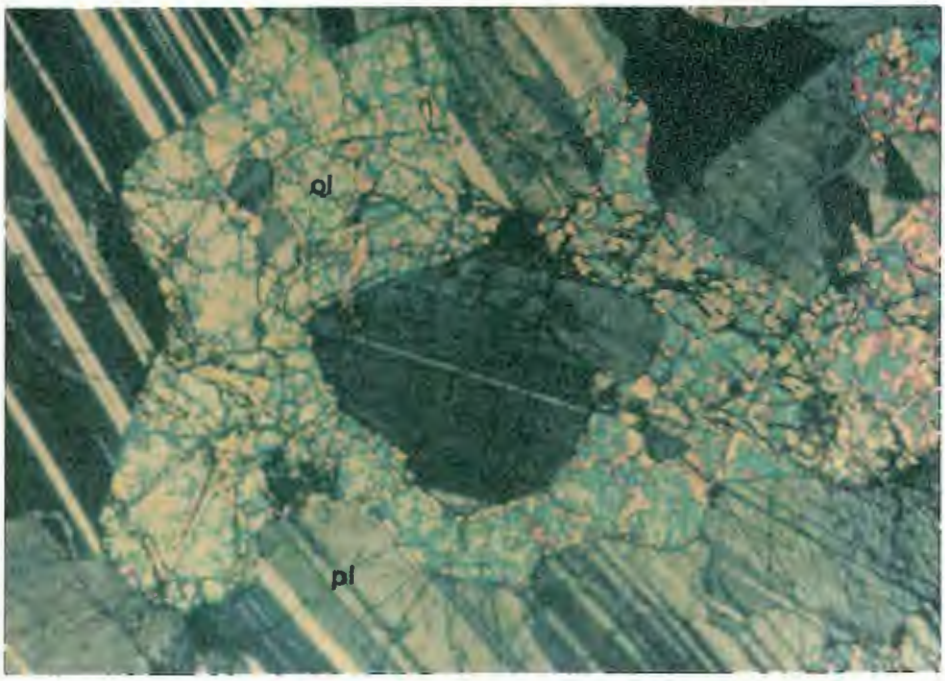

Fig. 13. Olivine oikocryst in unit 7. Olivine forms a single grain (colored) enclosing plagioclase (grey). (Field of view approx. 5 mm across, crossed polars)

Pegmatitic augite

Pegmatitic augite occurs within some outcrops in units 2a and 4 and on a very local scale in unit 7. The pegmatite ranges in size and shape from irregular "pods" 0.3 m to 1 m across, to ridges 15 m long by 1 m high, to veins 6 cm wide by 3 m long. This unit is characterized as a medium-grained olivine gabbro immediately adjacent to the pegmatitic augite with olivine composing less than 10% of the rock and coarse- to pegmatitic augite. Augite forms poikilitic grains with olivine and oxide inclusions near its edges and ophitic grains 0.5-20 cm across. Cleavage faces are typically discernable. Oxides composed predominantly of magnetite and lesser ilmenite are common and form 0.5-2 cm clusters made up of medium-size grains. Oxides compose 2-7% of the pegmatite.

Thin sections were made of the olivine gabbro. Plagioclase forms randomly oriented, equant to anhedral grains 2-6 mm across which are moderately fractured and altered to sericite-chlorite-epidote. Albite twins are locally bent approximately 10^{o} Olivine forms equant grains (0.5-1 mm) and anhedral grains 2-4 mm across. It is altered to iddingsite along fractures or to iddingsite-serpentine pseudomorphs. Augite is light pink in color. It forms poikilitic grains enclosing olivine and ophitic grains up to 1 cm across. Inclusions of opaque rods compose from 1-10% of the grain. Hornblende alteration is typical (5-10%). Ilmenite and magnetite form grains 0.2-3 mm across which are interstitial or included in plagioclase and/or augite.

Actinolite veins

Actinolite veins were seen in all units except units 1, 3, 2b and 4. They appear as black to greenish-black ridges 0.3-1 cm high and 0.5-2 cm wide on the outcrop surface (Fig. 14). They commonly occur in groups of 2 to 6 within 1-5 m. One vein system is traceable along strike for 122 m at N65^{o} W, dipping 84^{o} NE.

In thin section the veins are composed of fibrous actinolite in an olivine-bearing anorthosite. Both plagioclase and olivine form subhedral grains which are progressively more altered within 1.5 cm of the vein. Plagioclase (An_{71}) is altered to sericite, clay and chlorite. Olivine is altered to iddingsite, talc, chlorite, and magnetite. Actinolite forms patches of 0.5-3 mm long blades and fibers perpendicular to the length of the vein.

F. Structure

The structure in the map area is based on the attitudes of plagioclase foliation, actinolite veins, and joints. The poles to 45 plagioclase foliation planes, eleven actinolite veins and 18 joints are plotted and contoured on the southern hemisphere of a Schmidt equal area net (Figs. 15, 17, and 18 respectively).

Plagioclase foliation shows attitudes with two centers of concentration at N8^{o} E, 22^{o} SE, and N46^{o} W, 35^{o} NE (Fig. 15). This contrasts with that reported by Cooper (1978) for foliation in the Partridge River troctolite who gives a center of concentration at N45^{o} E, 11^{o} SE (Fig. 16). Cooper (1978) noted five joint sets in the PRT (Fig. 17). They are 1) N51^{o} W, vertical; 2) N42^{o} W, vertical; 3) N14^{o} W, vertical; 4) N11^{o} E, 85^{o} NW, and 5) N44^{o} E, 42^{o} NW. The second set

Fig. 14. Actinolite veins in unit 2a.

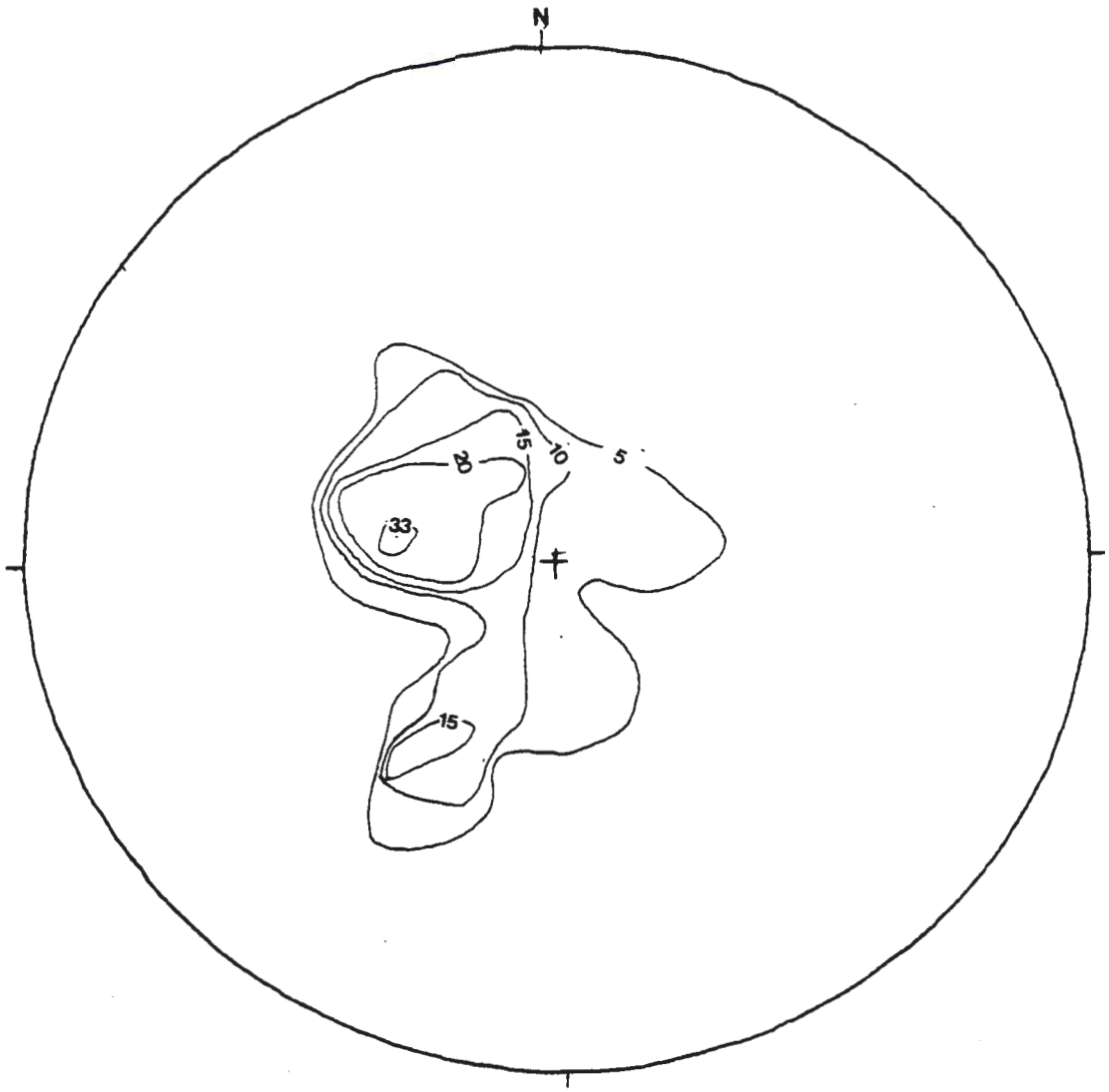

Fig. 15. Equal area projection on the southern hemisphere of 45 poles to plagioclase foliation in the study area. Contours are percentage of data per 1% area. Centers of concentration are approximately N 8° E, 22° SE, N 46° W, 35° NE.

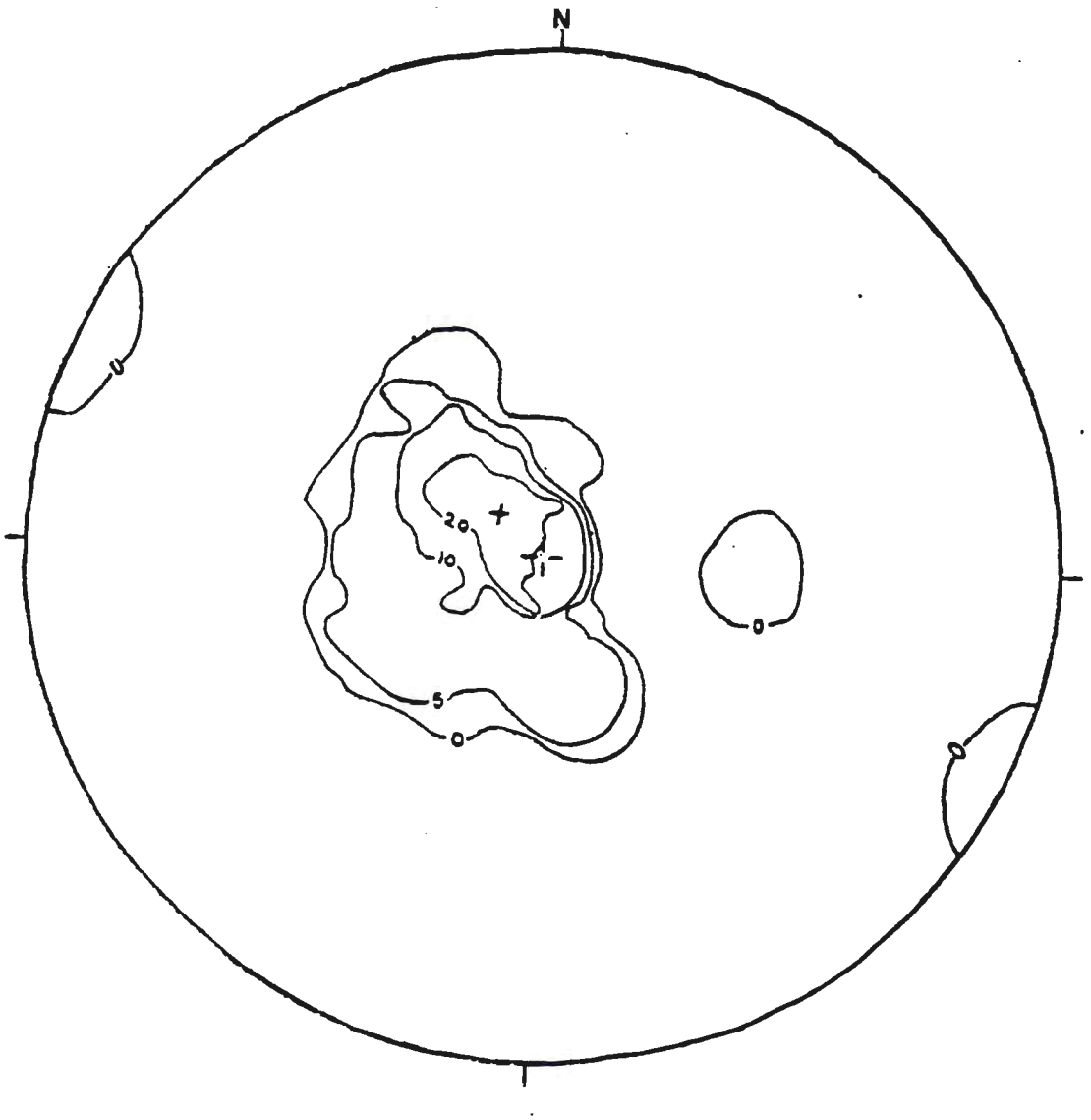

Fig. 16. Equal area projection on the southern hemisphere of 34 poles to foliation in the Partridge River troctolite. Contours are percentage of data per 1% area. Center of concentration is approximately N 45° E, 11° SE.
(From Cooper, 1978)

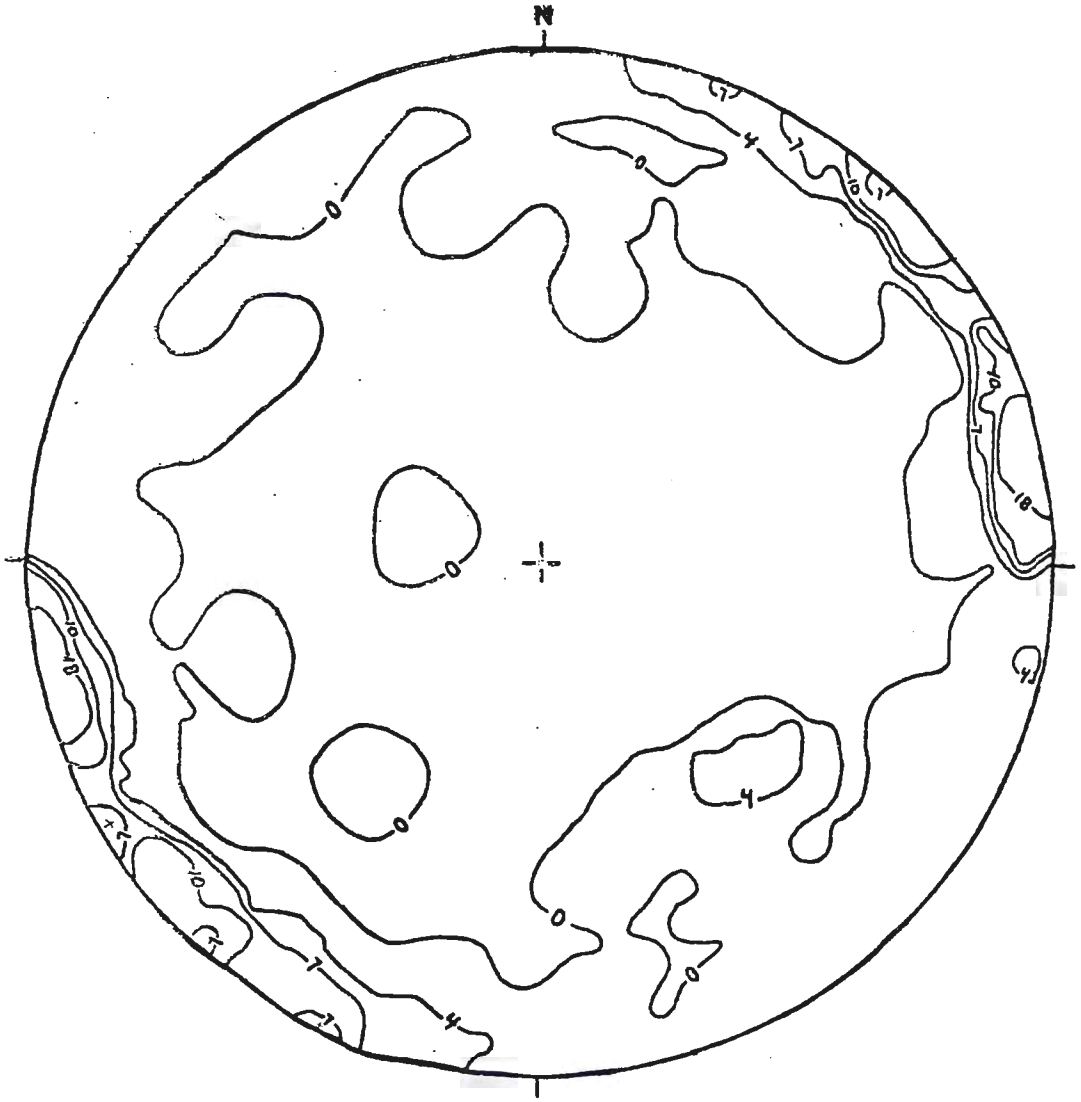

Fig. 17. Equal area projection on the southern hemisphere of 333 poles to joint planes in the Partridge River troctolite. Contours are percentage of data per 1% area. Joint sets include: N 51° W, vertical; N 42° W, vertical; N 14° W, vertical; N 11° E, 85° NW; and N 44° E, 42° NW. (From Cooper, 1978)

is characterized by pyroxene fillings and/or stringers which are in close agreement with the actinolite veins which show a center of concentration at N62° W, 79° NE (Fig. 18). The first and fourth joint sets appear to be late joint sets as the joints are commonly sheared. The joints in the present study area show concentrations at N88° E, 80° NW and N22° E, 80° SE (Fig. 19). The latter concentration is similiar to Cooper's (1978) number four joint set.

G. Interpretation

All rock units are plagioclase-olivine mesocumulates with the exception of the oikocryst variety of unit 7 and unit 3 which are plagioclase mesocumulates, and unit 8 which is an olivine mesocumulate. In the plagioclase-olivine mesocumulates both plagioclase and olivine typically display overgrowth resulting in subhedral to anhedral grains and augite and oxides invariably occur as intercumulus minerals. Plagioclase typically shows patchy zonation. The rare occurrence of oscillatory zonation in plagioclase can be explained by reaction between the grains and the intercumulus or cumulate liquid which is changing composition. The oxide euhedra near the edge of plagioclase in some units can be explained by crystallization contemporaneously with plagioclase overgrowth. Orthopyroxene rims on olivine can form from olivine reacting with intercumulus and cumulate liquid (with Ca, Na, and Al) that is changing composition. Unit 3 and the oikocryst variety of unit 7 are plagioclase mesocumulates with olivine forming as rare nuclei. These nuclei could have formed along with or after plagioclase. In the olivine adcumulate of unit 8, olivine is the

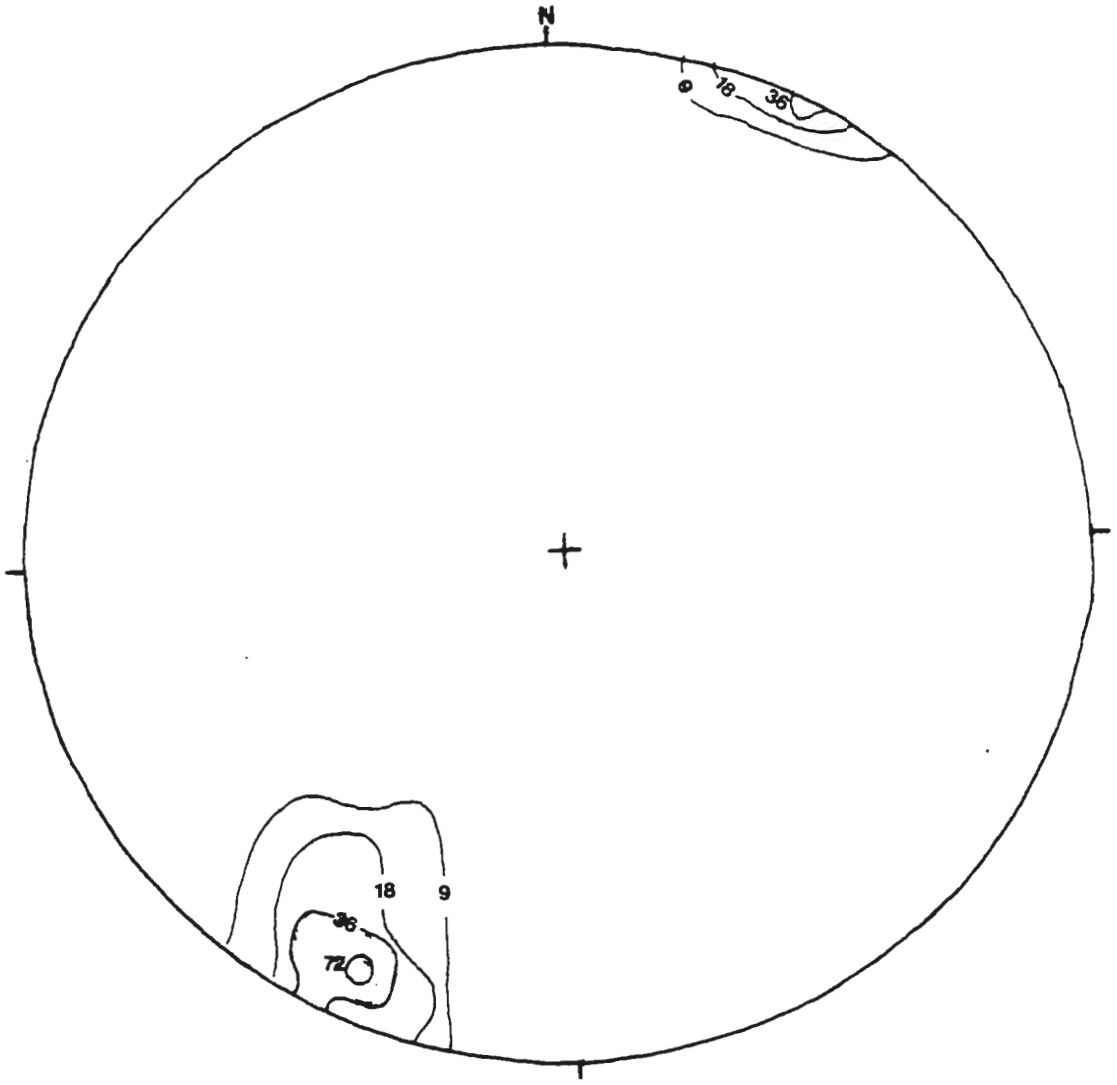

Fig. 18. Equal area projection on the southern hemisphere of 11 poles to actinolite veins in the study area. Contours are percentage of data per 1% area. Center of concentration is approximately N 62° W, 80° NE.

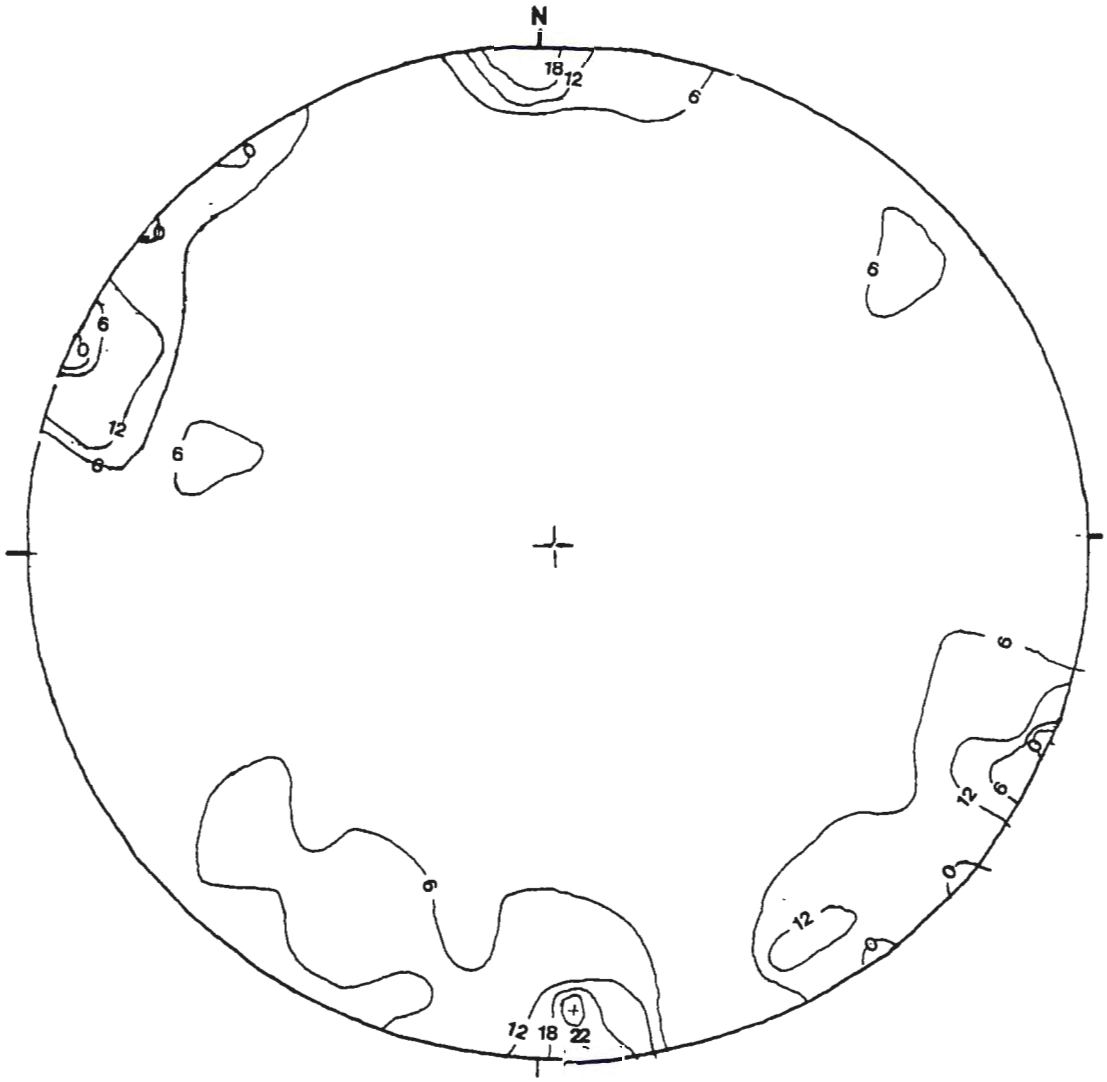

Fig. 19. Equal area projection on the southern hemisphere of 18 poles to joints in the study area. Contours are percentage of data per 1% area. Centers of concentration are at approximately N 88° E, 80° NW; and N 22° E, vertical.

cumulate phase followed by plagioclase which fills the pore space. Biotite is a deuteric alteration product in all cases.

The general crystallization sequence of cumulus plagioclase-olivine followed by augite and oxides corresponds to that reported by Bonnichsen (1972) and Tyson (1979) for other troctolites in the Hoyt Lakes-Babbitt area.

Examination of one polished section of the black rods in augite identified the rods as ilmenite. The rods in plagioclase were to small to positively identify. Both Bonnichsen (1972) and Tyson (1979) attributed these to ilmenite exsolution in plagioclase and exsolution of ilmenite and rutile in augite for troctolites in the Hoyt Lakes-Babbitt area. Mainwaring (1975), however, concluded from microprobe study of augite in host troctolite rocks of the Water Hen intrusion that the rods were hematite.

Plagioclase ranges in composition from An_{66} to An_{75} as determined by the Michel-Levy method. This is within the range of Tyson's (1979) findings of An_{51} to An_{75} in the core and An_{53} to An_{66} in the mantle of plagioclase from troctolitic rocks determined by measuring the index of refraction on (001) by the dispersion method (Morse, 1968).

The origin of the anorthosite-rich zones within unit 7 is not clear. Anorthositic series blocks ranging from meters to several kilometers are not uncommon in the troctolite series (Bonnichsen 1972). Bonnichsen (1972) noted that in the troctolites southeast of Birch Lake, anorthosite, troctolitic anorthosite, and gabbroic anorthosite bodies ranging from inches to hundreds of feet across occur within troctolitic rocks. Although some are clearly inclusions, some might be

cogenetic plagioclase-rich segregations.

No field evidence was encountered, either textural or structural, that defines the relationship between the Duluth Complex and the Longnose Peridotite in the field area. However, the Longnose Peridotite is here thought to be intruding the Partridge River troctolite based on drill core evidence from the Longnose Peridotite (see chapter 3). A zone of weakness, such as a fault, would serve as a conduit for intrusion. However, no lineament was observed either on air photos of the area or on the topographic map to support this hypothesis.

Chapter 3

Petrography of the Longnose Peridotite

A. Introduction

This chapter presents a petrographic description of the rocks studied from four drill cores penetrating the Longnose Peridotite. The format of the chapter consists of detailed description of the rock types followed by interpretation. Study of the Longnose Peridotite entailed hand sample desription of four drill cores BA-6, LN-2, LN-6, and LN-5, followed by examination of 89 thin sections (TS), 59 polished sections (P), and 14 polished thin sections (PT). The logs of the four drill holes studied are depicted in Plate 2. Each drill hole log shows, from left to right, 1) the rock types, 2) the mineral modes of the four major primary silicates olivine, augite, plagioclase, and hornblende, and the oxides, 3) the ratio of ilmenite to titanomagnetite based on hand sample description and polished section, and 4) the plot of weight percent TiO_2 (supplied by Nicor Mineral Ventures). Alteration is not shown. Drill hole BA-6 was drilled at 90^{o} the other three were drilled at 45 plus or minus 3^{o} to the northwest along the geophysical grid line (see Fig. 45). Measurements are reported in feet as that is how the drill core was initially marked, followed by metric in brackets.

Appendix 2 contains the mineral modes, type of texture, crystallizaiton sequence, and deformation features for all thin sections. All sections were chosen to represent rock types and/or

textures, or to confirm mineralogy. They do not therefore always represent the mineral mode of the unit.

B. Rock types

Seven rock types (units) were delineated using Phinney's classification (1972) shown in Fig. 4, with some modification to include the oxide content because most rock types contain greater than 10% oxides. The oxide classification is as follows:

Rock name	%Oxide
oxide + rock name	10-50%
semi-massive + rock name + oxide rock	51-80%
massive oxide rock	81-100%

The seven silicate - dominated rock types are: 1) troctolitic anorthosite with minor pegmatitic olivine gabbro and picrite (country rock), 2) oxide clinopyroxenite and oxide olivine clinopyroxenite, 3) oxide peridotite (wehrlite) to oxide feldspathic peridotite with local hornblende gabbro, 4) oxide dunite, 5) massive oxide rock, 6) oxide feldspathic dunite, and 7) picrite. For ease of discussion, clinopyroxenite is herein shortened to pyroxenite. Semi-massive oxide rock and massive oxide rock zones are discussed in chapter 4. Each rock type is discussed in the order of a) distribution and b) petrography.

Terminology used in the discussion of textures follows that of Wager, Brown and Wadsworth, (1960) (Appendix 3). Special oxide textures follow that of Buddington and Lindsley (1964) and of Haggerty (1976); these textures are explained in the introduction of chapter 4, page 73. Grain size follows that used in describing igneous rocks:

fine-grained, less than 1 mm; medium-grained, 1-5 mm; coarse-grained, 5 mm to 1 cm; and pegmatitic, greater than 1 cm.

1. Troctolitic anorthosite/pegmatitic olivine gabbro/picrite

a. Distribution

These units are interpreted to be xenoliths of the footwall rock. Troctolitic anorthosite is the most abundant in volumne in this unit, and contains local zones of pegmatitic olivine gabbro and picrite. Troctolitic anorthosite commonly forms the cap rock and footwall rock in drill core (see chapter 5, Figs. 45 and 46), and occurs as inclusions 117′ (37 m) to 1′ (0.3 m) thick. All contacts between the troctolitic anorthosite and Longnose Peridotite rocks are sharp (less than 2 cm).

b. Petrography

In drill core, troctolitic anorthosite is similar to the field unit 2a. It is medium-grained, commonly fresh, and is fairly homogenous in texture and mineral modes, but may vary to a pyroxene troctolitic anorthosite. Plagioclase (85%) forms tabular to irregular grains 1-7 mm in length, averaging 4 mm in length. Foliation is rarely evident. Olivine (10-15%) is olive-green in color, and forms irregular to suboval grains 0.5-5 mm in diameter. Augite (0-5%) is light brown and forms subophitic grains. Oxides constitute between 1-3% of the rock and are interstitial. Deep brown colored hornblende and gold-brown colored biotite are minor alteration products of augite.

Pegmatitic olivine gabbro occurs as separate zones within troctolitic anorthosite with which it is in sharp contact. The

pegmatite is composed of irregularly shaped grains of plagioclase, olivine, and augite which measure up to 1.5 cm, 1 cm, and 4 cm across, respectively. Ilmenite occurs as irregular grains 2-4 mm across. Alteration is localized to olivine and augite. Olivine is altered to dark green serpentine and orange-red iddingsite (up to 80%), and augite is altered to hornblende and red biotite.

Gabbro to picrite is mottled green and white in drill core, and is medium-grained, non-foliated, and homogeneous.

All three rock types are moderately fractured. These fractures are filled with white talc or dark green serpentine and rust red hematite. Fractures occur about 1-2 per foot and dip 30-65° to the core axis. Extreme alteration zones occur in LN-6 on either side of the troctolitic anorthosite between 245′ (74.7 m) and 362′ (110 m). The bottom alteration zone is 11′ thick and contains pegmatitic plagioclase, hornblende, ilmenite, and biotite in a dark green, fine-grained matrix. Biotite forms euhedral books the width of the core axis and in one case forms a grain 8 cm in length which is bent into a recumbent fold. An ilmenite grain 3 cm long and 0.5 cm wide is curved around plagioclase. The top alteration zone is 3′ thick, and consists of a very fine-grained to aphanitic medium green chloritic rock with euhedral, light yellow apatite and black tourmaline up to 7 mm long and 3 mm in diameter, and coarse-grained calcite pods.

2. Oxide clinopyroxenite

a. Distribution

Pyroxenite occurs at the top of BA-6 between 18 and 81′ (5.5 and 24.7 m), and at the base of LN-2 from 452 to 557′ (137.7 and

169.8 m). The base of the pyroxenite in both holes is in sharp contact with troctolitic anorthosite country rock. The pyroxenite is altered to actinolite/tremolite, chlorite, and talc at the contact. The contact of the pyroxenite with oxide peridotite in LN-2 is gradational over 3′ (0.9 m) and is marked by an olivine horizon at 430′ (Plate 2).

b. Petrograpy

In drill core, the pyroxenite is light brown to pinkish brown, medium- to coarse-grained (4 mm-10 mm across) with local pegmatitic zones 1-2 m wide. It is composed of 75-90% augite, 0-10% olivine, less than 2% plagioclase, and 10-15% oxides. Augite occurs as inequigranular, anhedral grains with mutually sinuous grain boundaries.

In the pegmatitic zones augite reaches 10 cm across. It poikilitically encloses olivine and oxides. Olivine forms disseminated light green-brown oval grains 0.5-7 mm across and locally forms stringers 1-2′ thick composed of 25-40% olivine. Plagioclase occurs very sporadically as isolated, anhedral grains 1-3 cm across which are in sharp contact with augite. Both augite and oxides may be included on the edge of plagioclase, or plagioclase may subpoikilitically enclose augite. Oxides occur as anhedral to subequant grains (0.25-4 mm) in a disseminated or broken net-textured fashion and occasionally in irregular shaped clusters 1-4 cm across in which case they compose up to 80% of the rock.

In thin section, augite is pinkish in color. It typically forms anhedral grains with mutually sinuous boundaries, and poikilitically encloses olivine and oxides or embays the oxides. Euhedral augite 2-4 mm long with a blue pleochroic chlorite rim occurs in only one sample

(13036) and is associated with calcite alteration. Particular features of augite include: 1) intergrowths of augite grains (Fig. 20) or of augite and oxides; 2) single twins; 3) wavy extinction; and 4) exsolved ilmenite platelets (Fig. 21) as identified by SEM methods (see chapter 6). These platelets are .05-.2 mm long, are parallel to prismatic cleavage, and occur in local concentrations. They also vary in concentration between drill holes; in LN-2 they are minor where as in LN-6 they are abundant (compare Figs. 20 and 21). A thin rim of hornblende may surround the platelets.

Olivine occurs as 0.3-7 mm grains of oval to stubby shape which are included in augite or concentrated in small clusters or strings of 2-10 grains on the edges of augite. The olivine is moderately fractured and filled with serpentine, secondary magnetite, and hematite. The fractures terminate at the olivine edge. Plagioclase occurs only in one thin section (13037) as a 7 mm anhedral grain slightly altered to a brown clay.

The ratio of ilmenite to titanomagnetite varies greatly between polished sections (Appendix 3). Both oxides occur predominantly as interstitial grains of fine- to medium-grain size and anhedral to subequant shape. Both may occur as inclusions in augite or interstitially where they embay augite. Some ilmenite contains inclusions of augite or titanomagnetite. Ilmenite typically displays (white) hematite along {0001} planes with grey spinel disks (see Fig. 35). Titanomagnetite has ilmenite lamellae parallel to {111} planes and grey spinel rods and blebs parallel to {100} (Haggerty, 1976 a).

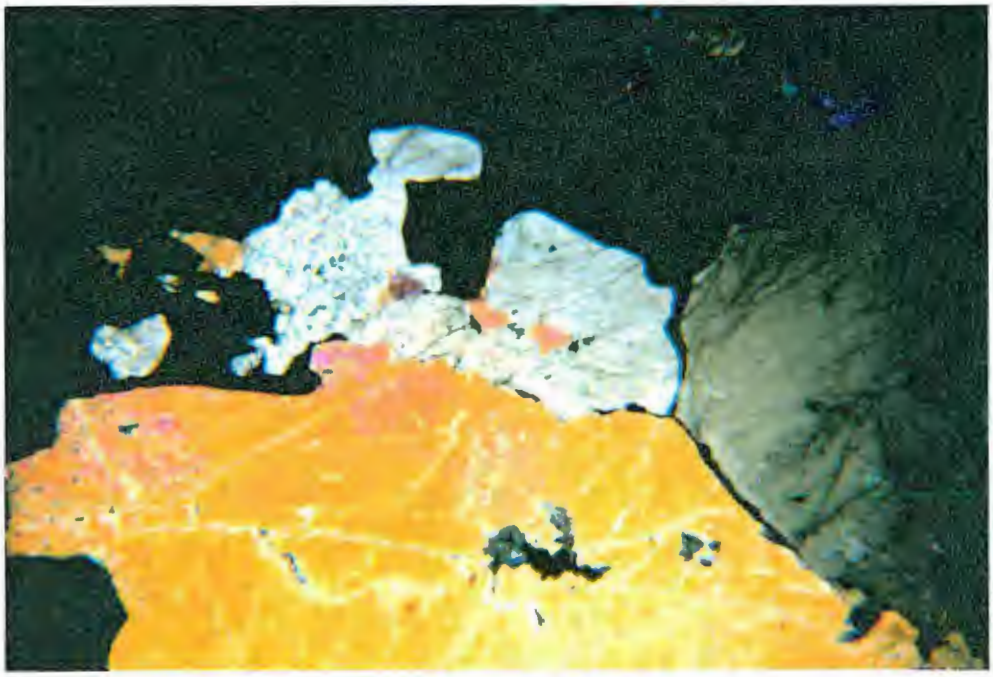

Fig. 20. Intergrown augite grains (yellow and grey) in oxide clinopyroxenite; LN-2, 507.5'. (Field of view approx. 2 mm across, crossed polars)

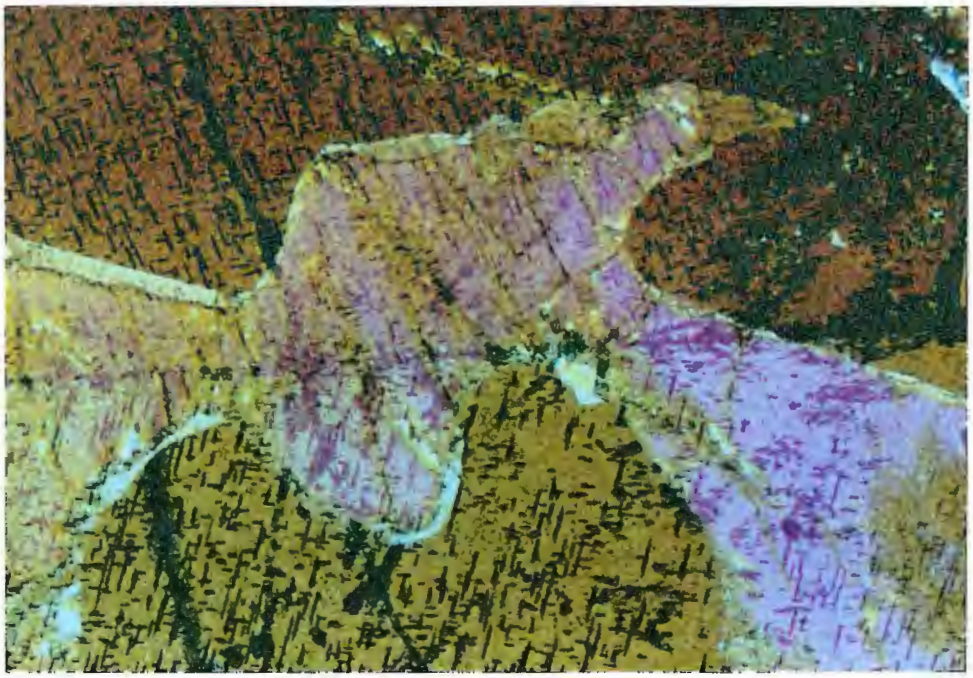

Fig. 21. Augite with exsolved ilmenite platelets in semi-massive oxide clinopyroxenite; LN-6, 494.7'. (Field of view approx. 2 mm across, crossed polars)

Alteration of augite varies between 5-60%. The major alteration minerals include hornblende, chlorite and talc. Minor alteration minerals include biotite and carbonate. Sphene occurs in trace amounts. Hornblende displays deep red-brown pleochroism. It typically forms epitaxial replacement near the center of augite, or as partial rims on oxides. Fractures in augite may continue through the adjacent oxides which give them a "moth-eaten" appearance. Recrystallized augite appears within 0.5 cm or adjacent to carbonate alteration as anhedral grains 0.1-2 mm across which form clusters within augite grains or between larger grains. Biotite displays deep red pleochroism. It forms a partial rim on augite when it is in contact with plagioclase.

Chalcopyrite occurs only in trace amounts near alteration of augite and rarely along the border of ilmenite. A trace of bornite was seen in one polished section (p 13037). It is purple and occurs as irregular blebs or flames in chalcopyrite.

3. Oxide Peridotite (wehrlite)

a. Distribution

Oxide peridotite contains approximately 55-75% olivine, 10-20% pyroxene, 5-15% plagioclase, and 10-25% oxides. The peridotite occurs above the pyroxenite in LN-2, in the lower third of LN-6, and sporadically throughout LN-5. It is a very inhomogenous rock, with sporadic zones centimeters to meters wide of feldspathic peridotite and feldspathic dunite. Both upper and lower contacts of peridotite are gradational over (0.7'-1.5' meters).

b. Petrography

In drill core, the peridotite is mottled brownish-olive green in color and hypidiomorphic and inequigranular in texture. It consists of medium-grained granular olivine and oxides which are subpoikilitically to pokilitically enclosed by coarse-grained (5 mm-5 cm), anhedral, augite. Augite is light brown and altered 10-50% to a medium blue-green. Plagioclase is light-cream, and occurs as medium size grains which subpoikilitically enclose subequant grains of olivine and oxides or as sporadically distributed coarse grains up to 3 cm across. Oxides form a broken net-texture, with sporadic stringers centimeters to 0.75 m thick which contain up to 100% oxides.

In thin section, olivine is the only cumulate phase. It is bimodal in grain size and texture, forming oval to stubby grains 0.5-1.5 mm in length which are poikilitically enclosed by augite and oxides; and larger, anhedral grains (2-7 mm across) which are embayed by oxides and occasionally intergrown with augite (Fig. 22). Both textures are present in the same thin section. Banded undulatory extinction is common in the large olivine grains (Fig. 23). Serpentine and secondary magnetite occur in thin veinlets replacing olivine, and terminate at the grains edge. Augite is pink, and forms anhedral grains (4 mm-1 cm across) which invariably contain exsolved opaque (ilmenite) plates occupying {100} and {001} parting planes (Irvine, 1974). The rods are absent near the grain edges. The larger grains vary in texture from poikilitic, enclosing smaller, subhedral olivine and oxide grains, to non-poikilitic. Plagioclase forms two distinct grain sizes; a) interstitial grains 2-5 mm in diameter which

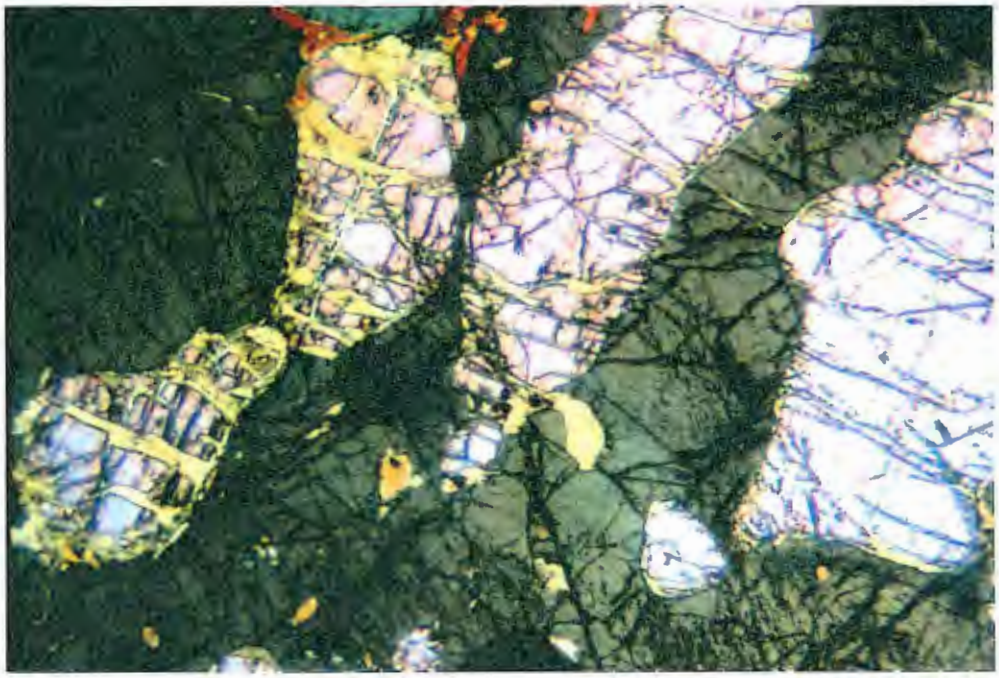

Fig. 22. Intergrown olivine (purple) and augite (brown) in oxide peridotite; LN-6, 464.1'. (Field of view approx. 5 mm across, crossed polars)

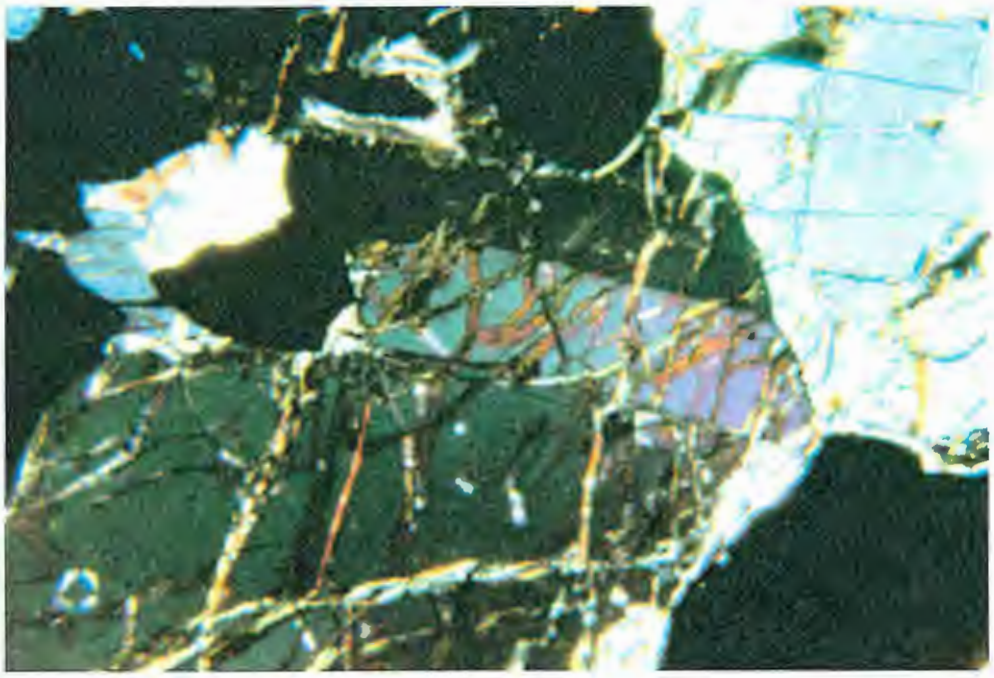

Fig. 23. Undulose banded zonation in olivine; LN-6, 524.5'. (Field of view approx. 2 mm across, crossed polars)

occasionally are intergrown with augite, and b) coarse grains (up to 1.5 cm) which host subequant grains of ilmenite (Fig. 24) and subpoikilitically enclose olivine, augite, and oxides along its outer edges. In one instance (ts 13104) plagioclase forms 0.2 mm round blebs in the center of olivine and a large plagioclase grain hosts about 20 anhedral small plagioclase grains, each aout 0.2 mm in diameter. Both grain sizes display undulose to patchy extinction with flared albite twins bent 5-10^{o} Plagioclase is unevenly altered from 10-80% to a fine mat of sericite and dark brown clay, or to epidote, chlorite and carbonate. Next to augite, plagioclase typically displays a rim of chlorite and epidote, and in one case (ts 13032) it is successively rimmed by red pleochroic biotite and red-brown pleochroic hornblende. Hornblende is a minor constituent of peridotite, occuring predominantly as an alteration product of augite and rarely as a primary phase in which it subpoikilitically encloses olivine and oxides (ts 13096). Hornblende displays oscillatory zonation with a deep red-brown pleochroic core and a light green-tan pleochroic rim. It is altered to plates of dark green chlorite (ts 13054).

Ilmenite is the dominant oxide and forms interstitial anhedral to subequant grains or granular-mosaic texture composed of fine- to medium-sized subequant grains with polygonal outline and triple-point junctions. Titanomagnetite is interstitial. Ilmenite varies in color from distinctly pinkish-brown with distinct pleochroism in LN-2 and LN-6, to nearly the same white color of titanomagentite with weak pleochroism in LN-5. Spinel-hematite bands occur along the {0001} plane. Ilmenite trellis and spinel rods are typical of titanomagnetite

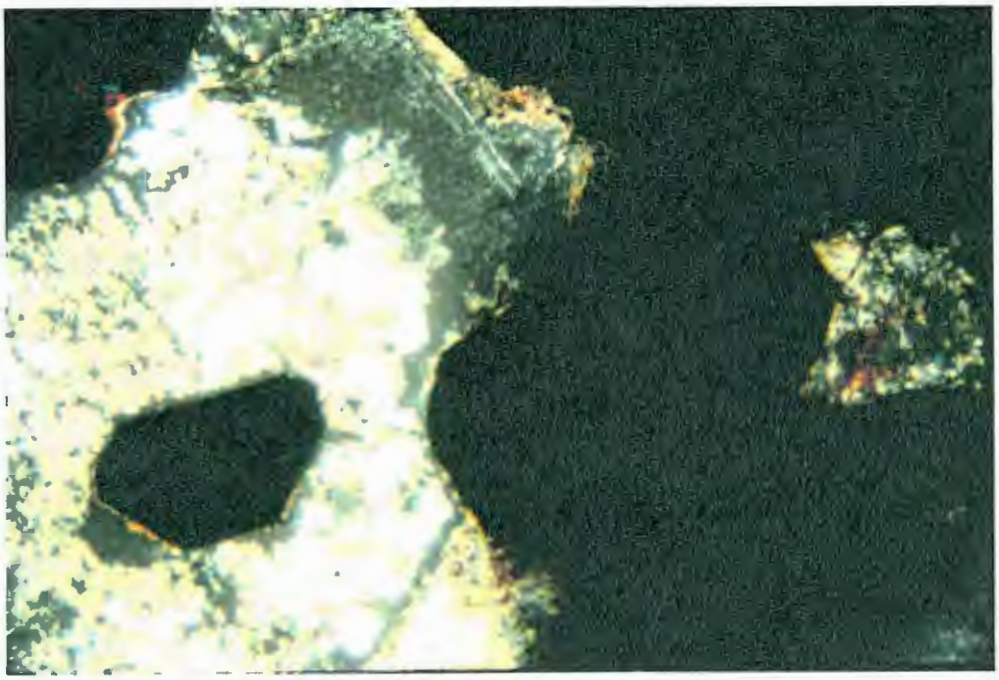

Fig. 24. Ilmenite euhedra in coarse-grained plagioclase in oxide peridotite; 440'. (Field of view approx. 5 mm across, crossed polars)

in LN-2 and LN-6 but absent in LN-5. The trellis occurs as fine lamellae along the {111} plane of the host titanomagnetite. Spinel is isotropic, grey, and occurs as exsolved blebs in the ilmenite trellis and as rods which occupy the {001} plane of augite. They are conspicuously absent near the edges of the grain and near ilmenite lamellae. Symplectites of spinel-ilmenite or spinel-titanomagnetite are common along ilmenite-titanomagnetite grain boundaries in LN-2 and LN-6.

Chalcopyrite varies in amount composing less than 1% of the rock in LN-2 and 1-3% in LN-5. It forms grains 0.1-2 mm in diameter which occur predominantly between the two oxides, in fractures, and to a lesser extent interstitial to the silicates. It is found rarely as small round inclusions in ilmenite.

Apatite occurs as an accessory mineral. It forms euhedral prisms 0.2-1 mm in length bewteen ilmenite and plagioclase (ts 13104).

4. Oxide dunite

a. Distribution

Oxide dunite occurs in the top 426´ (130 m) of LN-2 where it is interlayered with semi-massive oxide dunite and oxide rock, and as relatively minor zones within feldspathic dunite and peridotite of LN-6 and LN-5.

The contacts between dunite and the other various rock types are of varied character. The contacts with peridotite and troctolitic anorthosite are sharp within centimeters, whereas those with the feldspathic dunite are gradational over widths up to 1 m. The contacts with various oxide rocks are described in chapter 4.

b. Petrography

Oxide dunite contains 50-65% olivine, 10-50% oxides, and a total of 0-10% plagioclase and/or augite. In drill core, oxide dunite ranges in color from light olive green-brown to dark green with increasing serpentization, to dark green-black with increasing oxide content. Serpentine alteration ranges from 15% to 100%. Because the olivine grain boundaries are preserved in the serpentinite, it was logged as dunite. Texturally, it is either medium-grained and equigranular or medium- to coarse-grained and inequigranular. The contact between the two textures is sharp.

The equigranular texture is characterized by a medium grain size, paucity of plagioclase and augite, and net-textured to disseminated oxides. The inequigranular texture is characterized by sporadic individual coarse-grained augite, bimodal grain size olivine, and a thicker net-texture of oxides. Oxide stringers 5 cm to 0.75 m thick are common to both textures. The stringers are characterized by 1-3 cm long clots of medium-grained, subequant oxides. Augite is light brown with grey-blue alteration. It forms grains 0.5-3 cm in length which either poikilitically enclose olivine and oxides or are non-poikilitic.

Serpentine bands are common and occur as in feldspathic dunite. Fibrous serpentine (chrysotile) is rare, and displays fibers perpendicular to the strike of the band. The bands cross-cut all minerals. No relationship was observed between the concentration of these bands and the oxide content of the rock.

In thin section, the equigranular-textured oxide dunite is characterized by equant to subhedral grains of olivine 0.5-3.5 mm in

length with interstitial oxides (Fig. 25). Olivine shows no cataclastic granulation and only weak, patchy undulatory extinction. No cleavage or opaque rods were seen in olivine.

In zones of inequigranular-textured oxide dunite, olivine consists of suboval to subequant grains 0.5–2 mm across and suboval to anhedral grains 3 mm to 3 cm across (Fig. 26). Oxides are for the most part interstitial, but in one case ilmenite occurs as a subhedral plate in the middle of an olivine grain 3 cm in diameter. Olivine may subpoikilitically enclose a smaller subequant olivine grain. Plagioclase is common but modally minor in this texture. It forms anhedral grains 0.5–2 cm in length which poikilitically enclose oxides and in places contains 0.1 mm blebs of pyroxene. Albite twins may be bent 5–10^{o} within a grain. Plagioclase shows patchy extinction and is variably altered to sericite and clay. Augite is a minor constituent and occurs as sporadic coarse grains subpoikilitically enclosing olivine and oxides. Ilmenite exsolution platelets in augite are abundant and show a decrease in concentration around ilmenite inclusions (Fig. 27). Hornblende is a minor constitiuent of oxide dunite. It forms deep red-brown pleochroic rims around oxide inclusions in plagioclase.

In polished section, the ilmenite-titanomagnetite ratio in oxide dunite is seen to range within and between drill holes from about 87:13 to 30:70 (Appendix 3). Ilmenite forms interstitial, medium-size grains where it is disseminated and net-textured, and a granular mosaic texture when it is concentrated in clots. Spinel-hematite bands are present in most samples. Titanomagnetite occurs only as interstitial

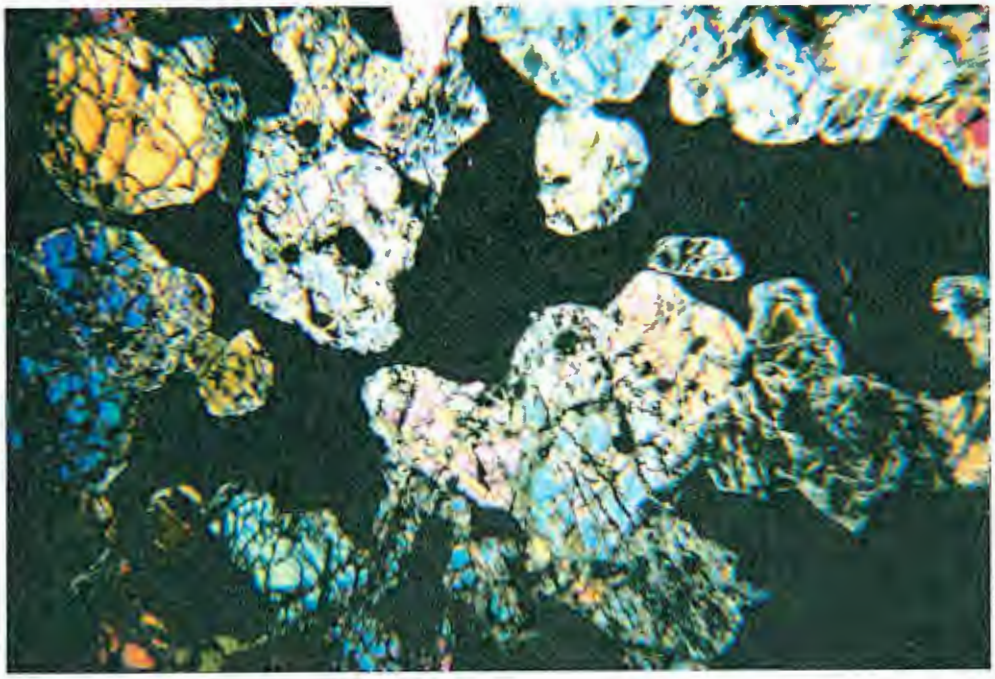

Fig. 25. Equigranular texture of cumulate olivine (colored) with interstitial oxides in oxide dunite; LN-2, 170.2'. (Field of view approx. 5 mm across, crossed polars)

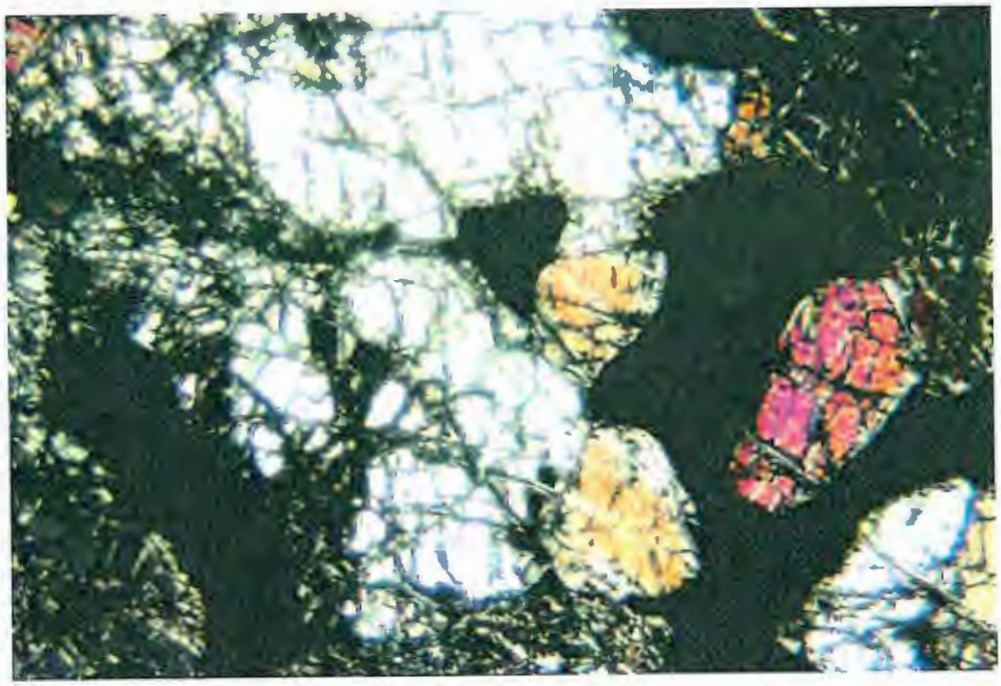

Fig. 26. Inequigranular texture of olivine (colored) with interstitial oxides (black) in oxide dunite; LN-2, 254.0'. (Field of view approx. 5 mm across, crossed polars)

Fig. 27. Augite with ilmenite inclusion in oxide dunite. Note paucity of exsoloved ilmenite platelets next to inclusion; LN-6, 408.2'. (Field of view approx. 2 mm across, plain light)

grains 0.5-3 mm across, which commonly host spinel disks parallel to {100} and ilmenite trellis along {111}. Symplectite of spinel in titanomagnetite grains next to ilmenite are present only in the oxide dunite of LN-6. The distribution of the above internal features of the oxides appears irregular (App. 3).

Serpentine and lesser secondary magnetite account for over 90% of the alteration in oxide dunite. Serpentine content increases with oxide content. In thin section serpentine ranges in color from light green to green-yellow and clear. In the less altered oxide dunite serpentine forms a mesh texture with islets of unaltered olivine. Secondary magnetite forms anhedral blebs which occur randomly or in a medial band between serpentine layers. Hematite is crimson red and may form a border on serpentine veinlets or a ring around olivine pseudomorphed by serpentine.

Accessory alteration products of olivine include carbonate, fine platy to radiating talc, deep green, blue and brown pleochroic chlorite, and tremolite/actinolite. Biotite forms partial rims on oxides. It is deep red to light brown and may show local epitaxial replacement by chlorite and magnetite parallel to cleavage.

5. Massive and semi-massive oxide rock

These rocks are described in Chapter 4.

6. Oxide feldspathic dunite

a. Distribution

Oxide feldspathic dunite is most abundant in LN-6 and LN-5 (Plate 2). The lower contact is gradational over 0.5-1 m with oxide dunite,

peridotite, and picrite, and is sharp with troctolitic anorthosite (country rock).

b. Petrography

In drill core, oxide feldspathic dunite is mottled dark green to light blue-green and white, non-foliated, inequigranular, and medium- to coarse-grained. It is composed of 55-80% olivine, 10-20% plagioclase, 10-30% oxides, 0-15% augite, and minor hornblende. The grain size and texture of olivine is the same as in peridotite. Plagioclase is white and forms medium to coarse, anhedral grains, some of which are poikilitic enclosing olivine and oxides. Augite occurs as sporadic, large, anhedral grains 0.5-1.5 cm in length. Oxides typically occur in a disseminated to broken net-textured fashion. Oxide "clots" with up to 70% oxides are uncommon. Deuteric red biotite and chalcopyrite are minor constituents composing less than 1% and 2% of the rock, respectively.

Serpentine bands are common. The bands are 0.5-2 cm thick, and consist of dark green bands of serpentine interlayered with or rimmed by secondary magnetite bands 0.5-1 mm thick. The surrounding olivine is easily distinguished from the bands by its lighter green-brown color. The dip of the bands is relatively constant at 30-45^{o} to the core axis.

In thin section, feldspathic dunite invariably shows hypidiomorphic, inequigranular texture. Olivine forms a bimodal arrangement in grain size and texture (Fig. 28), differing from its mode of occurrence in peridotite in that it also forms interstitially to plagioclase (Fig. 29). Undulose banding extinction and brown rods

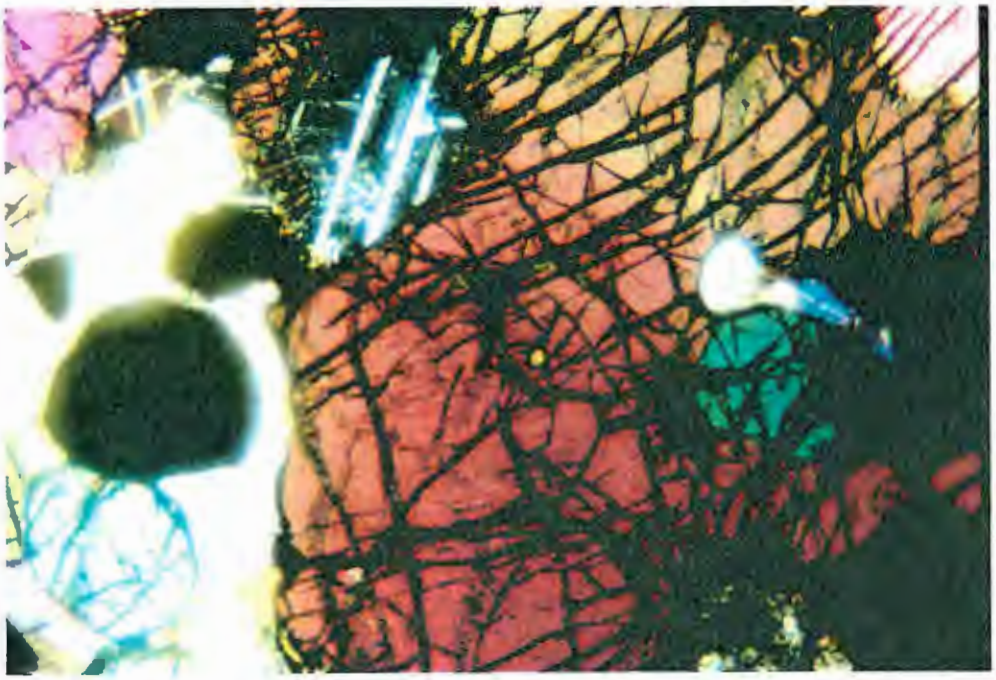

Fig. 28. Bimodal grain size of olivine in feldspathic dunite; LN-5, 455.1'. (Field of view approx. 5 mm across, crossed polars)

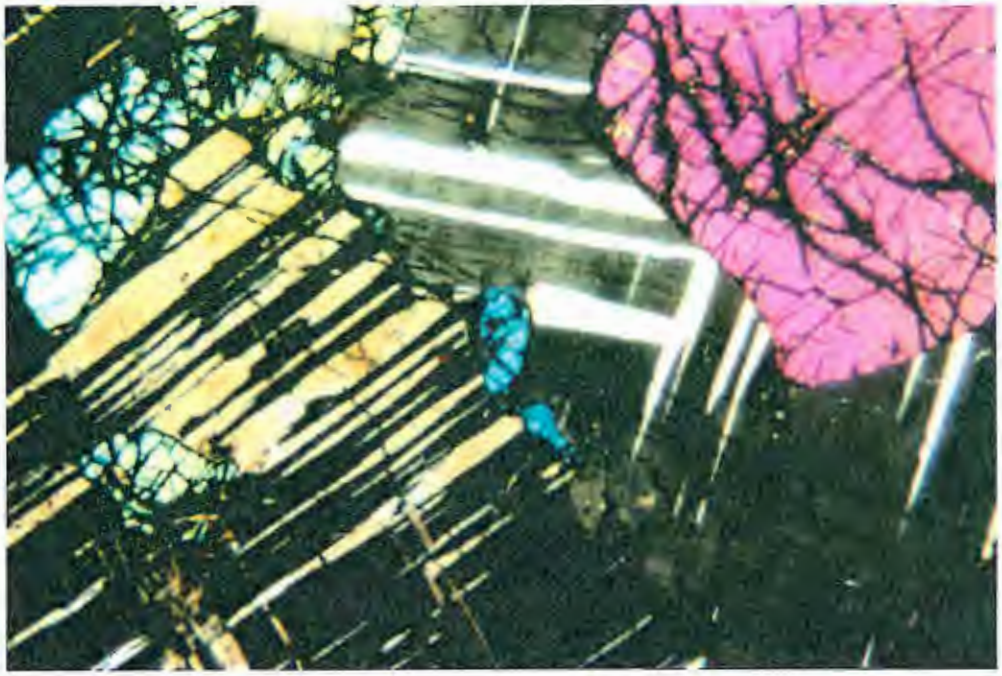

Fig. 29. Cumulate and interstitial olivine (pink and blue) in feldspathic dunite; LN-5, 454.3'. (Field of view approx. 5 mm across, crossed polars)

parallel to {100} or {001} parting planes (Irvine 1974) (Fig. 30) are common in the large, anhedral grains. Wavy extinction occurs in both the large, anhedral grains and the smaller, subhedral ones. Large grains are commonly found intergrown with plagioclase (ts 13064,13056), as apophyses embaying augite (ts 13102), as hosts to subround oxide inclusions, and subpoikilitically enclosing other small, round olivine grains.

Plagioclase forms interstitial non-poikilitic to subpoikilitic grains 1-4 mm in length and poikilitic grains 0.5-1 cm across which enclose several subhedral olivine and subequant ilmenite grains (Fig. 31). These ilmenite grains are rimmed by deep orange-red pleochroic biotite or hornblende, and the plagioclase itself is zoned around the ilmenite (ts 13051). Round plagioclase inclusions 0.1-0.2 mm across locally occur in olivine and vice versa (ts 13102). Plagioclase typically displays slightly bent albite twins and patchy zonation. Alteration is minor and local in occurrence, the main products being sericite and brown, nonpleochroic clay.

Augite occurs as isolated grains 1-2 cm in length and is always associated with large plagioclase grains. It subpoikilitically encloses subequant olivine and ilmenite grains and plagioclase grains 0.5-1 mm in length. In several cases augite also appears intergrown with plagioclase (ts 13051,13064). Internal features of augite include patchy extinction, exsolved ilmenite platelets, and hornblende alteration. The hornblende displays tan to deep brown-red pleochroism and forms as epitaxial replacements up to 1 cm in length (ts 13051). A minor amount of hornblende occurs as 3-5 mm thick, zoned selvages on

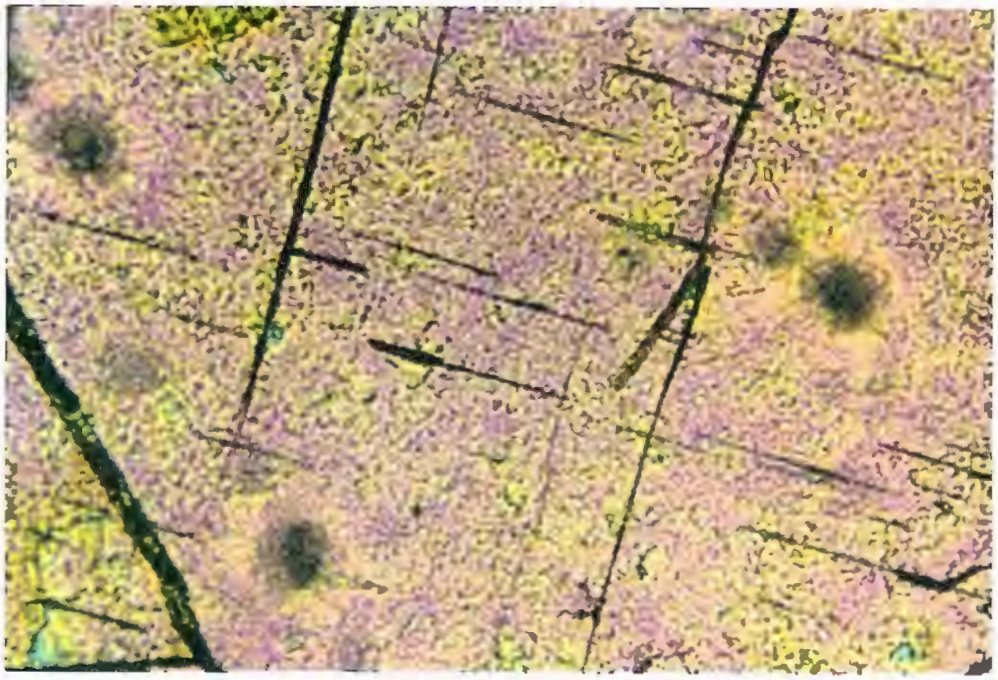

Fig. 30. Brown transparent rods parallel to {100} or {001} parting planes in olivine in feldspathic dunite, LN-5, 470.0′. (Field of view approx. 0.5 mm across, crossed polars)

Fig. 31. Cumulate olivine (colored) with subpoikilitic plagioclase (grey) and subequant oxides in feldspathic dunite, LN-6 171.2′. (Field of view approx. 5 mm across, crossed polars)

augite. The selvage is pleochroically zoned outward from deep red-brown to augite to tan-light green at the outer edge. Serpentine psuedomorphs of olivine occur as inclusions.

In polished section, the ilmenite: titanomagetite ratio is consistent at about 4:1 (App. 3). Ilmenite forms subequant to anhedral grains 1-3 mm across. Texturally, it is interstitial except where it composes more than 40% of the rock as a local, irregularly shaped oxide "clot" in which case the oxide texture is granular mosaic. Spinel-hematite bands parallel to {0001} and spinel symplectite occur in trace amounts in most samples. Textural relationships between ilmenite and the silicates include round ilmenite and augite, and round inclusions of plagioclase and augite in ilmenite. When rotated under crossed nicols, some ilmenite grains display internal "ghost" borders which are not discernable in plain light.

Titanomagnetite occurs as interstitial grains 1-4 mm across. Internal features common to most samples (App. 3) include ilmenite trellis and spinel disks. Chalcopyrite forms blobs 0.05-0.2 mm in size which occur between the silicates and either of the oxides, as inclusions near the edge of titanomagnetite, or as fracture fillings.

7. Picrite

a. Distribution

In drill core LN-5 there are several zones of picrite which are in contact with peridotite, feldspathic dunite, or troctolitic anorthosite. Contacts with the peridotite and troctolitic anorthosite are sharp and marked by olivine (up to 70%) in the picrite altered to a red-orange material (hematite/iddingsite) which progressively decreases

over 0.3 m to about 5% within 3 m of the contact. The contact with feldspathic dunite at depths of 455′ (77.9 m) is gradational over 0.5-1.5 m.

b. Petrography

In drill core, the picrite is mottled light olive green and white. It is composed of 50-70% olivine, 20-40% plagioclase, 1-10% augite, and 10-20% oxides. Texturally, it is medium- to coarse-grained, hypidiomorphic, inequigranular, and inhomogeneous. It grades locally into zones of feldspathic dunite to dunite on a scale of 0.3-1 m with gradational contacts of about 10 cm. Pegmatitic picrite forms zones 10 cm to 0.75 m wide in which plagioclase and olivine reach 2 cm in length.

Olivine is light olive-brown where fresh and is altered 10-100% to red-orange hematite/iddingsite. Olivine occurs as both anhedral grains 0.5-2 cm across and to a lesser extent as suboval grains 2-5 mm across. The plagioclase is white with 10-30% light blue alteration. Grains are anhedral and medium-grained. Augite is light brown, and forms subpoikilitic to poikilitic grains 0.5-1 cm across which enclose olivine and oxides. Oxides occur as anhedral medium size grains in a disseminated to net-textured fashion and locally form oxide aggregates 0.5-1.5 cm across. Hornblende is dark brown and is associated with pegmatitic zones. It is anhedral and grains reach 2 cm in size.

In thin section, olivine is altered 10-15% to serpentine and lesser actinolite-tremolite, talc, and carbonate. Deep green pleochroic chlorite occasionally rims olivine where it occurs next to plagioclase. The large anhedral olivine grains host inclusions of anhedral plagioclase with patchy extinction. Plagioclase forms

anhedral grains 0.3-1 cm in length which subpoikilitically enclose both subequant olivine and oxide grains 1-3 mm in length. The included oxide grains are commonly rimmed by zoned biotite showing dark green and red-brown pleochroism. Plagioclase is altered locally to saussurite. Augite is a minor constituent in the picrite. It is colorless in plain light, intergrown with olivine, and contains no ilmenite exsolution platelets. Hornblende grains embay olivine and plagioclase, and host inclusions of ilmenite. It dispays deep red-brown pleochroism.

Ilmenite is the primary oxide (Appendix 3), forming anhedral to subequant grains 1-6 mm in length. More rarely, it also forms oxide "clots" up to 1 cm across with a granular mosaic texture, as laths up to 6 mm long, and as intergrowths with olivine. Inclusions of silicates in ilmenite are rare. Internal features are similiar to those found in feldspathic dunite. They include "ghost" borders, spinel-hematite bands, and parting. Titanomagnetite is minor in amount, and occurs intestitially. It commonly hosts spinel disks along {100} planes. No ilmenite lamellae are present. Secondary magnetite is common as an alteration product of olivine.

Chalcopyrite is a minor constituent amounting to less than 2% of the rock. Its mode of occurrence is the same as that in peridotite.

C. Interpretation

The paragenesis of the rock types can be deduced from the textural relationships between minerals (Table 1). All rock types are classified as heteradcumulate, as they all contain intercumulate minerals which do not form as cumulate minerals. In some cases, the

lack of, or paucity of cumulate grains possessing euhedral to subhedral shapes is interpreted to be the result of adcumulate overgrowth of interstitial liquid onto the original grain. Lack of zonation in grains suggest that the interstitial liquid was of the same composition as the original cumulate grain.

Augite typically displays a central "core" of irregular shape which hosts exsolved ilmenite platelets and a rim which is barren of the oxide platelets and commonly encloses olivine subhedra and subequant oxides. Pasteris (1985) attributed this texture as seen in augite in troctolitic rocks at the Inco property to be the result of cumulate growth (core with platelets) and intercumulus growth (rim). In cases where the platelets occur throughout the augite the platelets could form as a function of exsolution. The bimodal grain size and texture of olivine indicates that the large, anhedral grains represent a "second" generation of olivine and could form by adcumulate overgrowth of the smaller, subhedral grains (Irvine, 1974). Jackson (1961) believes that banded undulatory extinction in olivine is evidence of intergranular deformation after complete solidification of the rock. Ilmenite also typically displays adcumulate overgrowth with an ilmenite rim which is not in exact optical continuity with the rest of the grain and which hosts spinel symplectite or spinel forms a border between the ilmenite rim and the core (see Figs. 39 and 40).

The hornblende-biotite rims on augite where next to plagioclase, and the alteration of plagioclase in pyroxenite and peridotite are explainable by either deuteric alteration or late-magmatic disequilibrium between the phases.

TABLE 1

Cumulate textures of rock types in the Longnose Peridotite

RK Type	Texture	Cum mnrls	intercum	adc overgrowth
troctolitic anorthosite	adc	ol,pl	aug,ox	pl
oxide pyroxenite	het	ol,aug	plag,ox	aug
oxide peridotite	het	ol,aug	aug,pl,ox,hbl	ol,aug
oxide dunite-equi	het	ol, $\pm$ ox	ox	
oxide dunite-inequi	het	ol $\pm$	ox,pl,aug	ol
massive oxide rock	gran-mos	ilm/tmt	ilm/tmt	ilm
oxide feldspathic dunite	het	ol	pl,aug,ox	ol
picrite	het	ol,pl	aug,ox,hbl	ol,pl

Abbreviations

adc----------adcumulate
cum mnrls----------cumulate minerals
intercum----------intercumulate minerals
het----------heteradcumulate
  equi----------equigranular textured oxide dunite
  inequi----------inequigranular textured oxide dunite
gran-mos----------granular mosaic textured oxides

Minerals
  ol----olivine
  aug---augite
  pl----plagioclase
  ox----oxides, both ilmentie and titanomagnetite
  ilm---ilmenite
  tmt---titanomagnetite
  hbl---hornblende

The intergrowths of minerals in which the grain boundaries of the minerals forming the intergrowths are interpenetrating is thought to indicate simultaneous crystallization along a common cotectic. Intergrowths include: augite and oxides in pyroxenite, olivine and augite in peridotite, and olivine with plagioclase, augite, and oxides in feldspathic dunite. The round plagioclase inclusions in olivine which occur in peridotite and feldspathic dunite may be due to the orientation of the plane (thin section) through the two minerals. If this is the case then olivine and plagioclase are cogenetic rather than plagioclase forming first and olivine second. Alteration minerals include biotite, hornblende, and minor sphene after augite; serpentine, hematite, secondary magnetite, talc and carbonate after olivine; and saussurite after plagioclase.

Chapter 4

Ore Petrology

A. Introduction

An oxide zone is here defined as a rock which averages more than 50% oxides. Six oxide zones occur in core LN-2 on the basis of change in oxide content and/or mineralogy (Plate 2). Drill holes LN-6 and LN-5 both host one oxide zone. The characteristics within an oxide zone are distinctive enough to warrant each oxide zone to be described separately. The general characteristics of the oxides in polished section and polished thin section are listed in Appendix 4.

Ilmenite and titanomagnetite are the primary oxides with lesser spinel and hematite as exsolution products. In drill core, ilmenite is distinguished by a silver-black metallic luster and conchoidal frature. Titanomagnetite, in comparison, has a dull black metallic luster and commonly displays octahedral parting. Ilmenite and titanomagnetite form characteristic textures which are related to their relative modal abundance. In general, if 1) ilmenite is the dominant oxide, it forms a granular mosaic texture (Fig. 32) with interstitial titanomagnetite (Fig. 33); if 2) the ilmenite:titanomagnetite ratio is about 1:1 and the total oxide content of the rock is high, then both oxides form a granular mosaic texture together. If the oxide content is low, both are interstitial; 3) the ilmenite:titanomagnetite ratio is about 1:4, then titanomagnetite forms a granular mosaic texture with interstitial ilmenite.

In polished section, ilmenite typically hosts spinel-hematite

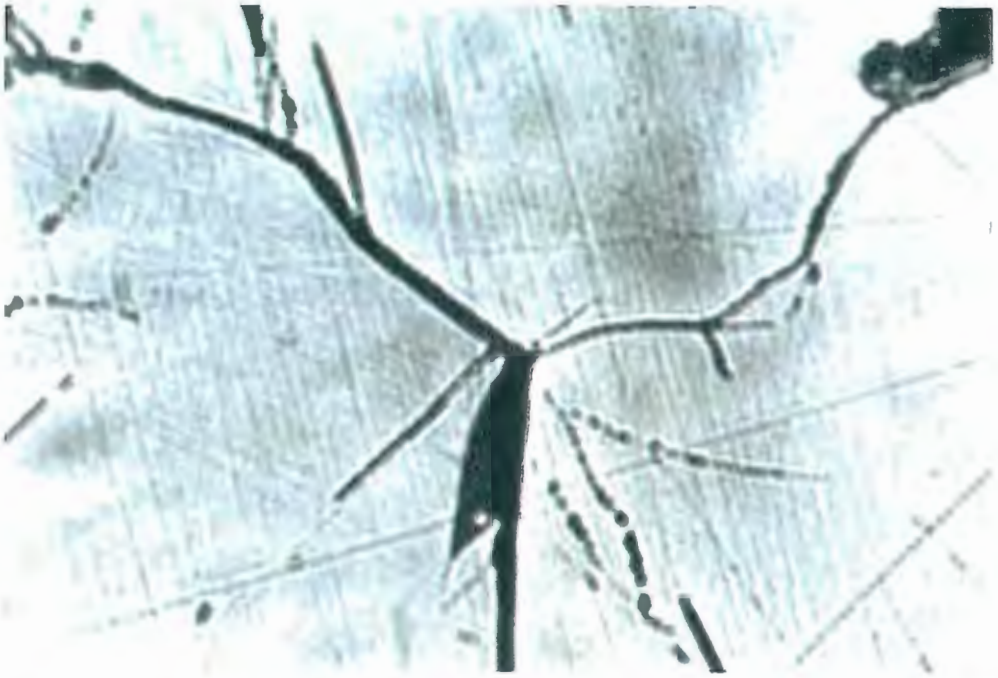

Fig. 32. Granular mosaic texture of ilmenite in massive oxide zone; LN-2, 200'. Note triple junction and approx. 120° angle. (Field of view approx. 1 mm across, plain reflected light)

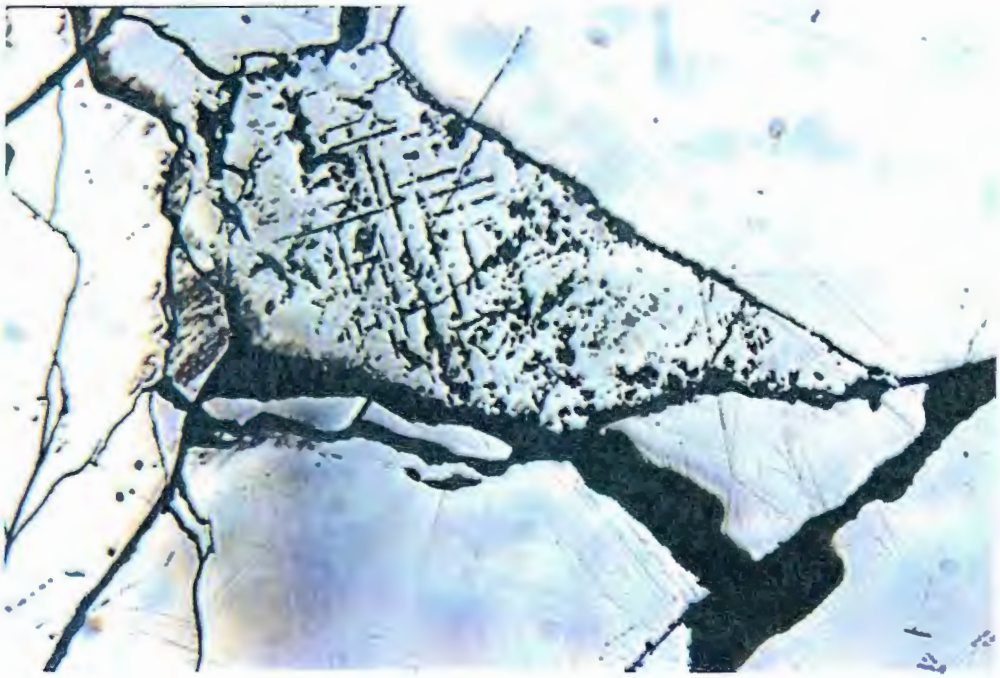

Fig. 33. Granular mosaic texture of ilmenite with interstitial titanomagnetite in oxide dunite; LN-2, 140'. (Field of view approx. 1 mm across, crossed polars)

bands which are parallel to {0001} (Fig. 34). The bands are approximately .05mm wide and less than 0.25 mm to 1 mm in length. They are estimated to compose less than 0.05% of any one grain.

Titanomagnetite shows a variety of internal textures, some of which are unique to a certain oxide zone. The textures are. 1) spinel disks (Haggerty, 1976, Von Gruenewaldt et al., 1985), 2) spinel-ilmenite sandwich, 3) ilmenite trellis (Buddington and Lindsley, 1964, Haggerty, 1976a), 4) ilmenite sandwiches (Buddington and Lindsley, 1964, Haggerty, 1976a), 5) internal and external composite ilmenite granules (Buddington and Lindsley, 1964, Haggerty 1976a), and 6) symplectites.

In type 1, the spinel disks are parallel to {100} planes (Fig. 35). The spinel is only observable in polished section, where it is grey, isotropic, and forms thin disks with rounded ends and/or is irregular in shape. A paucity of spinel is evident near the edge of the grain and the area immediately surrounding ilmenite lamellae.

In type 2, the spinel-ilmenite sandwich consists of a central spinel disk which is bordered by titanomagnetite and an outside ilmenite lamellae. The spinel forms a continuous disk or occurs in segments. The ilmenite lamellae are of about the same length as spinel disk, and do not host exsolved spinel.

In type 3, ilmenite forms oxidation-exsolution lamellae parallel to {111} (Fig. 36). The lamellae taper at the end and rarely reach the titanomagnetite grain edge. The lamellae invariably contain a later generation of spinel exsolution blebs along the inside edge of the lamellae and medially (Fig. 37). The trellis structure is parallel to

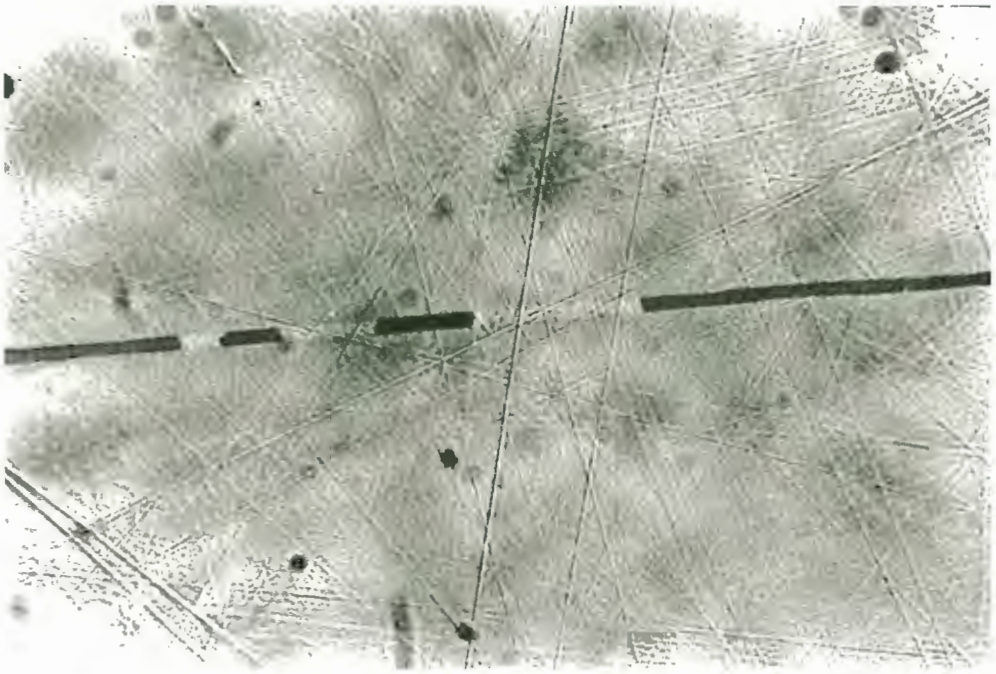

Fig. 34 Spinel (dark grey)-hematite band (light brown) along the {0001} plane in ilmentie in oxide dunite, LN-2, 151.0′. (Field of view approx. 0.5 mm across, crossed polars)

Fig. 35. Spinel disks along the {100} plane in titanomagnetite. Note spinel rim on titanomagnetite and lack of spinel disks at grain′s edge, LN-5, 232.5′. (Field of view approx. 1 mm across, plan reflected light)

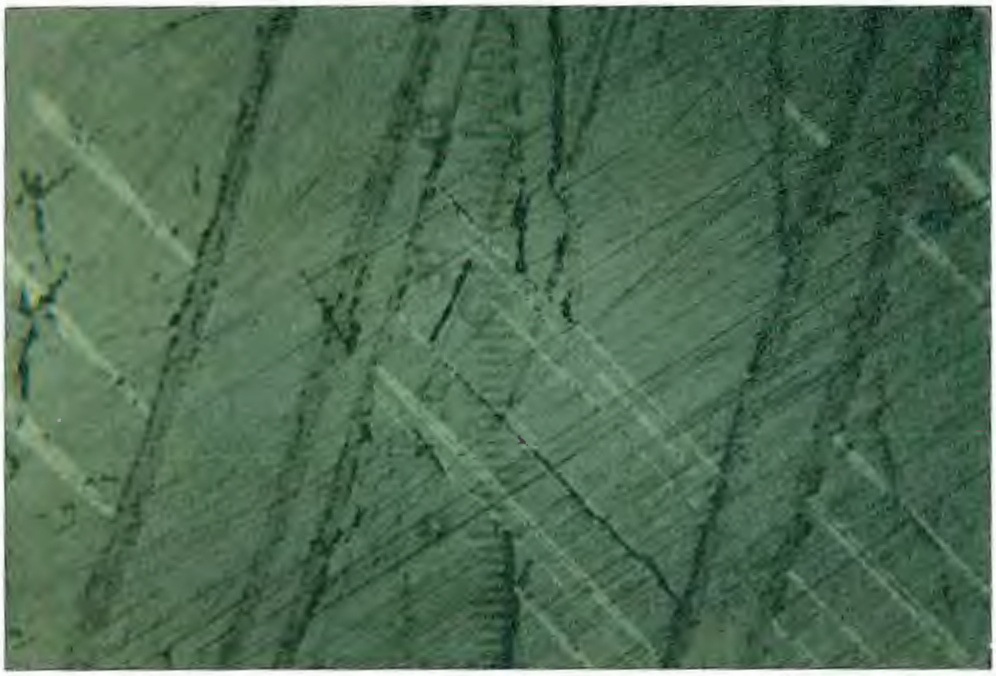

Fig. 36. Type 3 texture in massive oxide rock. Ilmenite (dark) brown and light green) forms oxidation-exsolution trellis parallel to the {111} plane in titanormagnetite. Note grey spinel in the trellis, LN-2, 389′. (Field of view approx. 1 mm across, crossed polars)

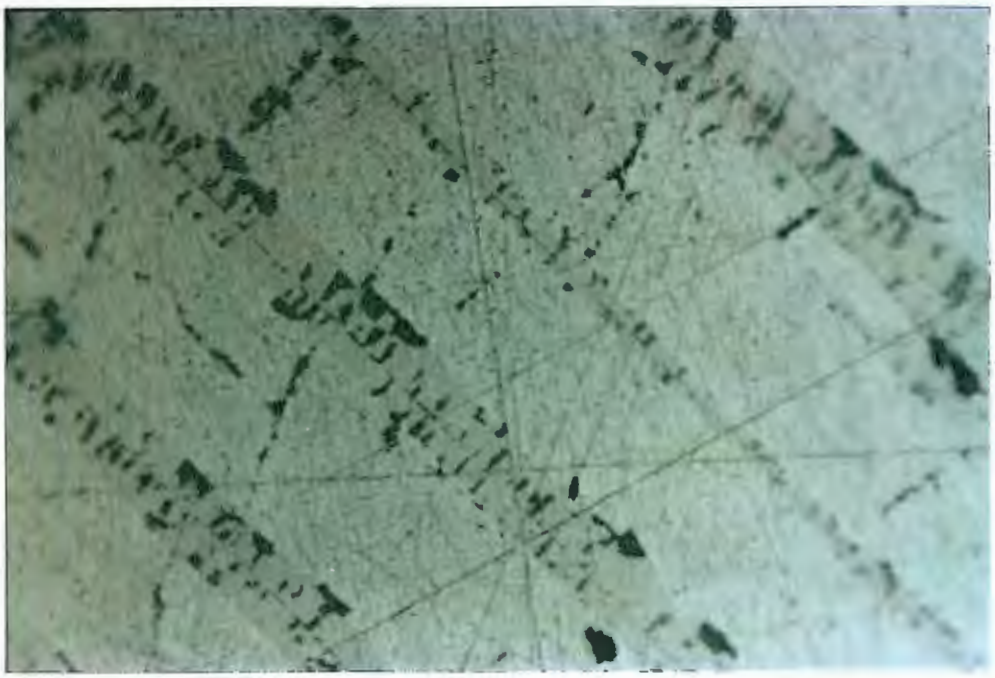

Fig. 37. Magnification of texture in Fig. 36. Note that the spinel (dark grey) is oriented 90° and parallel to the ilmenite lamellae (brown) LN-2, 389'. (Field of view approx. 0.5 mm across, crossed polars)

any one set of octahedral planes and is in optical continuity, displaying identical anisotropy and bireflectance. The trellis is of fairly uniform width within any one grain, but several generations of lamellae along different octahedral planes commonly display distinctive thicknesses.

Type 4 is restricted to titanomagnetite-rich zones. The ilmenite sandwich is distinguished from the ilmenite trellis of type 3 by being thicker, occurring in smaller numbers and along only one set of octahedral planes. Spinel exsolution blebs in the sandwich are common.

In type 5, the ilmenite composite granules are labeled internal or external depending on whether they occur inside or outside the host titanomagnetite (Buddington and Lindsley, 1964, Haggerty, 1976a). Internal granules form anhedral grains with poorly defined edges. They commonly occur at the end of ilmenite sandwiches of type 4, although they also coexist with titanomagnetite devoid of ilmenite trellis (Fig. 38). External granules are anhedral and display well defined edges.

In type 6, the sympletite most commonly consists of spinel blebs in the outer edge of ilmenite next to titanomagnetite (Figs. 39 and 40). Variations include a ragged border between ilmenite and titanomagnetite grains with small blebs of ilmenite and spinel in titanomagnetite and/or titanomagnetite and spinel blebs in ilmenite.

Oxide zones in core LN-2

In drill core, zone I (429.5′-393.5′) is marked by a sharp lower contact with a marked decrease in augite/oxide ratio. Augite ceases at 413′ and the result is a semi-massive dunitic oxide rock with oxide stringers. The stringers are 1" to 1′ thick, have gradational contacts

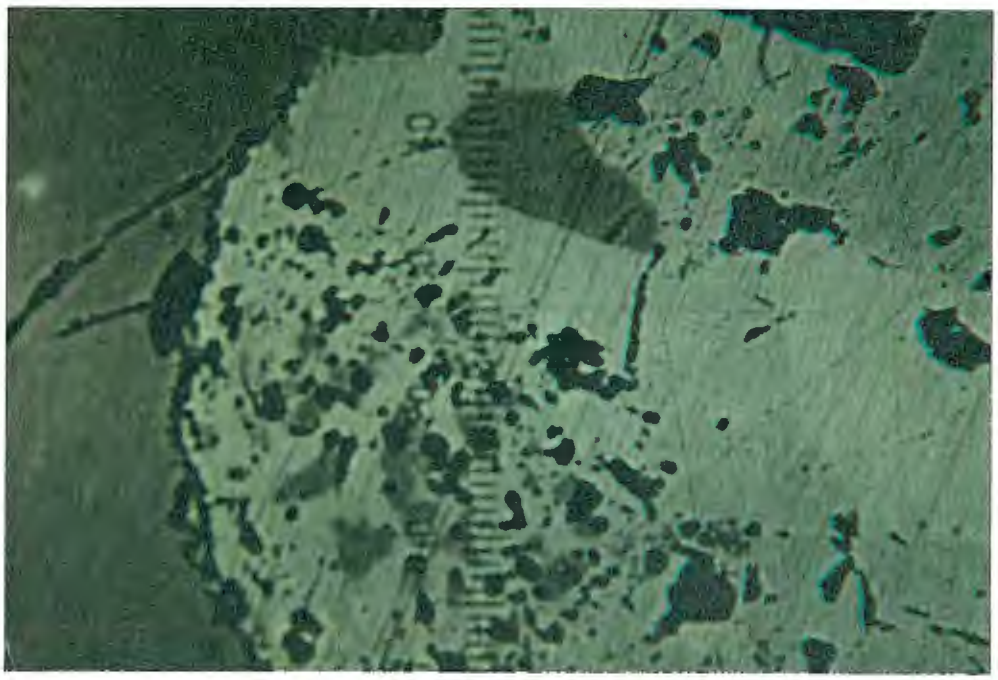

Fig. 38. Type 5 texture: Internal composite ilmenite granules (brown) in titanomagnetite (grey). Note the lack of ilmenite trellis and spinel; LN-2, 389'. (Field of view approx. 4 mm across, crossed polars)

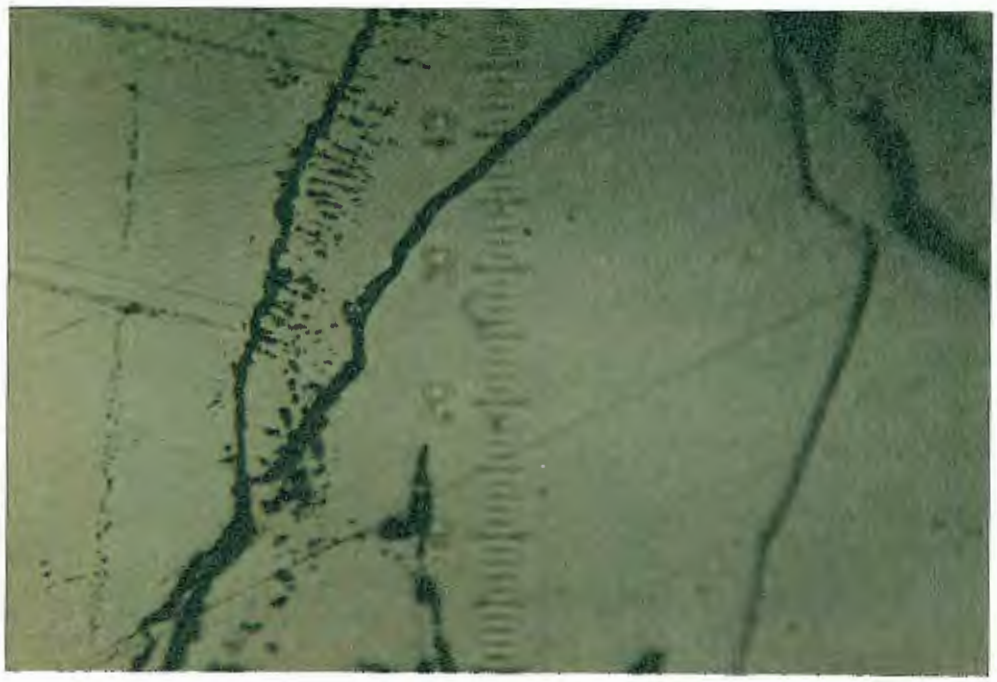

Fig. 39. Type 6 texture: Spinel symplectite (dark grey blebs) on edge of ilmenite rim. The rim is not in exact optical continuity with the rest of the grain. Titanomagnetite is on the left hand side of photograph with ilmenite trellis; LN-2, 389'. (Field of view approx. 0.5 mm across, crossed polars)

Fig. 40. Type 6 texture. Similar to Fig. 39, except that the ilmenite (upper grain) overgrowth is delineated by the spinel inclusion (dark grey blebs) border. Titanomagnetite is in far left and bottom right of photograph; LN-6, 518.2'. (Field of view approx. 1 mm across, plain reflected light)

over 3-5", and consist of 80-100% oxides.

In polished section, the ilmenite.titanomagnetite ratio is about 1.2.5 (Appendix 4). Both oxides are medium-grained (1-4 mm) and interstitial. No internal features were observed in either oxide.

In drill core, oxide zone II (393.5'-380.5') is in sharp contact with zone I, and is marked by the absence of olivine. Titanomagnetite is medium- to very coarse-grained (0.3-1.5 cm), but locally is pegmatitic with grains up to 4.5 cm across (384.5'-387'). It forms a granular mosaic texture in which ilmenite trellis along octahedral parting is visible. Ilmenite forms fine- to medium-size, interstitial grains. Ilmenite gradually decreases from 15% at the base to 5% at 388'. The zone is lightly fractured (1 fracture/2') with a decrease in fractures at 391'. Fractures are coated with white kaolinite (based on hand-samples). Serpentine (less than 5%) disappears at 390'.

In polished section, internal textures of titanomagnetite vary between samples (Appendix 4), but include all textural types. Type 2 texture is unique to this zone.

Oxide zone III (380.5'-334.5') is marked by a decrease in oxide/olivine ratio. Brecciated oxides occur from 381' - 380.8' with slickensides of serpentine or calcite. There are also vugs lined with 0.5-1 mm calcite crystals. Olivine forms suboval grains 1-3 mm in length which can occur as aggregates up to 1.5 cm across. Olivine is altered to about 70% serpentine and lesser magnetite and hematite. Massive oxide zones 0.25' to 5' thick have gradational contacts over 1-3", although in one case (at 361.8') the upper contact is sharp. The

oxides are medium-grained, net-textured and interstitial except when they form a local aggregate in which case a granular-mosaic texture results. The ilmenite-titanomagnetite ratio is fairly constant at about 40.60, although in once case (373′) the ratio is about 70.30.

In polished section, ilmenite and titanomagnetite may both occur interstitially to olivine, or both may form a granular mosaic texture where they form a local oxide clot (Appendix 3, Plate 2). Both oxides are fine- to medium-grained, measuring 0.3-4 mm across. Some ilmenite hosts spinel without hematite bands. Subequant grains of titanomagnetite are surrounded by, or included in ilmenite, and embay ilmenite. Textural types 1, 3, 5, 6, and a trace of 4 are present in titanomagnetite.

Oxide zone IV (334.5′-274′) consists of three subzones, as follows. 1) Massive oxide rock with 2-4′ stringers with 5-40% olivine (334.5-314.4′). The lower contact is gradational over 1.5′. 2) Semi-massive dunitic oxide rock from 314.5′-293′. The lower contact is gradational over 1.5′ and is heavily fractured. 3) Massive oxide rock from 293′-274′. The upper contact is gradational from 272′-274′. Zone IV is brecciated in 1-3′ zones between 334.5′-293′. Calcite forms crystals 0.2-0.5 mm in length in vugs and is anhedral along fractures. It composes up to 10% of the rock.

In zone IV, ilmenite.titanomagnetite ratio increases gradually going up section from 1.4 at the base to about 1.1 at 313′, above which the ratio sharply increases to about 9.1. A concomitant change in texture occurs with the changing oxide ratio. Titanomagnetite forms a granular mosaic texture with interstitial ilmenite from the base up to

313′, and a decrease in grain size from coarse-grained (up to 1 cm across) to medium-grained (1-4 mm) at 326′. Above 313, ilmenite forms a granular mosaic texture with interstitial titanomagnetite.

In polished section, the textures are as described above (Appendix 3), with the exception of one corroded titanomagentite grain in ilmenite (ps LN-2, 331′). Internal textures in ilmenite include spinel-hematite bands in all samples, and some ilmenite is twinned or displays "ghost" borders. Titanomagnetite invariably hosts spinel disks and ilmenite trellis, only at the base of zone IV (ps 331′) does titanomagnetite show internal composite grains of ilmenite.

Oxide zone V (274′-247′) is a semi-massive dunitic oxide rock. The lower contact is gradational from 272′-274′ with a marked decrease in oxide content to 70% compared to 100% in zone IV. The oxide content decreases gradually from 65% at 260′ to 30% at 252′. A five foot thick oxide zone with about 70% oxides occurs between 252′-247′. The ilmenite.titanomagnetite ratio varies between 1.1 to 100% ilmenite in an irregular fashion. Oxides are medium-grained, anhedral to subequant in shape, and net-textured. The silicate mineralogy is the same as in oxide dunite. Olivine forms suboval grains 0.5-5 mm in length which have been about 90% serpentinized and/or hematitized 5-90%.

Oxide zone VI (213.0′-180′) consists of medium-grained, granular, massive oxide rock. Olivine stringers and net-textured oxides occur between 213.0′ and 201.8′. The lower contact is gradational over 2′ with an increase in oxide content from 30% to 80%. The upper contact is brecciated from 180′-182′, and contains 2 mm wide calcite veins with apparently irregular orientation and calcite vugs. The silicate

mineralogy is the same as in the inequigranular oxide dunite variety. Olivine is altered to 70-100% serpentine and lesser secondary magnetite and hematite. The ilmenite.titanomagnetite ratio is fairly constant between 213′ and 197′ at about 19.1, and changes at 197′ to about 1.1 where it remains constant to 180′. Texturally, the oxides fall under the type 1 category, ilmenite is subequant and titanomagnetite is subequant to interstitial.

In polished section, the massive oxide rock (213′-180′) shows a decrease in the ilmenite.titanomagnetite ratio from 96% ilmenite at 200.0′ to about 1.1 at 194.3′ (see App. 4 and compare to oxide zone IV). A change in oxide texture parallels the change in oxide ratio, ilmenite forms a granular mosaic texture with subequant grains 0.5-3 mm in length with interstitial titanomagnetite at 200′, and at 194.3′ titanomagnetite forms rare subequant grains, although it is largely still interstitial. Ilmenite also forms rate round blebs 0.5 mm across in plagioclase.

Ilmenite hosts spinel-hematite bands, and titanomagnetite hosts type 1 and 3 textures. Ilmenite also forms a unique trellis in which the ilmenite lamellae are short, and lack exsolved spinel. Symplectite is common, and occurs as ilmenite and spinel within the border of titanomagnetite or as spinel in an overgrowth rim of ilmenite.

Chalcopyrite composes less than 0.1% of the rock and occurs as 0.5 mm blebs between silicates and ilmenite or with alteration of silicates.

Oxide zone in core LN-6

One major oxide zone occurs in LN-6 between 520′-488′. The zone

consists of 1-6′ zones of massive to semi-massive oxide rock interlayered with pegmatitic oxide peridotite to oxide olivine clinopyroxenite. Both upper and lower contacts are sharp. The contacts of the massive oxide zones are sharp to gradational over 0.5′. Fracture concentration is about 1/foot, fractures are coated with kaolinite or calcite. In one case, the top of a massive oxide zone (514′-509′) is brecciated. The contacts are apparently at random angle to the core axis.

Texturally, the massive oxide zones are medium- to coarse-grained and granular with titanomagnetite forming subequant grains 0.3-1.5 cm across with interstitial grains of ilmenite 2-3 mm across. The semi-massive oxide zones are fine- to medium-grained (0.5-4 mm) and net-textured.

The texture of the oxide peridotite changes up section. The rock is homogeneous and medium-grained between 520′ and 498′. The pegmatite consists of irregular augite grains 1-5 cm in diameter which poikilitically enclose olivine and oxides, and lesser irregular plagioclase grains (less than 5% of the rock) up to 5 cm across with oxide inclusions. Olivine forms both oval grains 1-3 mm across and larger anhedral grains up to 1 cm across.

In polished section, the ilmenite.titanomagnetite ratio is about 1.4 in the lower two thirds of the zone and shows a marked change in ratio at 494.7′ to about 2.3.1 (App. 3). This change is accompanied by a textural change in the oxides. In the first case, titanomagnetite forms irregular grains 1-4 mm across and rare oval grains 0.2 mm across which are included in serpentine (Fig. 46). The ilmenite content

consists predominantly of trellis, sandwiches, and composite granules within titanomagnetite grains. Some ilmenite external composite grains host anhedral titanomagnetite with ragged edges and which in turn host internal ilmenite composite grains. In the latter case, ilmenite forms subequant grains in a granular mosaic texture and titanomagneite is interstitial.

Oxide zone in core LN-5

A single semi-massive oxide zone with 1 to 2′ stringers of massive oxide occurs between 587.5′ and 602′. The zone is very inhomogeneous mineralogically, varing sharply between pegmatitic feldspathic hornblendite and hornblende-bearing gabbro. The upper contact is sharp with the appearance of a massive oxide stringer followed by pegmatitic hornblende. A pegmatitic zone of hornblende and plagioclase and gabbro occurs between 589.5-602′ with pegmatitic grains of augite and plagioclase.

Hornblende, augite, plagioclase and biotite form grains up to 4 cm across. Olivine forms oval cumulate and irregular interstitial grains. Ilmenite forms 2-4 mm equant grains and is poikilitically enclosed by hornblende, augite, and plagioclase. Titanomagnetite is interstitial. The ilmenite.titanomagnetite ratio varies unsystematically between 9.1 to 19.1.

In polished section, ilmenite forms subequant to irregular grains 2-4 mm across. At 588.8′ ilmenite forms subequant grains with interstitial hornblende (Fig. 41) and becomes massive with a granular mosaic texture in the bottom half of the thin section, giving an appearance of layering. Titanomagnetite forms irregular to subequant

Fig. 41. Intergrown hornblende and ilmenite; LN-5, 588.8'. (Field of view approx. 4 mm across, crossed polars)

grains with cuspate to straight edges at 588.8′. In the rest of the zone however it is interstitial or occurs as an alteration product of olivine. It may host grey spinel along cubic parting planes and minor ilmenite trellis along octahedral parting planes.

Sulfides

Sulfides are a minor constituent in the Longnose Peridotite. Chalcopyrite accounts for about 99% of the sulfide content, with bornite and chalcocite occurring in only trace amounts in association with chalcopyrite. Generally, chalcopyrite accounts for less than 0.2% of the rock in core LN-2, and averages about 2% in cores LN-6 and LN-5, with local concentrations of up to 5% in association with heavily altered zones.

In drill core, chalcopyrite forms irregular grains 0.2-4 mm across which occur interstitially between either oxide grains or oxides and silicates. In polished section, chalcopyrite occurs between either of the two oxides (Fig. 42) and the silicates as 0.1-0.5 mm blebs and rarely as inclusions within either of the oxides. Bornite may form "flames" in chalcopyrite which are related to microfractures in the latter and therefore appear to be an alteration product of chalcopyrite.

C. Interpretation

Ilmenite forms as both a primary phase along with titanomagnetite, and also as a secondary phase as ilmenite trellis in titanomagnetite. Buddington and Lindsley (1964) demonstrated by phase equilibrium experiments in the system $FeO-Fe_2O_3-TiO_2$ (Fig. 43) that subsolidus oxidation of magnetite-ulvospinel solid solutions (Mt-Usp ss) resulted in "exsolved" ilmenite lamellae along the {111} planes of the host, and

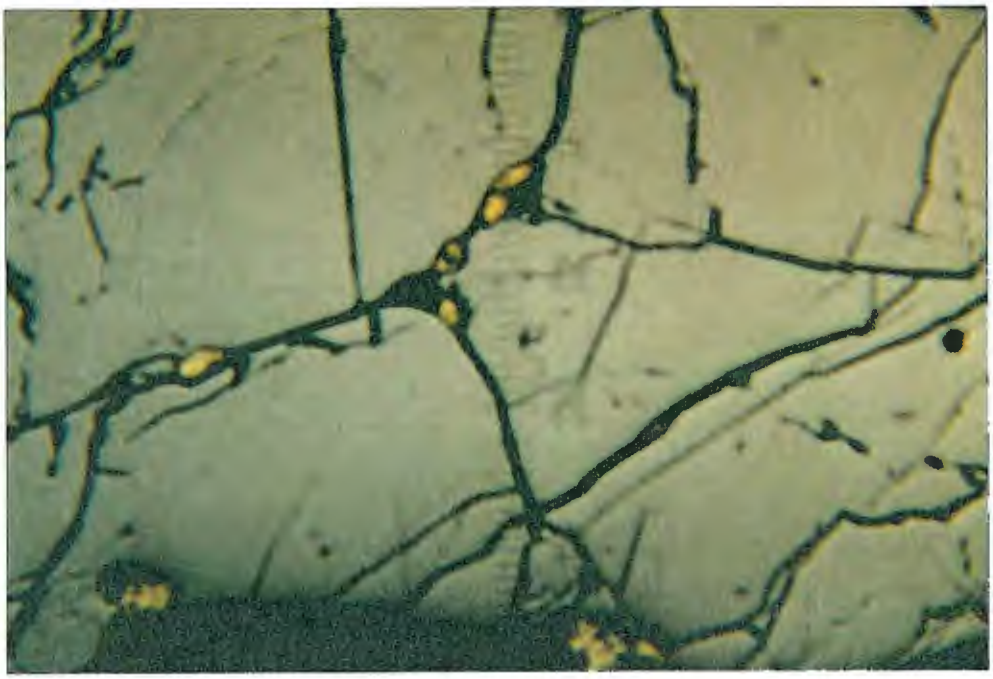

Fig. 42. Granular mosaic texture of ilmenite with interstitial chalcopyrite in oxide feldspathic dunite; LN-5, 189.2'. (Field of view approx. 4 mm across, plain reflected light)

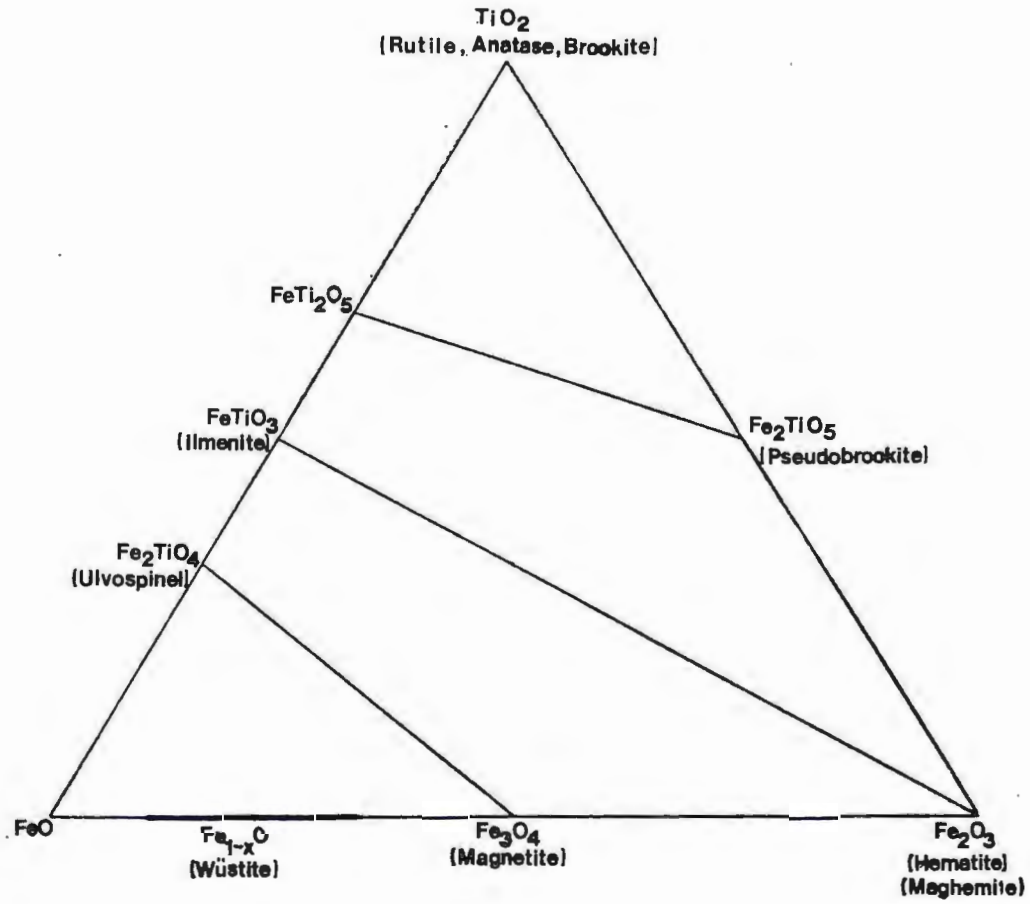

Fig. 43. Ulvospinel-magnetite and ilmenite-hematite solid solution series in the system FeO - Fe_2O_3 - TiO_2. (From Buddington and Lindsley, 1964)

that the density and abundance of the lamellae was a qualitative measure of the oxygen fugacity at the time of oxidation-exsolution.

The origin of ilmenite sandwiches and composite granules is uncertain, and may be the result of oxidation-exsolution or they may have crystallized as a primary phase from the melt. The presence of all three textural types (trellis, sandwich, composite) of ilmenite precludes the possiblility that the composite grains are the result of oxidation. Lamellae terminate sharply at the composite granules and therefore post-date the granules. If the granules developed under conditions of high diffusion rates and high temperature, most if not all of the ulvospinel would be oxidized at a relatively early stage, and further diffusion at lower temperatures to form ilmenite trellis and/or sandwiches is unlikely (Haggerty, 1976a).

The spinel (pleonaste) exsolved from Mt-Usp ss above the Mt-Usp solvus is indicated from textural evidence (Haggerty, 1976b) and from homogenization experiments of Mt-Usp exsolutions (Price, 1981). Pleonaste exsolution can occur earlier, contemporaneously, or later than the oxidation-exsolution of coexisting titanomagnetite. The process of spinel exsolution is an imposed exsolution induced by saturation of the host in Al_2O_3 and MgO (Haggerty 1976b).

The presence of spinel in ilmenite trellis is probably a result of simultaneous oxidation-exsolution of the ilmenite and exsolution of the pleonaste into the {111} parting of the Mt-Usp ss (Von Gruenwaldt et al., 1985, Haggerty, 1976a).

In the titanomagnetites of the Longnose Peridotite, at least 2 stages of spinel exsolution are indicated by texture, and in some cases

3. The paucity of spinel along {100} next to ilmenite lamellae which host spinel, indicates that the spinel along {100} are later than those in the ilmenite lamellae. A third generation of exsolution is evident where spinel forms symplectite along the edges of titanomagnetite grains.

Haggerty (1976a) noted seven oxidation assemblages of primary ilmenite (involving assemblages of ferrian rutile, titanohematite, and pseudobrookite). None of these assemblages however, are present in ilmenite of the Longnose Peridotite. The spinel-hematite bands are interpreted by the author to be composed of exsolved spinel along a twin plane in ilmenite which displays different anisotropy from the main ilmenite grain.

The granular mosaic texture of the oxides can be ascribed to the process of annealing whereby individual grains are consolidatd into more dense aggregates by heating and overgrowth at high subsolidus temperatures. The process involves growth of the grain by diffusion and results in polygonal grains with triple point junctions with interfacial angles of about 120^{o} (Reynolds, 1985).

Chapter 5

Stratigraphy & Structure of the Longnose Peridotite

A. Stratigraphy

The stratigraphy of the Longnose Peridotite is based on gravity data (Fig. 44), longitudinal and cross-sections based on drill core (Figs. 45 and 46, respectively) and the law of superposition, all cores other than those studied in this thesis were logged by Sarah Mills (1984), and supplied by American Shield Company along with the gravity data. All drill holes are drilled parallel to geophysical grid lines with an inclination of 45^{o} plus or minus 3^{o} to the NW, except drill holdes BA-6 and Al-1 which are vertical.

The gravity contours (Fig. 44) are based on modeling of gravity data and density contrasts using the program Forgave, by Petrospec. Actual gravity values are not shown as the data is proprietary information. The required data are the vertices that describe each anomalous body and its density contrast. The density contrast is the difference between the gravity of the Duluth Complex in the Hoyt Lakes area and that of the Longnose Peridotite. The gravity of the Longnose Peridotite is based on gravity tests of similiar rocks in the Water Hen intrusion. The body is drawn to meet the gravity curve. The gravity contours increase from the outside to the inside of the body. The outer limits of rock types in Figures 45 and 46 are based on the gravity countours in Figure 44. In the case of the Longnose Peridotite, a sill is unlikely as it is too fat and short. The best fit is an asymmetrical bowl (Ulland, pers. comm., 1986).

The general stratigraphy consists of a basal oxide pyroxenite to

Fig. 44

General gravity field of the Longnose Peridotite

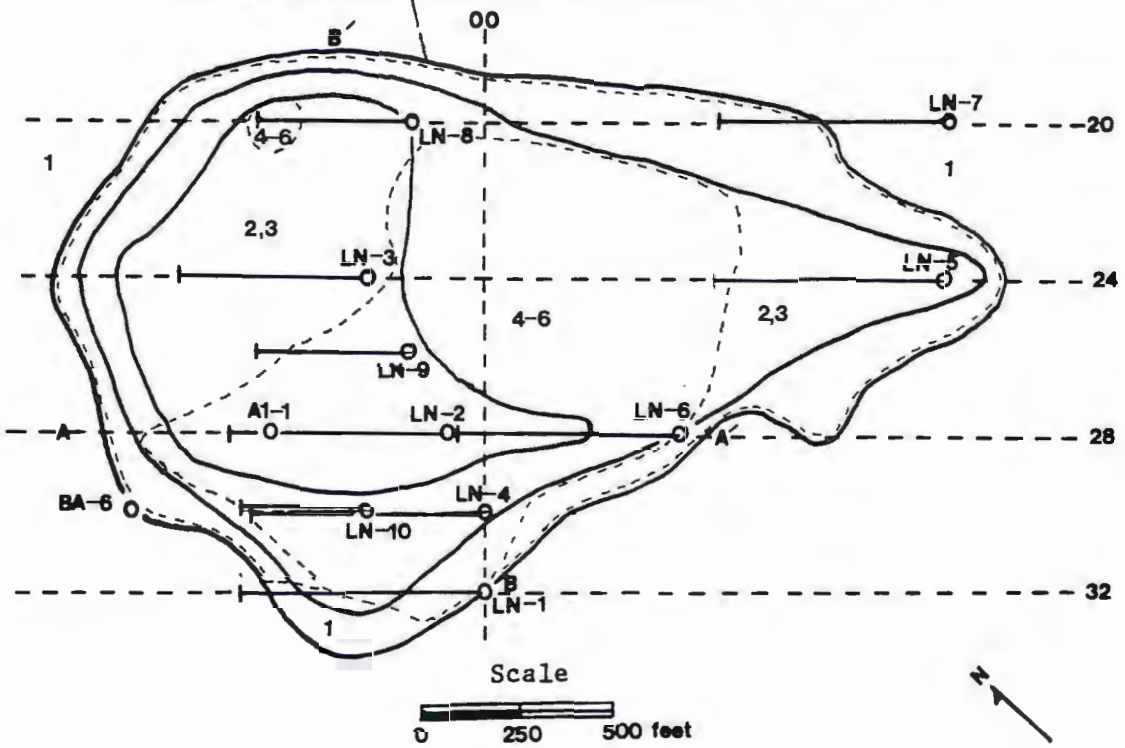

SYMBOLS

----- Contact, based on rock types in drill holes projected to surface from 45° plane.

⊢——o Drill hole, showing top of hole (o), bearing, and bottom of hole. Length based on actual footage, inclination is 45°± 3°

o Drill hole, vertical

— — Fault, inferred (Severson, 1988)

——— Gravity contours; gravity increases going inward

— — — Geophysical grid line

Longitudinal section A - A' and cross-section B - B'

ROCK TYPES

4-6 Oxide dunite / oxide feldspathic dunite / oxide rock

2,3 Oxide clinopyroxenite / oxide peridotite

1 Country rock (troctolitic anorthosite)

(After Ulland, 1985)

Fig. 45 Longitudinal section A - A' along grid line 28. Scale 0 100 FT.

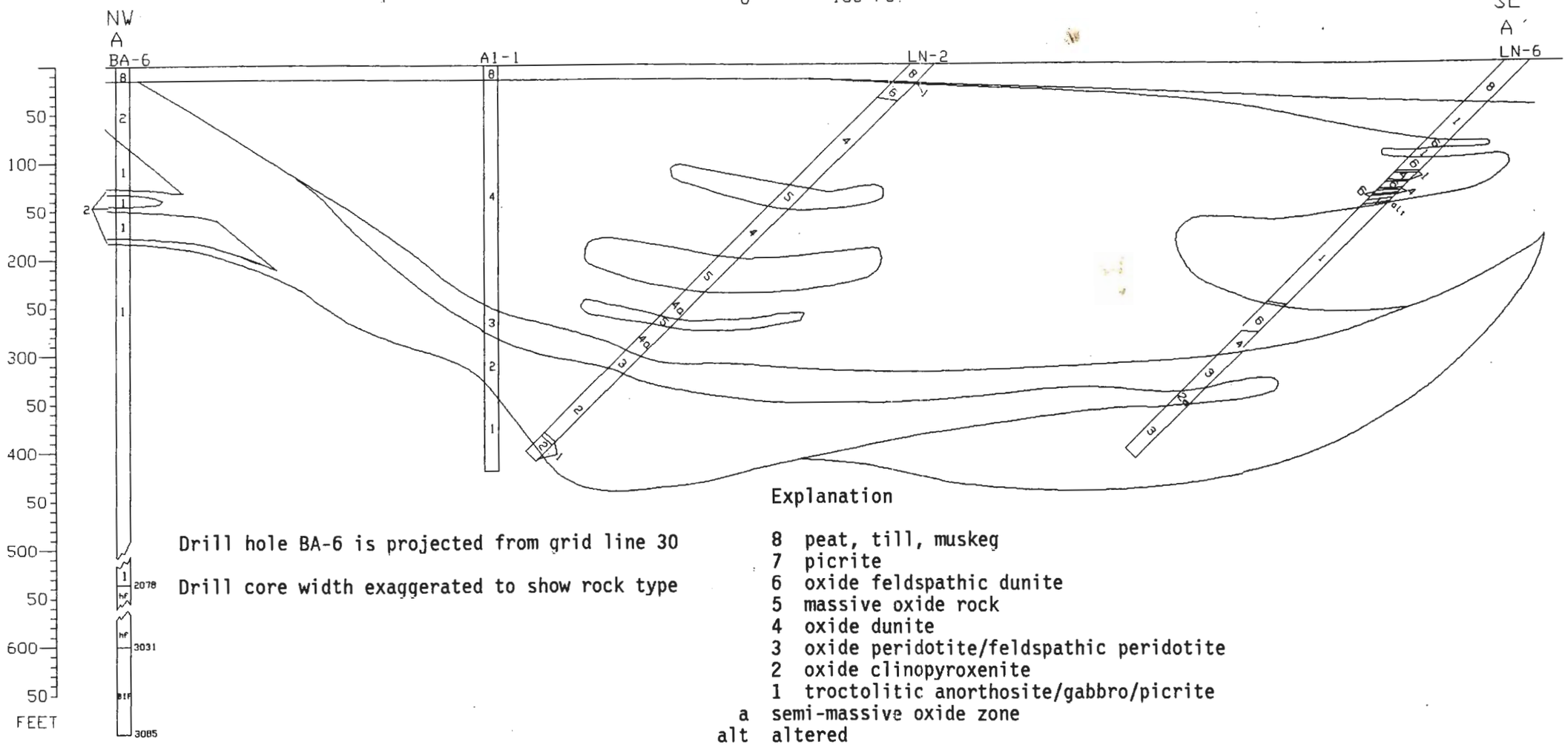

Drill hole BA-6 is projected from grid line 30

Drill core width exaggerated to show rock type

Explanation

- 8 peat, till, muskeg
- 7 picrite
- 6 oxide feldspathic dunite
- 5 massive oxide rock
- 4 oxide dunite
- 3 oxide peridotite/feldspathic peridotite
- 2 oxide clinopyroxenite
- 1 troctolitic anorthosite/gabbro/picrite
- a semi-massive oxide zone
- alt altered
- BIF Biwabik Iron Formation
- hf hornfels
- contact inferred

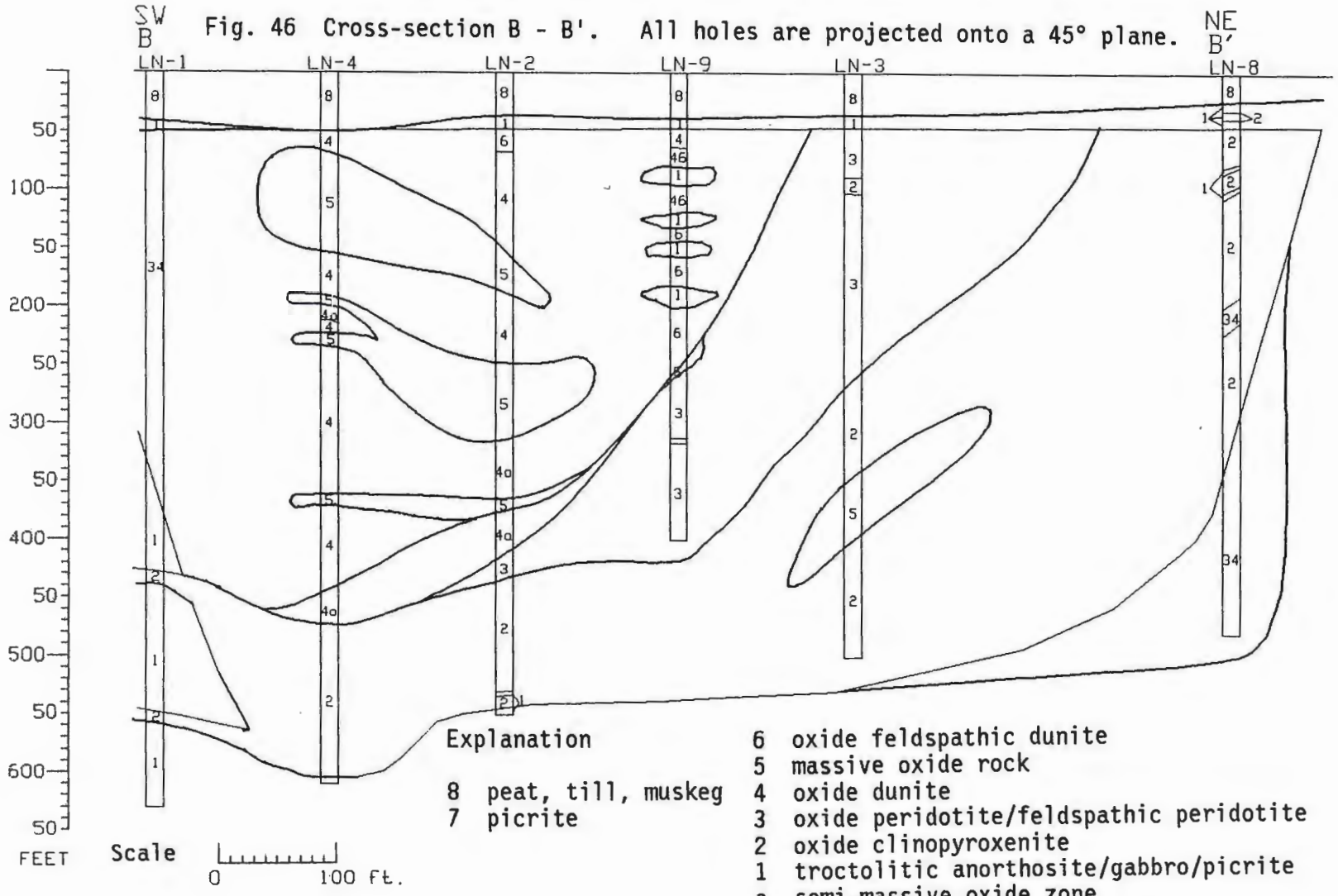

Fig. 46 Cross-section B - B'. All holes are projected onto a 45° plane.

olivine pyroxenite (unit 2) 80-180′ (24-55 m) thick, overlain by oxide peridotite to oxide feldspathic peridotite (unit 3) with a maximum thickness of 120′ (37 m) which pinches out to the NW and SW. Above the peridotite, in the south central portion of the body, is semi-massive dunitic oxide rock (unit 4a), dunite (unit 4), and massive oxide rock (unit 5). The oxide zones can be correlated between drill holes LN-4 and LN-2 (Fig. 46), but other oxide zones at the base of drill holes LN-6, LN-5, and LN-3 cannot be correlated.

The above stratigraphic sequence does not occur in drill holes LN-8 and LN-5 which are located on the NE and SE edges of the body, respectively (Plate 2, Fig. 46). Here the strata may be reversed with dunite/feldspathic dunite occurring below, or interlayered with peridotite or pyroxenite.

The footwall rock consists of Duluth Complex troctolitic anorthosite, which also apparently forms a cap to the deposit. The cap is overlain with 18-45′ (6-14 m) of muskeg and till.

B. Structure

Drill core logs and gravity data suggest that the Longnose Peridotite forms an asymmetrical bowl which dips very steeply on the NE, SE and SW sides and less steeply on the NW side. In plan view it is shaped like a tear-drop (Plate 1, Fig. 44), with the long axis striking approximately N 140^{o} E. This strike cross cuts the foliation trend of the country rocks. In plan view the body is 2500′ (762 m) long by 1600′ (487 m) wide at the base of the tear and narrows to approximately 250′ (76.2 m) at its tip. The depth of the pluton ranges from 81′ (24.7 m) in BA-6 to 448′ (136.5 m) in LN-1.

C. Interpretation

Severson and Hauck (1990) have delineated several oxide-bearing ultramafic intrusions (OUI) within the Partridge River troctolite intrusion (PRTS). The authors concluded that, in almost all cases, the OUI bodis in sharp contact with PRTS units are clearly younger. In drill core this is demonstrated by 1) near vertical, sharp contacts (in most cases), 2) the abundance of ultramafic stingers or apophyses in the PRT, 3) PRTS xenoliths in the OUI, and 4) where the OUI is in sharp contact with altered-foliated PRTS units, the adjacent OUIs are generally void of alteration and foliation. In this thesis, criteria #2, #3 and #4 were observed. Criteria #1 is thought to apply based on the longitudinal cross sections.

The Longnose Peridotite is interpreted by this author to have been intruded into the Duluth Complex (specifically the PRTS) in three stages to form a series of nested sills resembling small lopoliths (Fig. 47). The first stage consisted of a feldspathic dunite mush with crystals of olivine which was then quickly followed by an oxide dunite phase with crystals of olivine and oxides. The bimodal grain size of olivine could be explained by the formation of earlier olivine crystals that then grew larger by adcumulate overgrowth along with the euhedral - subhedral medium-grained olivine crystals. The second stage consisted of the intrusion of oxide peridotite beneath the oxide dunite. During the third stage oxide clinopyroxenite was emplaced both beneath the oxide periodite and as large apophyses into it (see Fig. 45, drill hole LN-6) or into first phase rocks (see Fig. 46, drill hole LN-8).

Fig. 47

Schematic cross-section of the Longnose Peridotite
(based on longitudinal section A - A')
not to horizontal or vertic1 scale

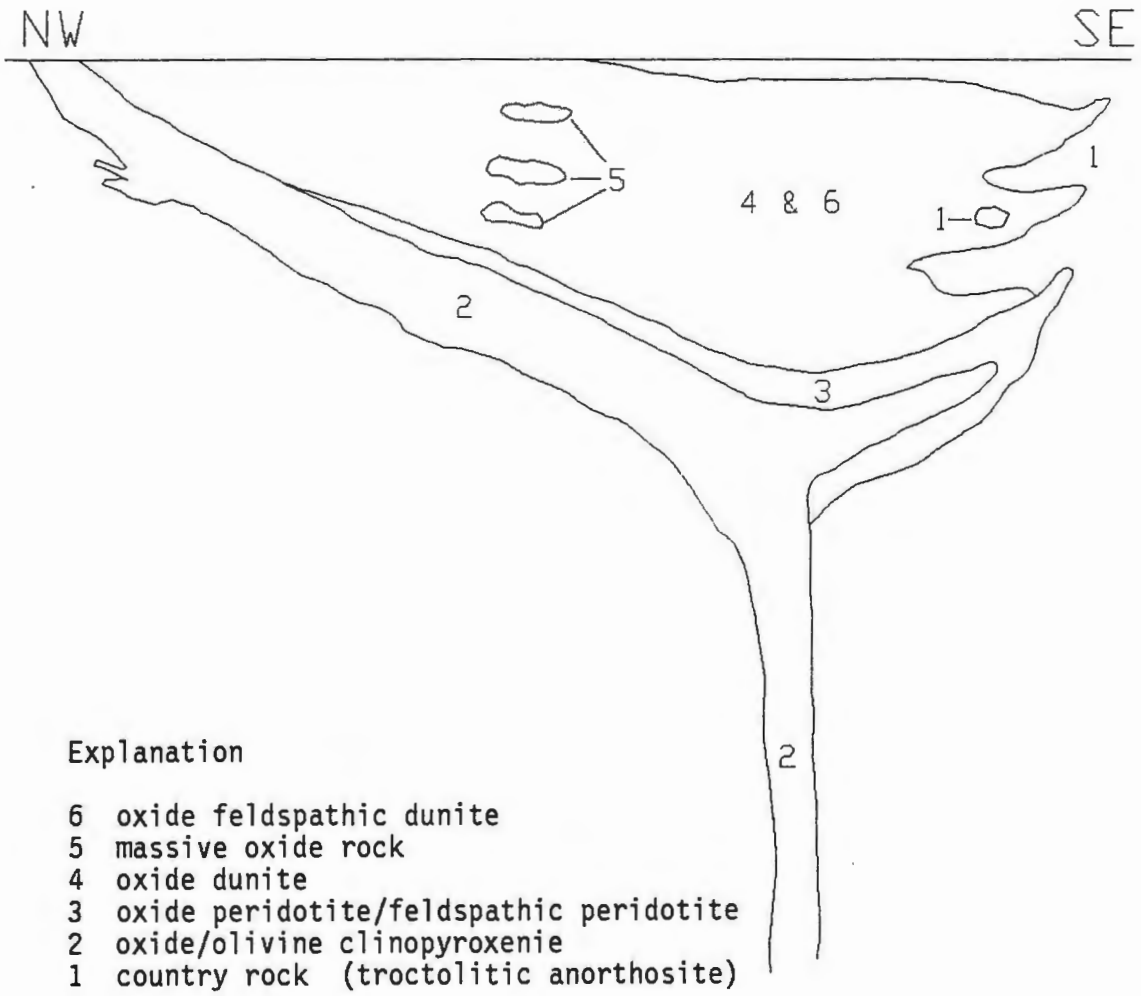

Although no textural evidence of major faulting was observed either in the mapping of the country rock or in drill core to account for the path of origin of the Longnose Peridotite, the textural evidence in drill core demonstrates that the Longnose Peridotite is intrusive in nature. A zone of weakness, such as a fault, would provide a path for the intrusion.

Severson (1988) delineated a series of inferred faults in the Partride River troctolite and surrounding Virginia formation. One of these faults, noted as fault #1, starts in Sec. 9, T. 59 N., R. 13 W., and strikes to the SE where it cuts through the Long Ear and terminates at the Longnose Peridotite. The fault is interpreted to be pre-Duluth Complex? in age and its motion being down on the SW block and up on the NE block. Reactivation of the fault during syn to post - Duluth Complex would provide a conduit for the intrusion of the Longnose Peridotite (and Long Ear).

Chapter 6

Mineral Chemistry

A. Introduction and methods

This chapter deals with compositions of olivine, plagioclase, augite, ilmenite and the spinel group minerals titanomagnetite and pleonaste. Selected mineral grains on ten polished thin sections were analyzed on a fully automated Jeol JSM 35c SEM with a Kevex-ray 3203-35 energy dispersive system. The standards are natural minerals and synthetic products of independently determined composition (App. 5). The operating conditions were 15 kV accelerating voltage and a current of 50 nA. All analyses were made with about a 5 um beam, except for the analyses of spinel and in some cases of titanomagnetite in which a spot beam of approximately 1 um in diameter was used. Approximately 167 analyses were made. The raw data were corrected by the Bence & Albee (1968) method. The oxide analyses were further corrected for Fe_2O_3 by standard stoichiometric recalculations.

B. Results

The composition of olivine in the ultramafic rocks ranges between 60-66 mole percent Fo (App. 6). Despite a small total range, the Fo content of the olivine appears to increase systematically (based on the six samples analyzed) in drill hole LN-2 going up section from Fo 60% at 455.5′ in pyroxenite to a maximum of Fo 66% at 254.0′ in oxide dunite, and then gradually decreasing to Fo 64% at 59.2′ in feldspathic dunite (App. 6). In the three troctolitic anorthosite samples of the country rock, Fo ranges between 59 and 62 mole percent. Traverses made across olivine grains with banded undulatory extinction indicated no

chemical zonation. In relation to other troctolitic and gabbroic rocks in the Duluth Complex, the Fo content in the Longnose Peridotite is similar in composition (Table 2), however, compared to the composition of other peridotitic rocks in the Duluth Complex (Weiblen and Morey, 1980, Bonnichsen, 1972), the Fo content in the Longnose Peridotite is considerably higher, although it is within the range of the basal dunite in the Water Hen (Table 2). Compared to the Duke Island ultramafic complex in S.E. Alaska (Irvine, 1967), the Fo content in all rocks of the Longnose Peridotite is considerably less (Table 2).

Compositional ranges of augite area also very small within and between rock types (App. 6.1). In an individual grain, analyses were made in areas of exsolved ilmenite rods, and on the edge of the grain where the edge was devoid of ilmenite rods. The zones with exsolved ilmenite show a slightly higher ferrosilite content (up to 4% higher) with the exception of sample 12119-3. Results are plotted on a Wo-Fs-En diagram (Fig. 48). Compared to other mafic and ultramafic bodies in the Duluth Complex, the Longnose Peridotite is slightly richer in enstatite content, but compared to the Duke Island ultramafic complex, the Longnose Peridotite is richer in ferrosilite component (Table 2).

The anorthite content of plagioclase ranges from An 50 to An 76 in the ultramafic rocks, and between An 57 to An 81 in troctolitic anorthosite (App. 6.2). The An content varies as much as 14% within a grain with patchy zonation, and up to 20% An between grains with patchy zonation. Mainwaring (1975) reports a range in composition of up to 10 mole percent anorthite in individual grains with patchy zonation in the

TABLE 2

Mineral Chemistry comparisons between the Longnose Peridotite and other mafic and ultramafic rocks

Mafic rocks

Area	Author	Rk type	Ol(Fo%)	Plag(An%)	En	Fs	Wo
DC-Babbitt	Hardyman (1969)	troc-gb	44-67	50-64	38-47	12-21	39-48
DC-Babbitt	Tyson (1979)	troc	33-72(63)		28-51	5-31	35-46
DC-Duluth	Taylor (1964)	gb	53-61	53-65	36-45	18-26	35-39

Ultramafic rocks

DC-Longnose Per. (This thesis)		dun-pxt-per	60-66	50-77	40-43	13-15	43-36
DC-Water Hen		basal zone	56-62	80-84			
Mainwaring & Naldrett (1977)		basal dun	63	-	-	-	-
		layered	50-60	40-75	-	-	-
Boulder Lk	Bonnichsen (1972)	per	41-50	50-65	33-40	18-24	41-49
DC-Duluth	Weiblen & Morey (1980)	per	55		42	17	41
Duke Island	Irvine (1967)	dun	91-81				
		ol cpx	84-78		44	8-9	47-48
		per	83-79		43	10	48

Abbreviations

Rock types

Dc----------Duluth Complex
dun----------dunite
gb----------gabbro
ol cpx----------olivine clinopyroxenite
per----------peridotite
pxt----------pyroxenite
troc----------troctolite

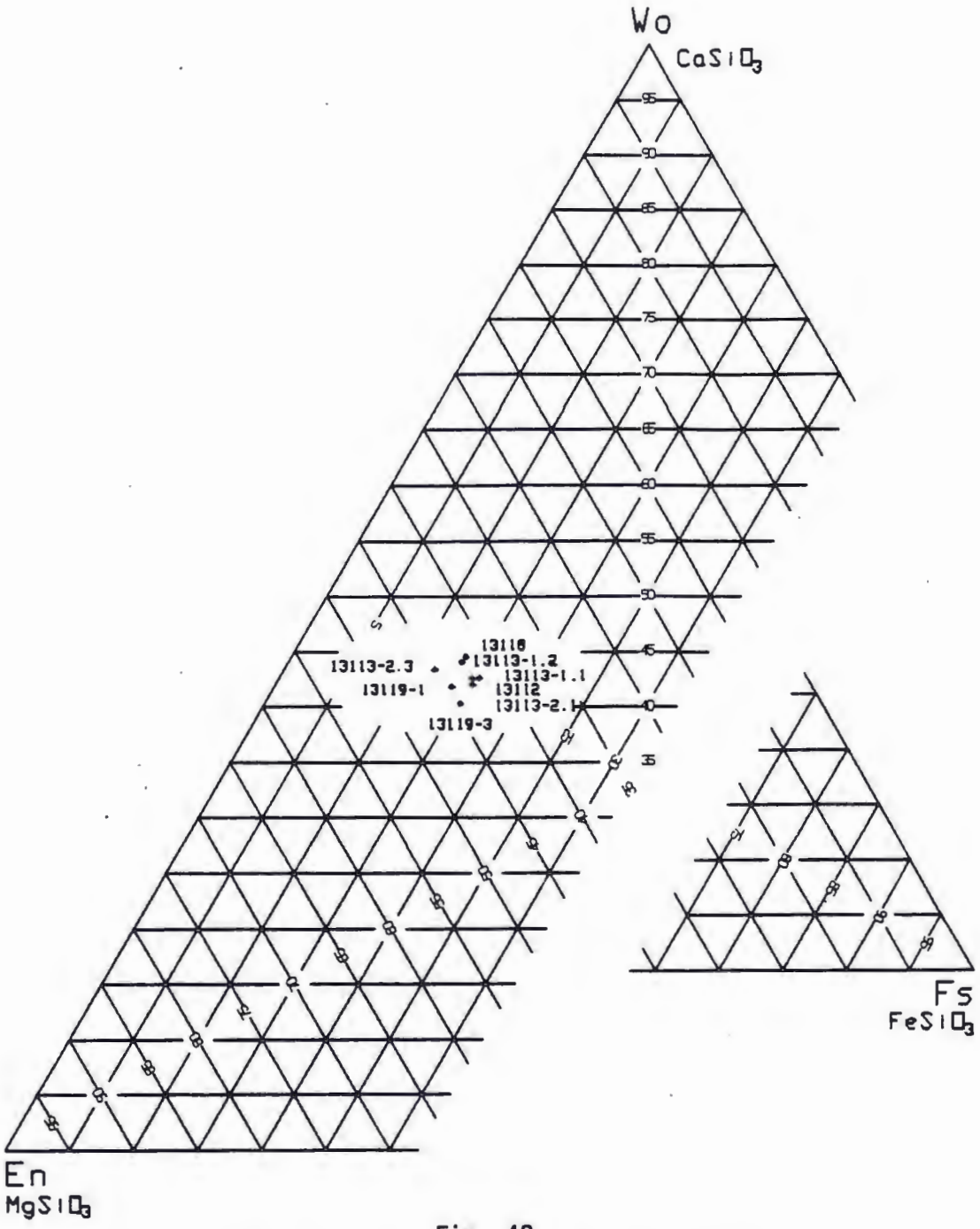

Fig. 48

En - Fs - Wo plot of augite samples

Water Hen intrusion. Some plagioclase from troctolitic rocks in the Kiglapait intrusion show reversed zonation with a composition gradient of 28% anorthite content over a distance of 40 um within an individual grain. This difference is attributed by Morse (1984) to a low diffusion coefficient for intracrystalline exchange of NaSi and CaAl. The large difference in An content within samples makes it difficult to identify any trends between rock types in the Longnose Peridotite. In relation to other mafic and ultramafic rocks in the Duluth Complex (Table 2), the plagioclase in the Longnose Peridotite and associated country rock has similar compositions (labradorite) with the exception of sample 13120 (An 81), which is exceptionally high.

Ilmenite is close to its end member composition and shows only minor chemical variation. The major solid-solution affecting ilmenite is Mg and Fe+3 (Pasteris, 1985). MgO ranges from 1.55 to 3.50 wt %, and Fe_2O_3 ranges from 7.17 to 11.11 wt % (App. 7.0-7.1). Chemical analyses done by Hardyman (1969) with ilmenite from the South Kawishiwi intrusion yielded 0.6-3.9 wt % MgO and 0.8-6.4 wt % Fe_2O_3. In respect to Hardyman's findings, the ilmenite in the Longnose Peridotite is thus similiar in MgO content but is higher in Fe_2O_3 content. FeO increases at the expense of Fe_2O_3 from pyroxenite to peridotite, then decreases slightly in oxide dunite. TiO_2 content does not display any systematic trends in drill hole LN-2.

The major trace element in ilmenite is V (0.18-0.67 wt % V_2O_3), and is restricted to ilmenite in the country rock and the feldspathic dunite at the top of drill hole LN-2. The presence of Al is now

associated with minute (exsolution) lamellae of spinel.

V and Cr contents are higher in titanomagnetite (1.36-2.49 wt % V_2O_3, and 0-4.76 wt % Cr_2O_3) than in ilmenite (App. 7.2). Titanomagnetite in pyroxenite and peridotite display slightly lower values of Mn and Cr, and higher values of wt % FeO relative to titanomagnetite in oxide dunite. As in the case of ilmenite, the Al content is thought to be associated with the spinel lamellae. According to Reynolds (1985 b), the Cr content, as well as the Al, could result by preferential partioning of these two elements into coexisting titanomagnetite during cystallization and subsequent subsolidua reequilibration. Spot analyses of exsolution-oxidation ilmenite lamellae in titanomagnetite found them to be enriched in spinel component associated with the lamellae.

Pleonaste is about 50% spinel ($Mg_{1/2}$ $Fe_{1/2}$ Al_2 O_4) in composition (App. 7.3). All spinels analyzed were hosted by titanomagnetite.

C. Interpretation

The origin of the Longnose Peridotite must account for the stratigraphy of the rock types and their mineralogy. The mineralogy of the Longnose Peridotite is similar to other troctolitic, gabbroic, and dunitic rocks (Water Hen intrusion) in the Duluth Complex. Chemically, the Longnose Peridotite has a higher Fo content than other peridotitic bodies, with the exception of the basal dunite in the Water Hen intrusion. The Longnose Peridotite resembles the ultramafic bodies of S.E. Alaska in many aspects. Both intrude older gabbroic bodies, have similar zonal arrangement of rock types, and display a systematic decrease in Fo content of the olivine going from a core of dunite

outward to pyroxenite (although the Fo content of the olivine in the Longnose Peridotite is considerable less). The Longnose Peridotite is also similar to the Water Hen intrusion in many aspects. Both bodies are similar in size. In plan view the Water Hen measures approximately 1600′ (487 m) by 500′ (152 m) and is 700′ (213 m) in depth. The Longnose Peridotite is 2500′ (762 m) by 1600′ (487 m), narrowing to 250′ (76.2 m) in plan view, with a depth of up to 448′ (136 m). Both bodies have marginal zones which are complicated in their stratigraphy and are rich in inclusions, olivine lacks compositional zoning, and the An content of plagioclase is quite variable within grains with patchy zonation. Major differences between the two bodies include the relative abundance of titanomagnetite in the Longnose Peridotite and the crude reversal of the two bodies stratigraphy. The Longnose Peridotite consists of a core of oxide dunite and feldspathic dunite which is enclosed by successive zones of oxide peridotite and clinopyroxenite going outward. The Water Hen intrusion consists of a basal plagioclase-ilmenite rock, overlain by a few hundred feet of dunite, above which is a layered sequence of troctolite and peridotite (Mainwaring, 1975). The Water Hen intrusion is thought to have been emplaced before the host troctolite had undergone much cooling as chilled or recrystallized margins are lacking (Bonnichsen, 1972).

The shape, distribution, and mineralogy of the oxide zones within the Longnose Peridotite impose certain constraints on its origin. The limited stratigraphic continuity between oxide bodies suggests that the oxide bodies are themselves discordant. The origin of discordant bodies composed largely of Fe-Ti oxides is disputed. Bateman (1951)

entertains the idea that formation of Fe-Ti rich aggregates is due to late gravitative liquid accumulation of a residual magma rich in Fe-Ti. Lister(1966) holds that the discordant oxide deposits he studied were formed by a variety of igneous processes. 1)accumulation by a Fe-Ti rich liquid by filter pressing or immiscible liquid, 2) injection of a Fe-Ti rich liquid, and 3) injection of a Fe-Ti rich basic pegmatite. In the Bushveld complex, Fe-Ti rich pegmatitic bodies are also thought to be intrusive in origin (Willemse, 1969, Viljoen, 1985), although many replacement models by metasomatism are also postulated (Cameron and Desborough, 1964, Irvine 1982). Philpotts (1967) established that phosphorus-rich Fe-Ti liquids may be immiscible in certain basaltic systems. In low phosphorus, low titanium tholeiitic magmas undergoing fractionation at low pressures, immiscibility is the rule rather than the exception (Philpotts and Doyle, 1983). If these conditions were valid for the Longnose Peridotite, it could explain the formation of the oxide zones. Reynolds (1985a) believes that concordant titaniferous magnetite rich layers are the result of fractional crystallization processes that resulted in concentration of Fe, Ti, and V in the residual magma. Precipitation of this liquid is the result of episodic increases in fO_2.

The genesis of oxide zones in LN-2 must account for 1) gradational and sharp contacts between oxide zones and silicate zones, 2) differences in the ilmenite.titanomagnetite ratio among oxide zones and change in the ratio within a zone.

In drill hole LN-2, the oxide texture changes in some instances from disseminated to net-textured to massive. In oxide dunite,

ilmenite is the dominant oxide (App. 3), but in the semi-massive dunitic oxide rock and massive oxide rock the ilmenite-titanomagnetite ratios change readily. The formation of oxide zones by an immiscible Fe-Ti phosphorus-rich liquid is rejected because apatite is a very minor accessory mineral, and was not observed in oxide zones. However, inclusions of round blebs of ilmenite in cumulate olivine and silicate blebs in oxides may suggest some liquid immiscibility.

The distribution and composition of primary opaque oxides in igneous rocks depends for the most part on initial titanium abundance and on the fO_2. The limiting factors chiefly responsible for the compositional variations between ilmenite and titanomagnetite are the initial ratios of Fe+2. Fe+3 and Fe.Ti which are dependent on temperature and fO_2 (Haggerty, 1976b). The abundance of titanomagnetite with exsolved ilmenite indicates that the oxides exsolved in an environment with a relatively high fO_2. The abundance of ilmenite suggests that it formed as a primary phase (along with titanomagnetite) from a Ti-Fe rich liquid. The annealed textures of both oxides in massive oxide zones suggest that both underwent annealing at subsolidus temperatures.

The textures, different modal amounts of the oxides within a given oxide zone, and the discordant nature of the oxide zones could be accounted for by either filter pressing or primary precipitation of the oxides in place with relatively little movement. Both processes would necessitate an environment with changing oxygen fugacity and variation in the composition of the magma. Both of these conditions could be met by multiple impulses of magma. The pegmatitic nature of the silicates

and presence of primary hornblende associated with the oxide zone at the base of LN-5 suggest that a hydrous, Fe-Ti rich fluid was involved in this specific case.

The layering in the Longnose Peridotite cannot be explained by any simple mechanism of fractional crystallization. The absence of lateral continuity of rock types and contradictory age relationships in the marginal zones that deviate from the typical sequence of clinopyroxenite - oxide peridotite - oxide dunite and feldspathic dunite, going up section, the absence of igneous foliation, and the rapid variability of mineral modes within rock types suggest that the body could have a similiar history to the Water Hen intrusion. Mainwaring and Naldrett (1977) suggest that the Water Hen intrusion formed by multiple injections of magma, the magma possibly containing abundant suspended crystals.

The Longnose Peridotite is interpreted to have been injected in three stages into the Duluth Complex (see interpretation, Ch. 5). The relatively small variation in olivine composition (7%) and augite between the oxide dunite/feldspathic dunite (first stage) and oxide clinopyroxenite (third stage) suggest that the magma of the Longnose Peridotite had not undergone extreme crystal fractionation before emplacement. The apparant systematic variation in Fo content of olivine in LN-2 may represent minor cryptic mineral variation or be the result of inadequate number of chemical analyses. The similarity of silicate mineral compositions in the Longnose Peridotite and the country rock (Duluth Complex) suggests that the basaltic magma from

which the Duluth Complex formed is also the source of the Longnose Peridotite.

Chapter 7

Summary and Conclusions

The Longnose Peridotite is a crudely zoned, titaniferous oxide-rich ultramafic complex hosted by the Partridge River troctolite (PRT) -- an intrusion of the troctolitic series which occurs near the base of the Duluth Complex.

Gravity data and drill cores delineate the body to be tear drop in shape, measuring about 760 m long and narrowing from 490 m at the widest point to 76 m at the narrowest point. The body has a maximum thickness of 167 m based on drill core. The intrusion can be divided mineralogically into 6 rock types. The relationships between rock types leads to a stratigraphic division of three main zones. These zones are, going up section, 1) oxide clinopyroxenite, 2) oxide peridotite, and 3) oxide dunite with or without oxide rock/ oxide feldspathic dunite -- picrite. This stratigraphy can be explained by three stages of magma injection.

The intrusive nature of the Longnose Peridotite is demonstrated in drill core by 1) apophyses of Longnose Peridotite stringers into the PRT, 2) PRT xenoliths in the Longnose Peridotite, which although commonly are unaltered, may display minor to pervasive alteration, and 3) lack of igneous foliation in the Longnose Peridotite. The Longnose Peridotite is interpreted to have been intruded as a crystal mush with intercumulate liquid acting as a lubricant. Evidence of a crystal mush is tentative, and includes the bimodal grain size of olivine in oxide dunite (this could also be explained by adcumulate overgrowth on one or more olivine grains to result in a larger grain) and the presence of

phenocrysts of plagioclase in oxide clinopyroxenite and oxide peridotite. Some of the plagioclase displays bent albite twins.

The proposed model for the genesis of the Longnose Peridotite is constrained by its petrographical, stratigraphic, and mineralogical characteristics. The ultramafic rocks are texturally heteradcumulates. Extreme adcumulate overgrowh has destroyed any euhedral augite crystals in oxide pyroxenite and oxide peridotite. In oxide dunite and oxide feldspathic dunite, adcumulate overgrowth or recrystallization of several smaller, euhedral olivine grains has resulted in large, unzoned, anhedral olivine. Plagioclase is an intercumulate precipitate in feldspathic dunite, but in other rock types appears to be phenocrystic in nature because of its large size and paucity in relation to other silicate and oxide minerals. The oxides ilmenite and titanomagnetite form disseminated to net-textured grains, and locally are massive in texture.

The first stage consisted of an impulse of feldspathic dunite/oxide dunite with local zones of oxide rock. The second stage consisted of an impulse of oxide peridotite beneath the oxide dunite. During the third stage an impulse of oxide clinopyroxenite was emplaced primarily beneath the oxide peridotite and also as apophyses. These apophyses enter all previous rocks, including the PRT.

Oxide rocks contain more than 51% of the oxides ilmenite and titanomagnetite. The ratio of these two minerals in oxide zones varies between 100% ilmenite to 100% titanomagnetite. Oxide zones are hosted predominately by dunitic rocks and to a lesser extent by clinopyroxenitic rocks. The zones vary from a maximum thickness of 30

m with a lateral extent of 130 m to less than 0.1 m in thickness. The lateral extent of most oxide zones is not known as the zones cannot be correlated between drill cores. This lack of continuity leads to the conclusion that the oxide zones are discordant in nature.

Similarity of mineral chemistry of the silicate minerals olivine, augite, and plagioclase between the Longnose Peridotite and other Duluth Complex rocks suggest that the basaltic magma from which the Duluth Complex formed is also the source of the Longnose Peridotite. Whole rock chemical analysis of the Longnose Peridotite is needed to further establish the petrology between the Longnose Peridotite and the Duluth Complex.

The basaltic magma must account for the Ti-Fe rich nature of the Longnose Peridotite. This could be done by the magma undergoing a period of fractional crystallization resulting in the concentration of substantial amounts Fe, Ti, and V in the body. The formation of the oxide zones is dependant on the Fe_2O_3/FeO ratio of the liquid which is, in turn, a function of the fO_2, temperature, and water content of the fractionating magma (Reynolds, 1985a). Massive oxide zones could form by a combination of processes or by just one process, 1) precipitation of copious amounts of Ti-Fe oxides as a result of episodic increases in the fO2 (Reynolds, 1985a), 2) late-stage injection of Fe-Ti rich fluid, or 3) by gravitative settling of individual oxide grains and/or development of oxide chains resulting in net-texture. Petrographic study of the oxide — silicate relationships suggest that processes 1 and 3 were involved in the formation of the oxide zones. Subsequent annealing to various degrees at elevated subsolidus temperatures could

result in the development of a wide range of ilmenite and spinel intergrowths in titanomagnetite. The type and relative abundance of these intergrowths reflect (in most cases) the composition of the oxides and the fO_2 conditions that existed during subsolidus cooling. Deuteric alteration consists largely of serpentinization (from 10% - 100%).

Although no textural or stratigraphic evidence of major faulting was observed either in the mapping of the country rock or in drill core to account for the pathway fo the magma in forming the Longnose Peridotite, an inferred fault delineated by Severson (1988) of pre-Duluth Complex age is shown to cut through the Long Ear intrusion and terminates at the Longnose Peridotite. This fault could have served as a conduit for the injection of the Longnose Peridotite.

REFERENCES

Bateman, A.M., 1951, the formation of late magmatic oxide ores. Econ. Geol., v. 46, p. 404-426.

Bence, A.E., Albee, A.L., 1968, Empirical correction factors for the electron microanalysis of silicates and oxides. Jour. Geol., v. 76, p. 382-403.

Bonnichsen, B., 1972, Southern part of Duluth Complex. in P.K. Sims & G.B. Morey eds., Geology of Minnesota. A Centennial Volume. Minn. Geol. Survey, St. Paul, MN., p. 261-287.

----1974, Geology of the Ely-Hoyt Lakes District, NE Minnesota. Minn. Geol. Survey, open-file.

Buddington, A.F., Lindsley, D.H., 1964, Iron-titanium oxide minerals and synthetic equivalents. Jour. of Petrology, v. 5, p. 310-357.

Cameron, E.N., and Desborough, G.A., 1964, Origin of certain magnetite-bearing pegmatities in the eastern part of the Bushveld Complex, South Africa. Econ. Geol., v. 59 p. 197-225.

Cooper, R.W., 1978, Lineament and structural analysis of the Duluth Complex, Hoyt Lakes-Kawishiwi area, northeastern Minnesota. unpub. Ph. D. Thesis, Univ. of Minnesota, 280 p.

Green, J.C., 1983, Geologic and geochemical evidence for the nature and development of the Middle Proterozoic (Keweenawan) midcontinent rift of North America. Tectphys, v. 94, p. 413-437.

Green, J.C., Phinney, W.C., & P.W. Weiblen, 1966, Gabbro Lake quadrangle, Lake county, Minnesota, 1.31680, Geol. Survey Misc. Map M-2.

Grout, F.F., 1950, The titaniferous magnetites of Minnesota. Iron Range Resources and Rehabilitation Comm., St. Paul, MN., 117 p.

Haggerty, S.E., 1976 a, Oxidation of opaque mineral oxides in basalts, Rumble III, D., ed., Oxide minerals. Mineralogical Society Amer., Short Course Notes, v. 3, p. 1-100.

----1976 b, Opaque mineral oxides in terrestrial igneous rocks, Rumble III, D., ed., Oxide minerals. Mineralogical Society Amer., Short Course Notes, v. 3, p. 101-276.

Hardyman, R.F., 1969, The petrography of a section of the basal Duluth Complex, St. Louis County, northeastern Minnesota. M.S. thesis, Univ. Minnesota, Minneapolis, Minnesota, 132 p.

Holst, T.B., Mullenmeister, E.E., Chandler, V.W., Green, J.C., and Weiblen, P.W., 1986, Relationship of structural geology of the Duluth Complex to economic mineralization. Minnesota DNR & NRRI, University of Minnesota, Duluth, unpub., 86 p.

Irvine, T.N., 1967, The Duke Island ultramafic complex, southeastern Alaska, Wyllie, P.J., ed., Ultramafic and related rocks. John Wiley & Sons, New York, p. 84-121.

----1974, Petrology of the Duke Island ultramafic complex, southeastern Alaska. Geol. Soc. America Mem. 138, 240 p.

----1982, Terminology for layered intrusions. Jour. Petrology, v. 23, p. 127-162.

Jackson, E.D., 1961, Primary textures and mineral associations in the ultramafic zone of the Stillwater Complex, Montana. USGS Prof. Paper, 358, 106 p.

Lister, G.F., 1966, The composition and origin of selected iron-titanium deposits. Econ. Geol., v. 61, p. 275-310.

Mainwaring, P., 1975, The petrology of a sulfide-bearing layered intrusion at the base of the Duluth Complex, St. Louis County, Minnesota. Ph.D Thesis, Univ. of Toronto.

Mainwaring, P.R., and Naldrett, A.J., 1977, Country rock assimilation and the genesis of Cu-Ni sulfides in the Water Hen intrusion, Duluth Complex, Minnesota. Econ. Geol., v. 72, p. 1269-1284.

Mancuso, J.D., and J.D. Dolence, 1970, Structure of the Duluth Gabbro Complex in the Babbitt area, Minnesota. Annual Institute Lake Superior Geo., abstracts, 16th Proceedings, p. 27.

Morey, G.B., 1972, Middle precoambrian general geologic setting. in P.K. Sims & G.B. Morey eds., Geology of Minnesota. A Centennial Volume. Minn. Geol. Survey, St. Paul, MN., p. 199-203

Morse, S.A., 1969, The Kiglapait layered intrusion, Labrador. Geol. Soc. America Mem. 112, 204 p.

----1984, Cation diffusion in plagioclase feldspar. Science, v. 229, p. 504-505.

Nathan, H.D., 1969, Geology of a portion of the Duluth Complex, Cook county. Univ. of Minnesota-Minneapolis, unpub. Ph.D Thesis, 198 p.

Pasteris, J.D., 1985, Relationships between temperature and oxygen fugacity among Fe-Ti oxides in two regions of the Duluth Complex. Can. Mineralogist, v. 23., p. 111-127.

Philpotts, A.R., 1967, Origin of certain iron titanium oxide and apatite rocks. Econ. Geol., v. 62, p. 303-315.

Philpotts, A.R., and Doyle, C,D., 1983, Effect of magma oxidation state on the extent of silicate liquid immiscibility in a tholeiitic basalt. Amer. Jour. Sci., v. 283, p. 967-986.

Phinney, W.C., 1969, The Duluth Complex in the Gabbro lake quadrangle, Minnesota. MGS Rept. Inv. RI-9, St. Paul, MN., p. 20.

----, 1972, Duluth Complex, history and nomenclature. in P.K. Sims G G.B. Morey, eds., Geology of Minnesota. A Centennial Volume. Minn. Geol. Survey, St. Paul, MN., p. 333-345.

----1984, personal communication.

Reynolds, I.M., 1985 a, The nature and origin of titaniferous magnetite-rich layers in the upper zone of the Bushveld complex. A review and synthesis. Econ. Geol., v. 80, p. 1089-1108.

----1985b., Contrasted mineralogy and textural relationships in the uppermost titaniferous magnetite layers of the Bushveld complex in the Bierkraal area north of Rustenburg. Econ. Geol., v. 80, p. 1027-1048.

Severson, M.J., 1988, Geology and Structure of portion of the Partridge River intrusion. Technical Report, NRRI./GMIN-TR-88-08, Duluth, MN., 78 p.

Severson, M.J., and S.A. Hauck, 1990, Geology, geochemistry, and stratigraphy of a portion of the Partridge River intrusion. NRRI, Duluth, MN., 236 p.

Stark, J.R., 1977, Surficial geology and groundwater geology of the Babbitt-Kawishiwi area, northeastern Minnesota with planning implications. Unpub. M.S. thesis, Univ. Of Wisconsin, Madison, 103 p.

Taylor, R.B., 1964, Bedrock geology of Duluth and vicinity, St. Louis county, Minnesota. Geologic Map series GM-1, Minn. Geol. Survey, Minneapolis, MN., p 12.

Tyson, R.M., 1979, The mineralogy and petrology of the Partridge River troctolite in the Babbitt-Hoyt Lakes region of the Duluth Complex, northeastern Minnesota. Unpub. Ph.D, Miami Univ., 179 p.

Ulland, W., 1985, personal communication.

----1986, personal communication.

Viljoen, M.J., and Scoon, R.N., 1985, The distribution and main geologic features of discordant bodies of iron-rich ultramafic pegmatite in the Bushveld Complex. Econ. Geol., v. 80, p. 1109-1128.

Von Gruenewaldt, G., Klemm, D.D., Henckel, J., and Dehm, R.M., 1985, Exsolutioon features in titanmagnetites from massive magnetite layers and their host rocks of the upper zone, eastern Bushveld Comple. Econ. Geol., v. 80, p. 1049-1061.

Wager, L.R., Brown, G.M., and Wadsworth, W.J., 1960, Types of igneous cumulates. Jour. of Petrology, v. 1, p. 73-85.

Weiblen, P.W., and G.B. Morey, 1980, A summary of the stratigraphy, petrology, and structure of the Duluth Complex. Am. J. Sci., 280-A, p. 88-133.

Willemse, J., 1969, The geology of the Bushveld igneous complex, the largest repository of magmatic ore deposits in the world. Econ. Geol., Mon. 4, p. 9-22.

Wright, H.E., Jr., 1972, Physiograpy of Minnesota. in P.K. Sims & G.B. Morey eds., Geology of Minnesota. A Centennial Volume. Minn. Geol. Survey, St. Paul, MN., p. 561-577.

Appendix 1

Mineral modes in outcrop and thin sections

sample #	plag	ol	aug	opx	oxides	biot	other
Unit 1							
otc.	75-87(77)	10-25(20)	0-5(2)	0-2(1)			
14495	86(An69)	10	3	0	1	0	0
Unit 2A							
otc.	68-83(0)	12-20(15)	5-12(7)	0	tr-2(.5)	1-2(1)	0
14490-36A*	80(An73)	4.7	9.8	0	1.2	.6	3.7
14490-36B	81(An)	6.0	10	0	1.0	0.5	1.5
14490-36C*	76.1(An71)	7.5	13.3	2	0.4	0.7	0
14491-37	79.1(An66)	17.9	0.4	1.0	1.6	0	0
Unit 2B							
otc.	55-70(65)	15-25(16)	15-20(19)	0	tr	0	0
1449(hnf)	68	15	17	0	tr	0	0
(tct)	73(An67)	25	2	0	tr	0	0
Unit 3							
otc.	87-93(92)	5-10(7)	0-3(1)	0	tr	0	0
14500	92(An75)	7.7	0	0.2	0.1	0	0
Unit 4							
otc.	65-80(75)	10-20(13)	5-15(10)	0	2	0	0
14489*	74.9(An70)	11.5	8.6	0	3.3	0	1.7(hbl)
14504	76	10	12.5	0	1	0.5	0
Unit 5							
otc.	80-90(87)	5-15(8)	3-10(5)	0	tr	0	0
Unit 6							
otc.	65-72(69)	28-35(30)	0-3(tr)	0	tr	0	0
14492*	67.8(An71)	29.6	2.5	0	0.1	0	0
Unit 7							
otc.	56-88(72)	12-46(25)	0-5(2)	0	0-2(tr)	0	0
14503	75(An73)	23	0.3	1.5	0.2	0	0
14494*	75.2(An70)	22.5	0.7	0.4	0.5	0	0.7(sym)
14996-52A*	82.2(An71)	16.6	0.6	0.5	0.1	0	0
14495-52B*	87.2(An71)	11.2	0.1	1.1	0.4	0	0
14496-52C	83(An72)	13	1	0.7	1.5	0.3	0.5(sym)
14496-52D*	80.6(An70)	14.4	3.8	1.1	0.1	0	0
14496-52E	see 52D*.						

Appendix 1.1

Unit 8							
otc.	5-60(30)	40-95(70)	0	0	2-5(3)	0	0
14497	37(An69)	55	0	0	8	0	0
Actinolite Vein							
14488	72(An71)	7	0	0	2	tr	18(act, talc,chl, ser)
14501	70	0	0	0	2	1	24(act) 3(chl)

Abbreviations and Explanation

* --------based on 1000 point counts
act ------actinolite
(An71) ---anorthite content of plagioclase
chl ------chlorite
hbl ------hornblende
hnf ------hornfels portion of thin section
otc ------the range and average (in parenthesis) of minerals estimated in outcrop
ser ------sericite
(sym) ----symplectite of plagioclase and oxides
tct ------troctolitic portion of thin section
(tr) -----mineral occurs in amounts of less than 1%

Appendix 2
Modal abundances of minerals by volume in thin sections fom drill hole LN-2

				Primary minerals				Alteration minerals					
spl type	spl #	rk	depth	ol/serp	plag	aug	ox	act/trem	ser	chl	biot	hbl	other
tpPT	13016	6	59.2	13/6	20	*	25	8		16	1	5	4 sym, sp
t	13017	6	64.2	17/8	21	5	20	6		15	1	5	
tp	13018	4	97.0	30/44		*	17		4	1.5		1	2.5 carb/hm
t	13019	4	109.0	13/5	5		55	1	4	11	1		5
tpPT	13020	4	170.2	35/50			15	*					
tp	13021	5	194.3	0/49			38			3		3	7 talc/hm/br-pn
tp	13022	5	205.0	0/17			80			1			2 carb/?
t	13023	4a	209.7	2/59		1	10			7	2	1	12 carb/talc/hm/?
t	13024	4	249.5	38/38			16			4			4 carb/talc
PT	13025	4	254.0	35/52			10			2.5			tr talc
t	13026	4a	257.0	9/20			40			28			3 carb/talc/hm
tpPT	13027	4a	301.0	0/53			40			2			5 ?
t	13029	4	405.5	15/60			22			3	*		
tPT	13030	3	418.2	28/7		45	20			*		tr	
tPT	13031	3	430.0	17/3		43	32					2	3 carb/talc/hm
LT	13032	A	440.0	2/*	5	8	5			*	5	7	68 epd/clay/carb/talc/ap
tPT	13033	3	448.5	60/2		12	21					4	5 clay/talc/ox
tPT	13034	2	455.5	*/1		76	10	3		1		8	1 talc
tp	13036	2	507.5			78	12			3		5	2 clay/carb
tp	13037	2	555.8		1	79	10	*		3	*	2	6 carb/talc/hm/clay
*t	13038	2B	555.9	10/?	3	6	20	24	27	5			5 talc/br
tp	13038	1B	555.9	7/1	65	4	7		16			tr	
tp	13039	1	561.5	12/*	65	4	5	2	16	1	*	1	* ap
LT	13040	2	534.2	*/5		84	8	*		1	*		2 carb/talc/sp
LT	13041	2	516.5										see spl 13040

Appendix 2.1
Modal abundances of minerals by volume in thin sections for drill hole LN-6

				Primary minerals				Alteration minerals					
spl type	spl #	rk	depth	ol/serp	plag	aug	ox	act/trem	ser	chl	biot	hbl	other
t	13075	1	52.1										
tp	13076	6	130.7	60/15	14		6		3			2	
t	13077	4	130.8	10/74	6		5			1	1	1	2 talc/carb
tPT	13078	6	167.1	ND									
tp	13079	4s	168.0	0/75	3		18			1	1	1	1 hm
t	13080	6	171.7	19/55	15		6	1			1	1	2 hm
t	13081	4	174.7	ND									
t	13082	C	212.2	8/10	10		5			27	*	*	40 talc
t	13083	D	218.0	8/5	20		55		3	2	1	1	5 talc/carb
t	13084	E	246.8										100 clay/carb/chl/toum
t	13085		328.3	ND									
tp	13086	6	371.0	69/2	6		17	*		5		*	1 talc/carb
tp	13087	6a	374.2	0/21			75				2	*	2 talc/carb
tp	13088	4	387.2	26/37			34			1		2	carb/hm
tp	13089	5	387.4			5	80	*				3	12 talc/carb/chl/serp/ap
tp	13090	4	398.1	66/7			20			2	1	2	2 talc/carb
t	13091	F	399.5										
t	13092		401.1	86/*			10			2			2 talc/carb
tp	13093	4	402.5	65/25			9				1		
t	13094	4G	408.2										
tp	13095	3	447.0	21/5		35	29				3	2	5 talc/ap/pleo/her
tp	13096	3	464.1	42/4		30	20			1		3	carb
t	13097	3	466.5	55/5		28	6			1		2	3 talc/carb
t	13098	3	468.7	45/4		40	7			2	*	1	1 talc/hm
tp	13099	1	494.7		7	25	30						38 clay/her
tp	13100	4	499.2	50/6	1	2	23			14		2	2 her/sch
tp	13101	2a	518.2	4/*		40	43			*		*	12 talc/carb/her
tp	13102	4	524.5	59/6	5	2	18		7	*		2	1 talc
tp	13103	3os	554.0				93			4			3 her
t	13104	1	573.1	17/3	35	13	20		8			2	2 clay
tp	13105	3	581.6	6/*		66	15		8			2	3 clay
tp	13106		581.7	10		72	18						

Appendix 2.2

Modal abundances of minerals by volume in thin sections for drill hole LN-5

				Primary minerals				Alteration minerals					
spl type	spl #	rk	depth	ol/serp	plag	aug	ox	act/trem	ser	chl	biot	hbl	other
t	13042	4	70.2	11/79			3			*	3	1	3 ox/hm/cc/epd
t	13043	3	89.9	30/40		20	5			*	*	3	1 talc
tp	13044	3	107.5	25/55	5	10	3			2			1 sd
tp	13045	4	111	30/48		8	8			1		2	3 hm
tp	13046	4	119	20/50	12	5	4	1		3	1	1	3 cc/hm
t	13047	4	119.9	70/20	3		5				1	*	1 sd
t	13048	4	122.2	70/20	3		4			1	1	1	
t	13049	4	158	75/20	3		2						*sd
t	13050	3	177	69/15			1			8	2	3	2 talc
tp	13051	1	187.2	0/21	20	26	27			2	1	1	2 cc/ap
tp	13052	4a	189.5										ND
tp	13053	6	231	64/7	12		2	8		4	1	1	1 talc/cc
t	13054	3	276.1	40/16	1	15	20	2		3		3	* cc
tp	13055	1a	308.5	*/0	32		65			*	*	2	
tp	13056	6	329.8	59/27	10		4						
tp	13057	2	336.5	7/1	2	54	30					6	
t	13058	1	349	1/*	49	36	6				1	5	2 ap
t	13059	1	357.3	5/0	84	7	*	1		1	1	1	* talc
tPT	13060	1H	396.1	5/*	79		4						12 chl/hbl/cc/clay
PT	13061	1	419.9		48	16	36						
t	13062	2	420		5	59	20					15	1 ap
tp	13063	7	447.3	60/1	15		5			3	*	15 P	1 talc
t	13064	1	454.3	40/2	53	1	3			*	*	1	
tp	13065	4	455.1	73/5	7	2	10					3	
t	13066	I	470										
tp	13067	4	514.5	65/15			17			1	2	*	* carb
t	13068	4	563.8	58/10	3		25	2		1		*	* carb
t	13069	4	575.5	74/7	5		5	3		3	1	2	1 talc/musc
t	13070	6	579.5	72/5	8		12			1	1	1	
tp	13071	J	588.8	2			60					38 P	
tp	13072	4	594.8	72/4	2		16					6 P	
t	13073		594.9	ND									
tp	13074	4os	598.7	25/5	2		65					3 P	

Appendix 2.3

List of abbreviations for appendix 2

* - trace
A - alteration zone
At - alteration
ND - no data
PT - polished thin section
act - actinolite
ap - apatite
aug - augite
biot - biotite
br - brucite
carb - carbonate
chl - chlorite
epd - epidote
hbl - hornblende
her - hercynite
hm - hematite
lt - large thin section
musc - muscovite
ol - olivine
ox - oxides
p - polished section
P - primary
plag - plagioclase
pleo - pleonaste
pn - pennine
rk - rock type
s - serpentine
sch - schorl
sd - sulfides
ser - sericite
serp - serpentine (includes secondary magnetite =/- hematite)
sp - sphene
sym - symplectite (oxides + opx)
t - thin section
tour - tourmaline
trem - tremolite

Rock Types

7 - picrite
6 - oxide feldspathic dunite
5 - massive oxide rock
4 - oxide dunite
3 - oxide peridotite
2 - oxide clinopytoxenite
1 - troctolitic aborthosite/pegmatitic olivine gabbro/picrite (Duluth complex)

Appendix 2.4

Explanation of Appendices 2.0 - 2.2

A. Pegmatitic plagioclase in peridotite

B. Contact between pyroxenite (2) and troctolitic anorthosite (1)

C. Alteration zone next to troctolitic anorthosite (1)

D. Pegmatitic plagioclase next to troctolitic anorthosite (1)

E. Alteration zone

F. Alteration between plagioclase and olivine

G. Relationship between pegmatitic plagioclase and augite

H. Contact between troctolitic anorthosite (1) and oxide feldspathic dunite (6)

I. Pegmatitic olivine and augite

J. Oxide hornblendite

Appendix 3

Cumulate classification

The classification of igneous cumulates by Wager and others (1960) is given here as it appears in Morse (1969).

A **cumulate** is a rock formed by gravity-induced crystal acumlation. **Cumulus** minerals are those whose crystals settle to form the rocks. **Intercumulus** spaces or liquids exist between settled cumulus crystals.

An **orthocumulate** completes its solidification by crystallization of intercumulus liquid around or onto the cumulus minerals. The cumulus crystals and their original intercumulus liquid constitute a closed system, final solidification is achieved only by zoning, change of liquid composition, and fall of temperature.

An **adcumulate** completes its solidification from intercumulus liquid which remains in diffusive communication with the overlying magma, so changing in composition in response to concentration gradients that cumulus crystals are enlarged at the same composition and at the same temperature until the intercumulus space is filled. Adcumulates show no mineral zoning. They are local open systems, and the components which are exchanged between magma and intercumulus space are to be considered perfectly mobile components in the sense of Korzhinskii, 1959.

A **heteradcumulate** contains intercumulus minerals not found among the cumulus species.

Mesocumulates are those rocks intermediate between ortho- and adcumulates.

Appendix 4

Oxide characteristics in LN-2

						ILMENITE		TITANOMAGNETITE						
									ILMENITE			COMP GR		
FT	RK	T%	ILM	MT%	CPY%	TEXT	SP-HM	TEXT	SP	TRELLIS	SAND	INT	EXT	SIM
59.2	6	25	87	13		I		I						
97.0	4	17	78	22		I		I	*	*				
140.0	4	90	92	8		G	*	I	*	*				
151.0	4os	97	98	2		G	*	I	*					
170.2	4	20	85	15		I	*	I	*					
183.0	5	97	50	50		G	*	GI	^	^				*
194.3	5	97	59	41		G	*	GI	^	^				*
200.0	5	97	96	4		G	*	I	*	*				*
205.0	5	100	75	25		G	*	GI	*	*				
254.0	4						*		*	*				
282.5	5	97	94	6		G	*	I	*	+				
301.0	5	97	89	11		G	*	I	*	+				*
318.5	5	100	55	45		G	*	GI	*	+				
331.0	5	100	20	80		GI	*	GI	*	+		^		*
372.0	4a	92	41	59		G		G	*	^	*	^	^	*
375.0	4a	57	44	56		I	*	I	+	+		^	^	*
383.8	5	100	7	93				G	+			*	*	
385.0	5	100	7	93				G	+			*		
389.0	5	100	15	85				G	^	+	*	*	^	*
418.2	3a	25	30	70		I		I						
30.0	3	30	50	50	*	GI		I	^	^				
48.5	3	20	25	75	*	I	*	I		^				
55.5	2	7	25	75	*	I	*	I	*	^				*
470.0	2	45	89	11		G	*	I						*
507.5	2	12	10	90	*	I	*	I	*	^		*		*
555.8	2	10	80	20		I	*	I	+	^				*
555.9	2	12	60	40		I		I	*	*				
561.5	1	5	60	40		I	*	I	*	*				

Appendix 4.1

Oxide characteristics in LN-6

						ILMENITE		TITANOMAGNETITE						
									ILMENITE			COM	GR	
FT	RK	T%	ILM%	MT%	CPY%	TEXT	SP-HM	TEXT	SP	TRELLIS	SAND	INT	EXT	SIM
130.8	6	12	0	88	12	I		I	^	^				
168.0	6	30	96	3	1	I	*	ALT						
243.0	1	30	83	7	10	I	*	ALT						
371.0	6	26	96	4	*	GI	*	ALT						
374.2	6	95	94	5	1	G	^	I	^					*
387.2	6	60	95	4	1	GI	*	I	^					
387.4	6	80	92	6	2	G	+	I	^					*
398.1	4	16	30	70	*	I	+	I	^					*
402.5	4	15	29	71	*	I	^	I	+	+		^		*
431.9	3	97	97	3	*	G	^	I	^					*
447.0	3	50	80	20	*	GI	*	I	+	^				*
464.1	3	21	96	4	*	EI	+	I	*	*		*		
494.7	3a	85	70	30	*	GI	^	I	^	^				*
499.2	2a	80	25	75	*	I	^	I		*	+	^	^	*
511.2	3os	100		15	85	0		G	^	^	+	^	^	*
518.2	2os	60	17	83	0	I		GI	+	^	*	*		*
524.5	3	30	97	3	*	G	*		*					*
554.0	3os	93	40	60	0	I	^	GI	^	+		*		
581.6	3	40	90	10	*	G	*		^	^				
581.7	3	93	99	1	0	G	*	ALT	*					

Appendix 4.2

Oxides in LN-5

						ILMENITE		TITANOMAGNETITE				
									ILMENITE		COMP GR	
FT	RK	T%	ILM%	MT%	CPY%	TEXT	SP-HM	TEXT	SP	TRELLIS SAND	INT EXT	SIM
107.5	6	5	50	40	10	I		ALT				
111.0	6	8	68	25	7	I		I				
119.0	4	30	91	7	2	IE		I	*	*		
133.0	4	25	75	23	2	I	*	I	^	*		*
187.2	3	27	89	7	4	GI	*	IALT				*
189.5	3	45	92	4	4	GI	*	ALT				
231.0	7	8	88	6	6	I	*	ALT				
232.5	7	65	61	34	5	G	*	GI	+		^	
284.0	3	40	92	5	3	I		ALT				
308.5	7os	65	97	1.5	1.5	I	*	ALT				
329.8	6	4	75	20	5	I		I	^	*		
336.5	3	30	90	10	*	I		ALT				
396.1	1	3	100	0	0	I	*					
419.9	1	37	100	0	0	EI	*					
447.3	7	20	98	0	2	EI	*					
455.1	6	10	68	30	2	I	*	I	*	*		
514.5	6	17	85	12	3	I	*	I	*			
541.0	6	22	80	15	5	I	*	I	*			
570.1	6	85	94	4	2	GI	*	I	*			
588.8	3bos	90	82	17	2	G	*	IALT	+	*		*
594.8	3b	75	95	4	1	EG	*	IALT		*		
598.7	3a	50	95	1	4	G	*	ALT				

Appendix 4.3

Abbreviations

FT-----footage
RK-----rock type
- 7---picrite
- 6---feldspathic dunite
- 5---massive oxide rock (greater than 80% oxides)
- 4a--semi-massive oxide dunite (50-80% oxides)
- 4---oxide dunite (10-50% oxides)
- 3b--hornblende gabbro pegmatite
- 3a--semi-massive oxide peridotite
- 3---peridotite
- 2---pyroxenite
- 1---troctolitic anorthosite

os-----oxide stringer
T%-----total oxide content in polished section or polished thin section
ILM%---percent ilmenite (primary only)
MT%----percent titanomagnetite (not including ilmenite trellis etc.)
TEXT---texture of oxide grains
- I---intercumulus
- G---granular mosiac
- ALT-alteration product
- E---euhedral

SP-HM--spinel-hematite bands in ilmenite
SP-----spinel platelets
TRELLIS-ilmenite oxidation-exsolution lamellae
SAND---ilmenite sandwich
COMP GR-composite grains of ilmenite
- INT---internal compsite granule of ilmenite
- EXT---external composite granule of ilmenite

SIM----simplectite of spinel and ilmenite, or titanomagnetite and spinel along ilmenite-titanomagnetite grain border
- +----abundant
- ^----common
- *----trace

Appendix 5

Standards used in microprobe analyses

Mnrl Anal	Elements Si	Ti	Al	Fe	Mn	Mg	Ca	Na	K
cpx	opx,cpx	ilm	Tib	opx,cpx	rhod	opx,cpx	cpx	Tib	-
ol	Marj	ilm	cpx	marj	cpx	Marj	cpx	cpx	cpx
plag	Barton OrlA	ilm	Barton		opx	-	-	Barton	Tib
							Cr	V	
ilm	-	ilm	ilm	ilm	rhod	spinel	chr	v	
mt	-	ilm	ilm	mag	rhod	spinel	chr	v	
spinel	-	ilm	ilm	mag	rhod	spinel	-	-	

Appreviations

Abbreviations under elements refer to standards

Barton-----Barton An85Ab15
chr--------chromite
cpx--------cpx 5-118
ilm--------ilmenite R1959
mt---------magnetite R1993
opx--------opx R1534
Marj-------olivine Marjalahitit
OrlA-------OrlA
rhod-------rhodonite R1826
spinel-----spinel
Tib--------Tib(albite)
v----------vanadium metal

The other standard used was garnet R1134

Appendix 6
Microprobe analyses of olivine

D.H.	LN-2	LN-2	LN-2	LN-2	LN-2	LN-2	LN-2	LN-2	LN-2	LN-2	LN-2	LN-6	LN-5	BA-6
Ft.	455.5	448.5	448.5	430.0	254.0	254.0	254.0	170.2	170.2	59.2	59.2	167.1	396.1	81.0
Spl #	13113	13112-1	13112-3	13111	13205-2	13205-1	13205-3	13108-1	13108-3.1	13107-1.1	13107-2.1	13115	13118	13120-1
# Anal	2	3	1	3	2	2	1	2	3	3	3	3	2	3
SiO2	36.2	36.5	36.8	36.8	37.6	37.3	37.6	37.6	37.3	37.1	37.4	37.4	36.6	36.6
TiO2	.18	.25	.13	.07	0.00	0.00	0.00	.09	0.00	.07	0.00	0.00	0.00	0.00
FeO	34.7	33.3	33.0	32.4	30.5	31.2	29.4	30.7	31.3	31.8	32.4	32.4	35.3	34.9
MnO	.42	.41	.39	.38	.35	.34	.28	.41	.34	.32	.45	.42	.47	.42
MgO	28.5	30.7	31.2	31.7	33.8	32.5	34.5	32.6	32.8	32.3	32.3	32.1	29.0	30.0
CaO	.08	.13	.17	.14	0.00	.08	0.00	.14	.14	.10	.08	.09	.10	.07
TOTAL	100.1	101.3	101.7	101.5	102.3	101.4	101.8	101.5	101.9	101.7	102.6	102.4	101.5	102.0
%Fo	59.8	62.2	62.8	63.6	66.4	65.0	67.7	65.5	65.1	64.5	64.0	63.8	59.4	60.5

Cations per 4 oxygen

Si	.99	.98	.98	.98	.94	.99	.99	1.00	.99	.99	.99	.99	.99	.98
Ti	0.00	0.00	0.00	0.00	0.00	0.00	0.00	0.00	0.00	0.00	0.00	0.00	0.00	0.00
Fe	.79	.75	.74	.72	.67	.69	.64	.68	.69	.71	.71	.72	.8	.78
Mn	.01	.01	.01	.01	.01	.01	.01	.01	.01	.01	.01	.01	.01	.01
Mg	1.18	1.23	1.25	1.26	1.32	1.29	1.35	1.30	1.29	1.28	1.27	1.26	1.17	1.20
Ca	0.00	0.00	0.00	0.00	0.00	0.00	0.00	0.00	0.00	0.00	0.00	0.00	0.00	0.00
TOTAL	2.97	2.97	2.98	2.97	2.94	2.98	2.99	2.99	2.98	2.99	2.98	2.98	2.97	2.97

Appendix 6.1
Microprobe analyses of clinopyroxene

D.H.	LN-2	LN-2	LN-2	LN-2	LN-2	LN-5	BA-6	BA-6
Ft.	455.5	455.5	455.5	455.5	448.5	396.1	73.0	73.0
Spl #	13113-1	13113-1.2*	13113-2.1	13113-2.3*	13112	13118*	13119-1	13119-3*
# Anal	1	1	3	1	2	1	2	1
SiO2	50.8	51.8	50.8	52.0	50.2	52.9	51.5	53.0
TiO2	1.34	0.62	1.02	0.68	1.35	0.62	0.88	0.60
Al2O3	2.44	1.79	2.50	1.78	3.16	1.42	2.35	1.56
FeO	9.43	8.29	8.95	8.50	8.71	8.16	8.89	9.31
MnO	0.22	0.22	0.16	0.11	0.00	0.22	0.24	0.16
MgO	13.8	14.0	14.0	14.7	13.7	14.3	14.6	15.2
CaO	21.8	22.7	21.6	22.6	21.9	22.8	21.8	21.2
Na2O	0.00	0.00	0.26	0.22	0.00	0.00	0.00	0.00
TOTAL	99.8	99.6	99.3	100.6	99.0	100.4	100.3	101.0
%En	41.8	42.5	42.5	44.9	42.4	42.1	45.5	44.9
%Fs	15.5	13.4	15.2	11.5	15.0	13.5	14.0	15.1
%Wo	42.8	44.1	42.2	43.7	42.6	44.5	41.6	40.9
Cations per 6 oxygen								
Si	1.90	1.94	1.91	1.93	1.89	1.96	1.92	1.95
Al	0.11	0.08	0.11	0.08	0.09	0.06	0.10	0.07
Ti	0.04	0.02	0.03	0.02	0.04	0.02	0.02	0.02
Fe	0.30	0.26	0.28	0.26	0.27	0.25	0.28	0.29
Mn	0.01	0.01	0.01	-	0.00	0.01	0.01	0.01
Mg	0.77	0.79	0.78	0.81	0.77	0.79	0.81	0.83
Ca	0.88	0.91	0.87	0.90	0.88	0.90	0.87	0.83
Na	0.00	0.00	0.02	0.02	0.00	0.00	0.00	0.00
TOTAL	4.01	4.01	4.01	4.02	3.94	3.99	4.01	4.00

* titanaugite grain edge without ilmenite platelets

Appendix 6.2
Microprobe analyses of plagioclase

D.H.	LN-2	LN-2	LN-2	LN-5	LN-5	LN-5	LN-5	LN-5	BA-6	BA-6	BA-6	BA-6	BA-6	BA-6	LN-6
Ft.	59.2	59.2	59.2	396.1	396.1	396.1	396.1	396.1	73.0	81.0	81.0	81.0	81.0	81.0	167.1
Spl #	13107-1	13107-1.2	13107-2	13118-1.1	13118-1.2	13118-2.1	13118-2.2	13118-3	13119	13120-1	13120-1.2	13120-2.1	13120-2.2	13120-3	13115
# Anal	1	1	2	1	1	1	1	1	2	1	1	1	1	1	5
SiO2	52.3	57.1	49.2	54.8	51.4	51.7	51.7	52.0	49.5	56.1	49.3	49.5	49.0	50.9	51.0
TiO2	0.06	0.07	1.35	0.08	0.09	0.00	0.00	0.12	0.00	0.00	0.00	0.08	0.00	0.00	0.00
Al2O3	30.7	28.9	31.1	30.6	33.2	32.2	32.4	32.2	33.7	29.7	33.8	26.8	34.3	33.4	33.3
FeO	0.71	0.00	1.68	0.00	0.11	0.16	0.00	0.00	0.17	0.00	0.00	0.00	0.00	0.10	0.23
MnO	0.08	0.00	0.00	0.00	0.00	0.00	0.00	0.00	0.00	0.00	0.00	0.00	0.00	0.00	0.00
MgO	0.00	0.00	0.68	0.00	0.00	0.00	0.00	0.00	0.00	0.00	0.00	0.00	0.00	0.00	0.00
CaO	12.5	10.5	13.6	12.1	14.8	14.3	14.4	13.8	15.9	11.4	16.2	18.6	16.9	15.6	15.0
Na2O	3.88	5.77	3.18	5.15	3.33	3.36	3.72	3.58	2.64	5.47	2.33	2.75	2.19	2.70	2.95
K2O	0.08	0.11	0.14	0.22	0.23	0.42	0.21	0.09	0.07	0.21	0.15	0.23	0.13	0.23	0.09
TOTAL	100.3	102.5	100.9	103.0	103.2	102.1	102.4	101.8	102.0	102.9	101.8	98.0	102.5	102.9	102.6
%An	64.1	50.2	70.3	56.6	71.1	70.8	68.1	68.0	76.9	53.5	79.3	78.9	81.0	76.1	73.7

Cations recalculated to stoichiometry with 20 cations per 32 oxygen

Si	9.46	10.0	6.67	8.97	9.63	9.09	9.20	9.27	8.88	9.84	8.85	9.36	8.77	9.03	9.07
Al	6.55	5.98	6.67	6.30	6.90	6.77	6.79	6.77	7.12	6.15	7.17	5.97	7.23	6.98	6.97
Ti	0.01	0.01	0.18	0.01	0.01	0.00	0.00	0.02	0.00	0.00	0.00	0.00	0.00	0.00	0.00
Fe	0.11	0.00	0.26	0.00	0.02	0.02	0.00	0.00	0.03	0.00	0.00	0.00	0.00	0.02	0.03
Mn	0.01	0.00	0.00	0.00	0.00	0.00	0.00	0.00	0.00	0.00	0.00	0.00	0.00	0.00	0.00
Mg	0.00	0.00	0.19	0.00	0.00	0.00	0.00	0.00	0.00	0.00	0.00	0.00	0.00	0.00	0.00
Ca	2.43	1.98	2.66	2.29	2.81	2.74	2.74	2.64	3.06	2.14	3.12	3.77	3.23	2.97	2.85
Na	1.36	1.96	1.12	1.76	1.14	1.16	1.29	1.24	0.92	1.86	0.81	1.00	0.76	0.93	1.02
K	0.02	0.02	0.03	0.05	0.05	0.09	0.05	0.02	0.02	0.05	0.03	0.06	0.03	0.05	0.02
TOTAL	20.0	20.0	17.0	19.4	20.6	19.9	20.1	20.0	20.0	20.0	20.0	20.2	20.0	20.0	20.0

Appendix 7

Microprobe analyses of ilmenite in drill core LN-2

Ft.	59.2	59.2	59.2	170.2	170.2	170.2	301.0	301.0	301.0	301.0	301.0	301.0	430.0	430.0
Spl #	13107-1	13107-2	13107-3	13108-1	13108-2	13108-3	13109-1.1	13109-1.2	13109-2	13109-3.1	13109-3.2	13109-3.3	13111-1	13111-2
SiO2	0.00	0.74	0.12	0.09	0.00	0.10	0.11	0.13	0.11	0.00	0.11	0.00	0.11	0.07
TiO2	47.8	47.8	48.5	49.4	49.3	49.3	48.8	47.7	49.2	48.9	48.7	48.6	49.0	49.8
Al2O3	0.00	0.34	0.00	0.00	0.00	0.00	0.00	2.62	0.16	0.00	0.00	0.29	0.00	0.00
Fe2O3	11.1	9.96	9.20	8.10	8.12	7.94	8.99	8.74	8.72	9.38	9.62	9.00	7.17	7.29
FeO	38.1	38.2	39.0	39.0	38.5	38.1	38.2	36.3	38.2	38.5	37.6	38.2	39.9	40.1
MnO	0.30	0.31	0.30	0.50	0.56	0.43	0.65	0.34	0.13	0.52	0.43	0.27	0.28	0.37
MgO	2.55	2.31	2.42	2.74	2.46	3.25	2.84	3.50	3.31	2.73	3.23	2.93	2.15	2.41
CaO	0.00	0.00	0.00	0.00	0.00	0.00	0.00	0.00	0.00	0.00	0.00	0.00	0.00	0.00
V2O3	0.42	0.34	0.44	0.23	0.35	0.00	0.18	0.18	0.19	0.43	0.22	0.21	0.39	0.39
Cr2O3	0.24	0.12	0.00	0.00	0.00	0.00	0.00	0.00	0.00	0.00	0.00	0.00	0.00	0.00
TOTAL	100.5	100.1	100.0	100.1	99.3	99.1	99.8	99.5	100.0	100.5	99.9	99.5	99.0	100.4
Cations per 6 oxygen														
Fe+3	0.40	0.38	0.34	0.30	0.30	0.30	0.34	0.33	0.32	0.36	0.36	0.34	0.26	0.27
Ti	1.80	1.80	1.82	1.85	1.85	1.85	1.84	1.83	1.84	1.81	1.82	1.83	1.87	1.84
Fe+2	1.58	1.59	1.62	1.61	1.59	1.59	1.59	1.57	1.58	1.60	1.55	1.59	1.67	1.63
Mn	0.01	0.01	0.01	0.02	0.02	0.02	0.03	0.02	-	0.02	0.02	0.01	0.01	0.01
Mg	0.18	0.18	0.18	0.20	0.21	0.24	0.18	0.27	0.24	0.20	0.24	0.22	0.15	0.18
V	0.02	0.02	0.02	0.01	0.01	-	0.01	-	0.01	-	0.01	0.12	0.02	0.04
Cr	0.01	-	0.00	0.00	0.00	0.00	0.00	0.00	0.00	0.00	0.00	0.00	0.00	0.00
TOTAL	4.00	3.98	3.99	3.99	3.98	4.00	3.99	4.02	3.99	3.99	4.00	4.11	3.98	3.97

Appendix 7.1
Microprobe analyses of ilmenite

D.H.	LN-2	LN-2	LN-2	LN-2	LN-2	LN-6	LN-6	LN-5	LN-5	BA-6	BA-6
Ft.	448.5	455.5	455.5	254.0	254.0	167.1	167.1	396.05	396.05	73.0	73.0
Spl #	13112-1	13113-1	13113-2	13205-1	13205-2	13115-1	13115-2	13118-1	13118-2	13119-1	13119-2
SiO2	0.09	0.07	0.12	0.14	0.16	0.11	0.00	0.00	0.00	0.17	0.15
TiO2	48.6	48.8	48.9	48.6	49.7	48.8	49.0	47.5	47.8	49.1	48.8
Al2O3	0.00	0.00	0.00	0.00	0.11	0.00	0.00	0.00	0.00	0.00	0.00
Fe2O3	8.88	7.88	8.67	9.55	8.84	9.39	8.06	10.9	9.61	8.47	8.19
FeO	38.4	38.4	38.5	38.9	37.7	40.0	40.9	38.0	39.2	38.5	38.4
MnO	0.43	0.34	0.52	0.43	0.54	0.55	0.39	0.29	0.31	0.38	0.64
MgO	2.74	2.87	2.82	2.48	3.60	1.82	1.55	2.50	1.95	2.95	2.71
CaO	0.00	0.00	0.00	0.00	0.00	0.00	0.00	0.00	0.00	0.00	0.00
V2O3	0.31	0.52	0.60	0.36	0.52	0.67	0.60	0.28	0.26	0.42	0.45
Cr2O3	0.00	0.00	0.00	0.00	0.00	0.00	0.00	0.08	0.15	0.00	0.00
TOTAL	99.5	98.9	100.1	100.5	101.2	101.3	100.5	99.6	99.3	100.0	99.3
Cations per 6 oxygen											
Fe+3	0.23	0.30	0.32	0.36	0.33	0.36	0.30	0.40	0.36	0.32	0.30
Ti	1.83	1.84	1.82	1.82	1.82	1.81	1.86	1.80	1.80	1.83	1.83
Fe+2	1.59	1.60	1.61	1.61	1.53	1.61	1.72	1.61	1.66	1.61	1.59
Mn	0.02	0.02	0.04	0.02	0.02	0.02	0.02	0.01	0.01	0.01	0.03
Mg	0.20	0.21	0.21	0.18	0.26	0.13	0.06	0.18	0.15	0.21	0.21
V	0.01	0.02	0.03	0.01	0.03	0.03	0.02	0.01	0.02	0.02	0.04
Cr	0.00	0.00	0.00	0.00	0.00	0.00	0.00	-	0.01	0.00	0.00
TOTAL	3.88	3.99	4.03	4.00	3.99	3.96	3.98	4.01	1.01	1.00	4.00

Appendix 7.2
Microprobe analyses of titonomagnetite

D.H.	LN-2	LN-2	LN-2	LN-2	LN-2	LN-2	LN-2	LN-2	LN-2	LN-5	BA-6	BA-6	BA-6
Ft.	254.0	301.0	301.0	430.0	430.0	430.0	448.5	455.5	455.5	396.0	73.0	73.0	81.0
Spl #	13025-1*	13109-2	13109-3	13111-1+	13111-2	13111-3+	13112-1	13113-1+	13113-2+	13118-1+	13119-1*	13119-2	13120-1+
SiO2	0.00	0.16	0.00	0.00	0.00	0.00	0.00	0.00	0.15	0.00	0.00	0.00	0.00
TiO2	6.20	2.62	3.16	2.32	11.1	8.37	6.50	3.20	9.51	7.60	1.31	6.25	6.46
Al2O3	3.09	0.68	1.60	3.25	2.72	4.00	2.32	1.27	2.67	3.99	2.16	8.54	3.44
Fe2O3	49.7	59.7	57.0	48.8	42.2	47.0	51.6	58.9	45.6	43.2	63.2	48.5	50.4
FeO	35.6	32.2	32.9	37.0	40.1	37.8	36.7	33.1	38.6	38.0	32.0	34.6	36.9
MnO	0.56	0.47	0.44	0.51	0.28	0.17	0.18	0.21	0.27	0.92	0.00	0.18	0.44
MgO	1.04	0.53	0.50	0.42	0.90	0.96	0.36	0.49	0.86	0.00	0.58	2.81	0.38
CaO	0.00	0.00	0.00	0.00	0.00	0.07	0.00	0.00	0.00	0.08	0.00	0.00	0.00
V2O3	2.08	2.26	2.49	2.24	2.18	1.89	1.99	2.37	1.90	1.98	1.93	1.80	1.24
Cr2O3	3.17	1.59	1.83	0.00	0.44	0.05	0.41	0.27	0.36	4.76	0.00	0.00	1.83
TOTAL	101.4	100.2	100.0	94.5	100.0	100.3	100.1	99.8	99.9	100.5	101.2	102.6	101.1
Cations per 32 oxygen													
Ti	1.38	0.64	0.72	1.63	2.12	1.86	1.45	5.25	2.14	1.70	0.27	1.34	1.43
Al	1.07	0.24	0.60	1.20	0.98	1.42	0.82	0.35	0.95	1.43	0.72	2.80	1.19
Fe+3	11.0	13.6	12.9	11.1	9.72	10.4	11.7	9.72	10.2	9.64	14.2	10.2	11.3
Fe+2	8.70	8.20	8.33	9.21	10.3	9.39	9.20	6.04	9.63	9.46	8.07	8.10	9.09
Mn	0.14	0.13	0.11	0.13	0.07	0.04	0.05	0.04	0.07	0.23	0.00	0.03	0.11
Mg	0.46	0.24	0.22	0.18	0.37	0.43	0.18	0.16	0.36	0.00	0.25	1.17	0.16
V	0.47	0.55	0.60	0.54	0.49	0.47	0.48	0.41	0.48	0.48	0.48	0.40	0.30
Cr	0.71	0.36	0.48	0.00	0.11	-	0.12	0.04	0.12	1.07	0.00	0.00	0.43
TOTAL	23.9	24.0	24.0	24.0	24.0	24.0	24.0	22.0	24.0	24.0	24.0	24.0	24.0

Appendix 7.3

Microprobe analyses of spinel in drill core LN-2

Ft.	254.0	430.0	448.5
Spl #	13025	13111-1	13112-1
SiO2	0.00	0.00	0.00
TiO2	0.86	0.47	0.35
Al2O3	57.9	63.7	63.9
Fe2O3	5.37	0.12	0.30
FeO	20.4	21.7	22.4
MnO	0.38	0.17	0.16
MgO	13.5	13.4	12.9
CaO	0.00	0.00	0.07
Na2O	1.86	1.74	1.56
V2O3	nt	nt	nt
Cr2O3	nt	nt	nt
TOTAL	100.3	101.3	101.6

Cations per 32 oxygen

Ti	0.13	0.07
Al	14.7	15.7
Fe+3	0.87	0.02
Fe+2	3.6	3.77
Mn	0.06	0.03
Mg	4.28	4.15
Ca	0.00	0.00
Na	0.40	0.38
TOTAL	5.7	24.1